



**Faculty of Engineering**

**BROAD-BAND DUAL-FREQUENCY MICROSTRIP PATCH ANTENNA  
WITH MODIFIED SIERPINSKI FRACTAL GEOMETRY**

**Chua Ting Ting**

**Bachelor of Engineering with Honours  
(Electronics and Telecommunication Engineering)  
2005**

# UNIVERSITI MALAYSIA SARAWAK

R13a

## BORANG PENGESAHAN STATUS TESIS

Judul: **BROAD-BAND DUAL-FREQUENCY MICROSTRIP PATCH ANTENNA  
WITH MODIFIED SIERPINSKI FRACTAL GEOMETRY**

SESI PENGAJIAN: 2005/2006

Saya **CHUA TING TING**  
(HURUF BESAR)

mengaku membenarkan tesis \* ini disimpan di Pusat Khidmat Maklumat Akademik, Universiti Malaysia Sarawak dengan syarat-syarat kegunaan seperti berikut:

1. Tesis adalah hakmilik Universiti Malaysia Sarawak.
2. Pusat Khidmat Maklumat Akademik, Universiti Malaysia Sarawak dibenarkan membuat salinan untuk tujuan pengajian sahaja.
3. Membuat pendigitan untuk membangunkan Pangkalan Data Kandungan Tempatan.
4. Pusat Khidmat Maklumat Akademik, Universiti Malaysia Sarawak dibenarkan membuat salinan tesis ini sebagai bahan pertukaran antara institusi pengajian tinggi.
5. \*\* Sila tandakan ( ✓ ) di kotak yang berkenaan

SULIT (Mengandungi maklumat yang berdarjah keselamatan atau kepentingan Malaysia seperti yang termaktub di dalam AKTA RAHSIA RASMI 1972).

TERHAD (Mengandungi maklumat TERHAD yang telah ditentukan oleh organisasi/ badan di mana penyelidikan dijalankan).

TIDAK TERHAD

Disahkan oleh

\_\_\_\_\_  
(TANDATANGAN PENULIS)

\_\_\_\_\_  
(TANDATANGAN PENYELIA)

Alamat tetap: No. 30, Lorong 8A2,

Jalan Sky Garden, 93150 Kuching,

Sarawak.

Cik Kho Lee Chin

Nama Penyelia

Tarikh: 15 May 2006

Tarikh: 15 May 2006

### CATATAN

- \* Tesis dimaksudkan sebagai tesis bagi Ijazah Doktor Falsafah, Sarjana dan Sarjana Muda.  
\*\* Jika tesis ini SULIT atau TERHAD, sila lampirkan surat daripada pihak berkuasa/organisasi berkenaan dengan menyatakan sekali sebab dan tempoh tesis ini perlu dikelaskan sebagai SULIT dan TERHAD.

Laporan Projek Tahun Akhir berikut:

Tajuk: **BROAD-BAND DUAL-FREQUENCY MICROSTRIP PATCH ANTENNA  
WITH MODIFIED SIERPINSKI FRACTAL GEOMETRY**

Nama penulis: **Chua Ting Ting**

Matrik: **8080**

telah dibaca dan disahkan oleh:

---

**Cik Kho Lee Chin**  
**Penyelia**

---

**Tarikh**

**BROAD-BAND DUAL-FREQUENCY MICROSTRIP PATCH ANTENNA  
WITH MODIFIED SIERPINSKI FRACTAL GEOMETRY**

**CHUA TING TING**

This project is submitted in partial fulfilment of  
the requirements for the degree of Bachelor of Engineering with Honours  
(Electronics and Telecommunication Engineering)

Faculty of Engineering  
UNIVERSITI MALAYSIA SARAWAK  
2005

Dedicated to my beloved family, my boyfriend, and my friends.

# ACKNOWLEDGEMENT

The author would like to express sincere appreciation and gratitude to the project supervisors - Ms Kho Lee Chin, Mr. Thelaha Masri, and Mr. Norhuzaimin Julai who have given the author tremendous support, encouragement and guidance throughout the project. Special thanks also go to all the lecturers and support staffs from the Faculty of Engineering, Universiti Malaysia Sarawak (UNIMAS) for their ongoing support during the duration of this Final Year Project.

Besides, the author would like to express appreciation to all her coursemates and friends for their valuable information and dynamic support.

Last but not least, the author would like to thank her beloved and supportive family for their encouragement and companionship in making this project a success.

# ABSTRAK

Teknologi antena berbentuk 'fractal' telahpun banyak diaplikasikan dalam rekaan antena 'multiband' untuk memenuhi tren pasaran telekomunikasi terkini. Antena Sierpinski merupakan contoh pertama antena berbentuk 'fractal' yang berfungsi 'multiband'. Antena 'fractal' mempunyai ciri untuk memancar gelombang elektromagnetik pada pelbagai frekuensi melalui ciri keserupaan fizikal bentuk 'fractal'. Dengan menggabungkan antena-antena berbentuk 'fractal', liputan meluas boleh dicapai. Antena jenis 'microstrip patch' berdasarkan geometri 'fractal' Sierpinski boleh dilaraskan melalui rekabentuknya untuk berfungsi pada liputan yang dikehendaki. Oleh sebab itu, matlamat utama projek ini adalah untuk mereka antena jenis 'microstrip patch' dengan geometri 'fractal' Sierpinski yang mempunyai liputan luas and ciri dwi-frekuensi dengan menggunakan perisian 'Microwave Office 2002'. Ciri-ciri liputan luas and kepelbagaian frekuensi antena akan ditunjukkan. Pencapaian antena jenis 'microstrip patch' berdasarkan bentuk Sierpinski klasik and bentuk Sierpinski yang diubahsuai akan dipersembahkan.

# ABSTRACT

Fractal antenna technology has currently been applied to the design of multiband antennas to provide a solution to the needs of nowadays telecommunication market trend. The Sierpinski gasket antenna was the first example of multiband fractal shaped antenna. Fractal antennas have the characteristic of radiating in multiple frequencies through the property of self-similarity that fractal shapes possess. By connecting fractal shaped antennas, wideband coverage can be achieved. Microstrip patch antennas with Sierpinski fractal geometry can be tuned, by design, to work exactly at the bands of interest, through judicious choice of the fractal designs and iteration. Therefore, the intention of this project is to design a broad-band dual-frequency microstrip patch antenna with modified Sierpinski fractal geometry by using Microwave Office 2002 simulation software. The broad-band and multiple frequency characteristics of fractal antennas will be demonstrated. The performance of microstrip patch antenna with the classic and modified Sierpinski fractal geometries will be presented.

# LIST OF CONTENTS

<b>CONTENTS</b>	<b>Page</b>
DEDICATION	ii
ACKNOWLEDGEMENT	iii
ABSTRAK	iv
ABSTRACT	v
LIST OF CONTENTS	vi
LIST OF TABLES	xii
LIST OF FIGURES	xiii
LIST OF ACRONYMS	xvi
<b>Chapter 1 INTRODUCTION</b>	
1.1 Introduction to Antenna	1
1.2 Background and History of Antenna	2
1.3 Project Overview	4
1.4 Project Objectives	6
1.5 Design Methodology	7
1.5.1 Information Searching and Focus on Topic	9
1.5.2 Study, Investigation, and Design Planning	9
1.6 Project Report Outlines	11

## **Chapter 2 LITERATURE REVIEW**

2.1	Fundamentals of Antenna	13
2.1.1	Electric Field	13
2.1.2	Magnetic Field	14
2.1.3	Electromagnetic Waves	15
2.1.4	Basic Microwave System	16
2.2	Antenna Design Parameters and Considerations	18
2.2.1	Radiation Pattern	18
2.2.2	Power Handling Capability	20
2.2.3	Frequency Range and Bandwidth	21
2.2.4	Power Gain	19
2.2.5	Polarization	22
2.2.6	Beamwidth	22
2.2.7	Coverage	23
2.2.8	Input Impedance	23
2.3	Microwave Transmission Line	25
2.4	Types of Antenna	27
2.4.1	Dipole Antenna	27
2.4.2	Horn Antenna	29
2.4.3	Yagi Antenna	30
2.4.4	Log-Periodic Antenna	31
2.4.5	Loop Antenna	32
2.4.6	Helical Antenna	33
2.4.7	Microstrip Antenna	34
2.4.8	Corner-Reflector Antenna	35

2.4.9	Array Antenna	36
2.4.10	Parabolic Dish	37
2.4.11	Smart Antenna	38
2.5	Fractal Antenna	39
2.5.1	Definition of Fractal Antenna	39
2.5.2	Fractal Theory	39
2.5.3	Fractal Geometry	39
2.5.3.1	Sierpinski Gasket	40
2.5.3.2	Sierpinski Carpet	42
2.5.3.3	Koch Curve	43
2.5.3.4	Koch Snowflake	44
2.5.4	Advantageous Characteristics of Fractal Antenna	45
2.5.4.1	Miniaturization and Space-Filling	45
2.5.4.2	Multiband Performance	45
2.5.4.3	Input Impedance Matching	45
2.5.4.4	Efficiency and Effectiveness	46
2.5.4.5	Improved Directivity	46
2.5.5	Fractal Antenna Applications	47
2.5.5.1	Mobile Devices	47
2.5.5.2	Radio Frequency Identification (RFID)	47
2.5.5.3	Wireless Network	47
2.5.5.4	Telematics	48
2.5.5.5	Military Defense and Intelligence Applications	48

### **Chapter 3 METHODOLOGY**

3.1	Design and Simulation	49
3.1.1	Antenna Design	49
3.1.2	Design and Simulation Process	51
3.1.3	Microwave Office	54
3.2	Analysis and Validation of Result	55
3.2.1	Smith Chart	55
3.3	Discussion and Conclusion	58
3.4	Compile of Report	58

### **Chapter 4 RESULTS & ANALYSIS**

4.1	Equilateral Triangular Single Patch Antenna with Length 5cm	59
4.1.1	Antenna Design	59
4.1.2	Simulation Results	63
4.1.3	Comparison of Simulation Results and Calculations	69
4.2	Equilateral Triangular Single Patch Antenna with Length 8cm	71
4.2.1	Antenna Design	71
4.2.2	Simulation Results	75
4.2.3	Comparison of Simulation Results and Calculations	80
4.3	Equilateral Triangular Single Patch Antenna with	81

Length 10cm	
4.3.1	Antenna Design 81
4.3.2	Simulation Results 84
4.3.3	Comparison of Simulation Results and Calculations 89
4.3.4	Comparison of 5cm, 8cm, and 10cm Single Patch Antennas 90
4.3.5	Causes of Inaccuracy in Simulation Results 91
4.4	Microstrip Patch Antenna with Classical Sierpinski Fractal Geometry 95
4.4.1	Antenna Design and Power Radiation Pattern 95
4.4.2	Determination of the Best Via Port Position 97
4.4.3	Simulation Results 99
4.5	Microstrip Patch Antenna with Modified Sierpinski Fractal Geometry 103
4.5.1	P3/5SPK Geometry 103
	4.5.1.1 Antenna Design 103
	4.5.1.2 Simulation Results 104
4.5.2	P3/4SPK Geometry 108
	4.5.2.1 Antenna Design 108
	4.5.2.2 Simulation Results 109
4.5.3	Comparison of Classical Sierpinski, P3/5SPK, and P3/4SPK Antennas 113

<b>Chapter 5</b>	<b>CONCLUSION &amp; RECOMMENDATION</b>	
5.1	Project Conclusion	116
5.2	Limitations and Difficulties	118
5.3	Recommendations	120
	<b>REFERENCES</b>	122
<b>APPENDIX A</b>	<b>Dimension and Cell Calculator</b>	125
<b>APPENDIX B</b>	<b>Substrates for Microstrip Antenna</b>	126

# LIST OF TABLES

<b>Table</b>		<b>Page</b>
1.1	Evolution History of Antenna	2
4.1	Parameters of Patch Antenna with Side Length of 5cm	59
4.2	Comparison of Frequencies from Simulation and Calculation	70
4.3	Parameters of Patch Antenna with Side Length of 8cm	71
4.4	Comparison of Frequencies from Simulation and Calculation	80
4.5	Key Parameters of Patch Antenna with Side Length of 10cm	81
4.6	Comparison of Frequencies from Simulation and Calculation	89
4.7	Summary of Important Parameters for Microstrip Single Patch Antennas	90
4.8	Average Bandwidth Corresponding to Different Via Port Position	98
4.9	Main Parameters of the Simulated Classical Sierpinski Antenna	101
4.10	Main Parameters of the P3/5SPK Antenna	106
4.11	Main Parameters of the P3/4SPK Antenna	111
4.12	Comparison of Classical Sierpinski, P3/5SPK, and P3/4SPK Antennas	113

# LIST OF FIGURES

<b>Figure</b>		<b>Page</b>
1.1	Project Methodology Flow Chart	8
2.1	Electric Field Associated with Positive and Negative Charge	13
2.2	Magnetic Field Resulting From a Flowing Current	14
2.3	Electromagnetic Wave	15
2.4	The Electromagnetic Spectrum	16
2.5	Basic Microwave Communication System	17
2.6	A Rectangular Azimuth Plot Presentation of a 10 Element Yagi Antenna	19
2.7	Polar Plot of a 10 Element Yagi Antenna	19
2.8	Main Lobe and Side Lobe in a Radiation Pattern	20
2.9	Diagram of Lossless Transmission Line with Load Showing Incident, Reflected-Transmitted Waves	26
2.10	Current and Voltage Distribution on a Halfwave Dipole	28
2.11	Power Pattern of a Halfwave Dipole	28
2.12	Horn Antenna	29
2.13	A Typical Multiple Elements Yagi Antenna	30
2.14	Horizontal Plane Pattern of a Yagi Antenna	30
2.15	The Typical Log-Periodic Antenna	31
2.16	Horizontal Plane Pattern of Log-Periodic Antenna	31
2.17	Magnetic Loop Antenna	32
2.18	Variations of Helix Antenna	33
2.19	Aperture-Coupled Patch Antenna	34
2.20	Corner-Reflector Antenna	35
2.21	Horizontal Plane Pattern of Corner-Reflector Antenna	35
2.22	A Typical Vertical Array Using Folded Dipoles	36
2.23	Vertical-Plane Radiation Patterns: (a) Single Half Wave Dipole, (b) Two-Element Array, and (c) Three-Element Array	36
2.24	Parabolic Dish Antenna	37
2.25	Configuration of Smart Antenna	38
2.26	Removal of Inner Triangle to Form Sierpinski Gasket	40
2.27	Sierpinski Gasket with Different Numbers of Iteration	41
2.28	First Four Iterations of Sierpinski Carpet	42
2.29	Construction of Koch Curve	43
2.30	Koch Snowflake	44
2.31	Directivity Versus Projected Arm Length for a Koch Fractal-Vee Dipole at Different Fractal Iterations	46
3.1	Iteration Function Process to Generate: (a) First Stage of the Classic Sierpinski Gasket, and (b) Perturbed Sierpinski Gasket	50

3.2	Iteration Function System Attractors:	50
	(a) Classic Sierpinski Gasket at Fourth Stage, and	
	(b) Perturbed Sierpinski Gasket at Fourth Stage	
3.3	Dimension and Cell Calculation in Mathcad	51
3.4	Setting Parameters and Graphs in Microwave Office Simulation	52
3.5	Design and Simulation Process Flow Chart	53
3.6	The Layout of Microwave Office	54
3.7	Example of a Smith Chart	56
4.1	Computation of Cell Size and Dimension by Using Mathcad	60
4.2	Entering Values of X-Dimension, Y-Dimension, X-Division, and Y-Division in Microwave Office	61
4.3	Information of Dielectric Layers	61
4.4	2D View of the 5cm Triangle Patch Antenna	62
4.5	3D View of the 5cm Patch Antenna	62
4.6	Return Loss Graph for 5cm Triangular Patch Antenna	63
4.7	Finding Bandwidth from VSWR Graph	64
4.8	An Ideal Phase Graph	66
4.9	Phase Graph of 5cm Triangular Patch Antenna	66
4.10	Finding Impedance from Smith Chart	67
4.11	Radiation Pattern of the 5cm Triangular Patch Antenna	68
4.12	Mathcad Computation of Cell Size and Dimension	72
4.13	Enclosure Information in Microwave Office	73
4.14	Substrate Information	73
4.15	2D View of 8cm Triangular Patch Antenna	74
4.16	3D View of 8cm Triangular Patch Antenna	74
4.17	Return Loss Graph for 8cm Triangular Patch Antenna	75
4.18	VSWR Graph of 8cm Triangular Patch Antenna	76
4.19	Phase Graph of 8cm Triangular Patch Antenna	77
4.20	Finding Impedance from Smith Chart	78
4.21	Radiation Characteristic Chart	79
4.22	Different Positions of Via Port Tested	82
4.23	10cm Triangular Patch Antenna Design with Via Port in Best Position	83
4.24	10cm Antenna Design in 3D View	83
4.25	Return Loss Graph for 10cm Triangular Patch Antenna	84
4.26	VSWR Graph of 10cm Triangular Patch Antenna	85
4.27	Phase Graph of 10cm Triangular Patch Antenna	86
4.28	Smith Chart for 10cm Triangular Patch Antenna Radiating at 9 GHz	87
4.29	Radiation Characteristics Chart for 10cm Triangular Patch Antenna	88
4.30	Actual Shape and Size of Antenna Patch	92
4.31	Antenna Patch Simulated By Microwave Office	92
4.32	(a) Initial Design of Classic Sierpinski Antenna, (b) Corresponding Power Radiation	95
4.33	(a) Improved Design of Classic Sierpinski Antenna, (b) Corresponding Power Radiation	96
4.34	Different Positions of Via Port	97
4.35	Return Loss Graph of Classical Sierpinski Antenna	99
4.36	Return Loss Graph of Classical Sierpinski Antenna	100
4.37	Smith Chart of Classical Sierpinski Antenna	100
4.38	Radiation Characteristics of Classical Sierpinski Antenna	102

4.39	(a) P3/5SPK Antenna, (b) Power Radiation	103
4.40	Return Loss Graph of P3/5SPK Antenna	104
4.41	VSWR Graph of P3/5SPK Antenna	105
4.42	Smith Chart From P3/5SPK Antenna Simulation	105
4.43	Radiation Characteristic of P3/5SPK Antenna	107
4.44	(a) P3/4SPK Antenna, (b) Power Radiation	108
4.45	Return Loss Graph of P3/4SPK Antenna	109
4.46	VSWR Graph of P3/4SPK Antenna	109
4.47	Smith Chart of P3/4SPK Antenna Simulation	110
4.48	Radiation Characteristic of P3/4SPK Antenna	112

# LIST OF ACRONYMS

AC	-	Alternating Current
AM	-	Amplitude Modulation
B	-	Magnetic Field
C	-	Capacitance
CDMA	-	Code Division Multiple Access
dB	-	Decibels
E	-	Electric Field Strength
EM	-	Electromagnetic
EPC	-	Electronic Product Code
F	-	Force
FM	-	Frequency Modulation
G	-	Conductance
GHz	-	GigaHertz
GSM	-	Global System for Mobile Communications
H	-	Magnetic Field Strength
HF	-	High Frequency
Hz	-	Hertz
$\dot{I}$	-	Time-Changing Current
IEEE	-	Institute of Electrical and Electronics Engineers
JTRS	-	Joint Tactical Radio System
L	-	Inductance
$\ell$	-	Length of Current Element
LHCP	-	Left Hand Circular Polarization
LPDA	-	Log Periodic Dipole Array
$\lambda$	-	Wavelength
m	-	Magnetic Charge
MIMO	-	Multiple Input Multiple Output
PCS	-	Personal Communications Services
PDA	-	Personal Digital Assistant
P3/4SPK	-	Perturbed $\frac{3}{4}$ Sierpinski
P3/5SPK	-	Perturbed $\frac{3}{5}$ Sierpinski
q	-	Test Charge
Q	-	Charge
r	-	Distance to Test Pole
R	-	Resistance
RADAR	-	Radio Detection and Ranging
RF	-	Radio Frequency
RFID	-	Radio Frequency Identification
RHCP	-	Right Hand Circular Polarization
RLC	-	Resistor Inductor Capacitor
SWR	-	Standing Wave Ratio
TV	-	Television

UHF	-	Ultra-High Frequency
$\mu$	-	Permeability
$v$	-	Time Change of Velocity
VSWR	-	Voltage Standing Wave Ratio
WiMAX	-	Worldwide Interoperability for Microwave Access
www	-	World Wide Web
$Z_o$	-	Characteristic Impedance
$Z_L$	-	Load Impedance

# CHAPTER 1

## INTRODUCTION

### 1.1 Introduction to Antenna

Antenna is a specialized transducer that converts radio frequency (RF) signals into alternating current (AC) or vice versa. There are two basic types of antenna:

- (i) The transmitting antenna, which is fed with AC from electronic equipments and generates an RF field
- (ii) The receiving antenna, which intercepts RF energy and delivers AC to electronic equipment

Antenna is three dimensional and lives in a world of beam area, steradians, square degree, and solid angle. It has self and mutual impedances. Antenna also has polarizations: linear, elliptical, and circular.

All types of antenna have the same basic principle that radiation is produced by accelerated (or decelerated) charge. The basic equation of radiation can be expressed as [1]:

$$\dot{I} L = Qv \quad (\text{Ams}^{-1}) \quad (1.1)$$

where  $\dot{I}$  = time-changing current,  $\text{As}^{-1}$

$L$  = length of current element, m

$Q$  = charge, C

$v$  = time change of velocity which equals the acceleration of the charge,  $\text{ms}^{-2}$

## 1.2 Background and History of Antenna

Since decades ago, antennas have become increasingly important to our society until now they are indispensable. The evolution and development of antennas have a long and fascinating history that can be summarized as in Table 1.1.

Table 1.1 Evolution History of Antenna

Year/Time	History
1885	<ul style="list-style-type: none"><li>• Thomas Edison developed the first mobile communication with wireless telegraph between trains and stations</li></ul>
1886-1887	<ul style="list-style-type: none"><li>• Heinrich Hertz built the first radio antennas</li><li>• He assembled a complete radio system operating at meter wavelengths with an end-loaded dipole as the transmitting antenna and a resonant square-loop antenna as receiver</li></ul>
1898	<ul style="list-style-type: none"><li>• Guglielmo Marconi started the real mobile communication services with wireless telegraph on ships by using long wire antennas in various forms such as T, inverted L, and umbrella shapes</li></ul>
1903	<ul style="list-style-type: none"><li>• Guglielmo Marconi and a team of colleagues demonstrated trans-Atlantic wireless telegraphy</li></ul>
1909	<ul style="list-style-type: none"><li>• Radio operator Jack proved the usefulness of wireless telegraphy by sending out a maritime distress call</li></ul>
1916	<ul style="list-style-type: none"><li>• Engineers and scientists at the Naval Research Laboratory transmitted the first practical amplitude-modulated (AM) radio signal</li></ul>
1921	<ul style="list-style-type: none"><li>• Wire antennas were firmly established</li><li>• The age of international amateur communications arrived</li><li>• The national identifiers in call signs became necessary</li></ul>

1930	<ul style="list-style-type: none"><li>• Radio communications and broadcasting experienced rapid development as technology and techniques improved</li></ul>
World War II	<ul style="list-style-type: none"><li>• Centimeter wavelengths became popular and the entire radio spectrum opened up to wide usage</li><li>• World War II is the first war to be fought with extensive electronics</li><li>• British developed RADAR (radio detection and ranging)</li></ul>

### 1.3 Project Overview

The aim of this project is to design a broadband dual-frequency microstrip patch antenna with modified Sierpinski fractal geometry. Dual-frequency antennas are useful where integration of two services are required such as in mobile communication systems (GSM900, GSM1800, UMTS, PCS) where two bands cooperate having similar radiation performance, i.e., bandwidth, radiation pattern, gain, etc. [2].

The Sierpinski gasket antenna was the first example of multiband fractal shaped antenna. This multiband behavior stems from the self-similarity property that all fractal shapes share. The whole shape is constructed by clusters which are scaled down versions of the whole structure. However, in this project, the antenna design will be obtained through a perturbation of the classic Sierpinski fractal based on a reduction of the fractal iteration and a modification of the scale properties.

This project is a combination of research and design that focuses on a few sub-elements which are done in stages as follow:

- a) Research basic issues related to antenna
  - i. Search and collect information on numerous antenna types
  - ii. Study antenna property definitions, RF propagation characteristics, application of different antennas, antenna design fundamentals and considerations
- b) Study IEEE journal “Broad-Band Dual-Frequency Microstrip Patch Antenna With Modified Sierpinski Fractal Geometry” presented by Jaume Anguera [2]
  - i. Investigate the proposed dual-frequency antenna based on the Sierpinski fractal with two parasitic patches for impedance bandwidth enhancement

- ii. Study the proposed electrical circuit model formed by RLC resonators to learn about the antenna physical behaviors and to achieve the dual band operation minimizing a trial-and-error numerical/measurement proofs
- c) Design and simulate microstrip single patch antennas of various sizes
- i. Observe simulation results and interpret graphs obtained from simulations
  - ii. Compare the resonant frequencies from simulation with that from calculation
  - iii. Study the effect of antenna size on resonant frequency
- d) Design and simulate antennas based on the Classical and modified Sierpinski fractal geometries
- i. Design a fractal antenna based on the Classical Sierpinski geometry
  - ii. Design a broadband dual-frequency/multi-frequency fractal antenna with modified Sierpinski geometry and simulate the design by using Microwave Office 2002
  - iii. Adjust design parameters (i.e. dielectric constant and thickness) in order to obtain the desired frequency range, maximum bandwidth and radiation patterns for optimized performance
  - iv. Organize and arrange the simulation results systematically
  - v. Compare the results with that of [2] which has been done using a method of moment commercial code
  - vi. Make adjustments to get simulation results similar to [2] for performance optimization

## **1.4 Project Objectives**

The main objectives of this project are as follow:

- (i) To acquire an understanding of a wide variety of antennas and RF propagation fundamentals
- (ii) Investigate the characteristics and properties of microstrip patch antenna with Sierpinski fractal geometry and rooms for improvement and advancement
- (iii) Learn about antenna design fundamentals and considerations, parameters, and understand the basic performance trade-offs associated with antenna design
- (iv) Design and simulate a broadband dual-frequency/multi-frequency microstrip patch antenna with modified Sierpinski fractal geometry by using Microwave Office 2002
- (v) Analyze and compare the results of simulation with that obtained by the original researcher, Jaume Anguera in [2], focusing on the radiation patterns and attainable bandwidth

## 1.5 Design Methodology

The development of this project consists of seven main stages that are conducted systematically in two semesters. The methodology flow chart for this project is illustrated in Figure 1.1.

Since the purpose of the project is to design a broadband dual-frequency fractal antenna, it is useful to refine the goals in order to obtain an appropriate design methodology:

- (i) To show the potential for application to common technology, the antenna must be designed for operation at two useful frequency bands.
- (ii) Efforts should be made to design for radiation properties similar to those of common systems.
- (iii) To achieve the desirable compact property, the antenna must be designed to occupy a portion of space more efficiently than other antenna types.
- (iv) The advantages of fractal antenna with modified Sierpinski geometry must be proven. It must be shown that the antenna has broadband and dual-frequency behaviors.
- (v) Given the academic nature of the design project, the monetary budget is limited. The design must thus employ technology that is low in cost.

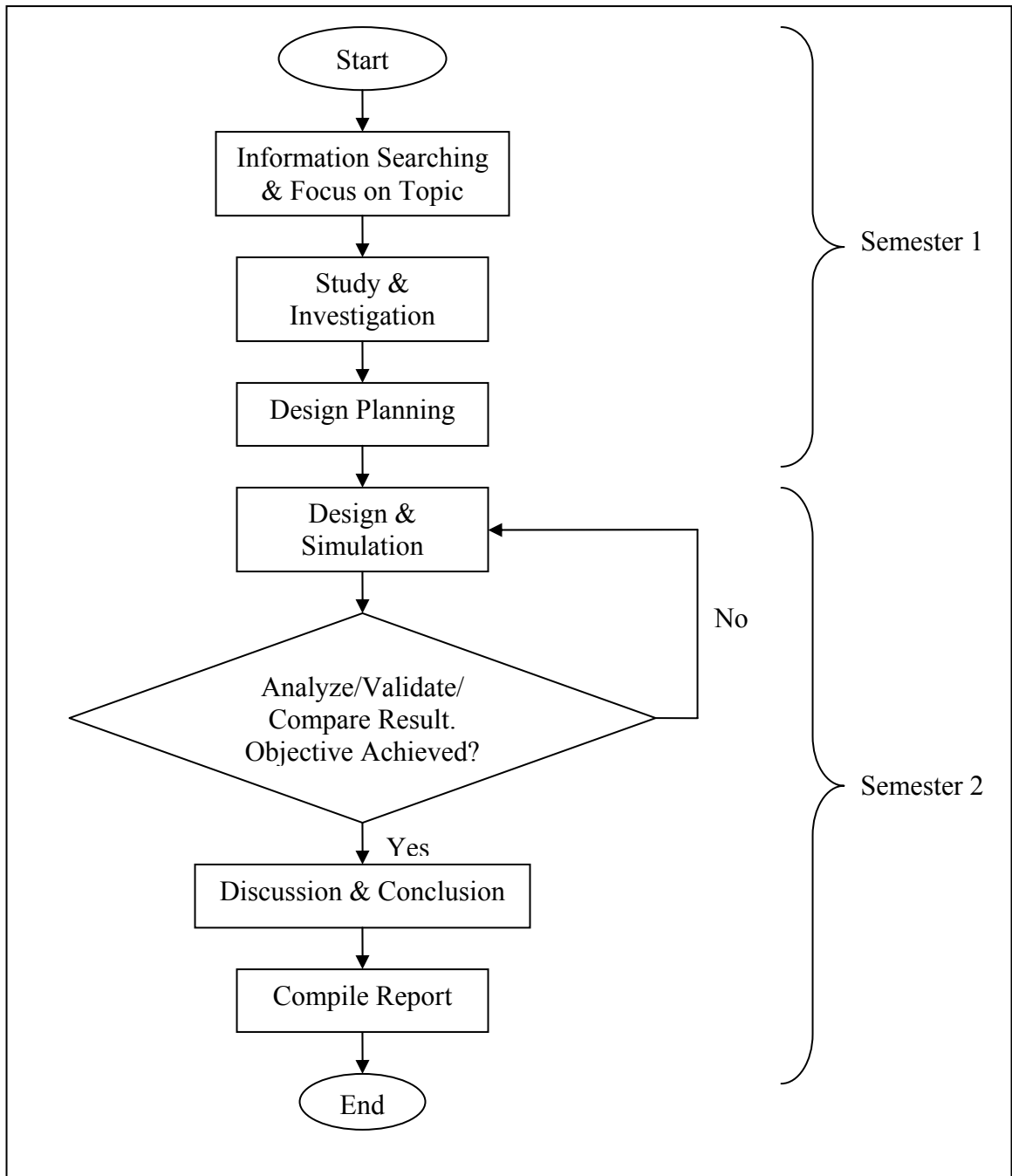


Figure 1.1 Project Methodology Flow Chart

### **1.5.1 Information Searching and Focus on Topic**

To begin with this project – Design of Broad-Band Dual-Frequency Microstrip Patch Antenna with Modified Sierpinski Fractal Geometry, the search and collect of information is essential. All the information for the purpose of this project is searched thoroughly from three main sources:

- (i) The World Wide Web (www)
- (ii) Journals
- (iii) Books

After the necessary information is collected, useful information for the topic of this project is marked and stored in relevant folders. With this, attention is focused on the main tasks of this project.

### **1.5.2 Study, Investigation, and Design Planning**

The information collected is studied and investigated thoroughly to come up with a design planning. The main areas of the study and investigation are as follow:

- (i) Various types of antenna and their characteristics
- (ii) Antenna design fundamentals and considerations, parameters, and basic performance trade-offs associated with antenna design
- (iii) Broad-band dual-frequency microstrip patch antenna based on the classical Sierpinski and modified Sierpinski fractal geometry
- (iv) Geometry drawing of triangular patch antenna by using Microwave Office 2002 simulation software

- (v) Determination of parameter values for antenna design and simulation in Microwave Office 2002
- (vi) Interpretation and analysis of graphs obtained from Microwave Office 2002 simulations
- (vii) Calculation algorithms and methods by using Mathcad v.12 software

## **1.6 Project Report Outlines**

This project report consists of six main chapters written in systematic order. As the introduction, Chapter 1 outlines a brief definition of antenna, as well as the history of antenna and its evolution. It also gives an overview of the project.

A literature review of the project is outlined in Chapter 2. This section explains about various types of antenna and propagation topics. It provides an understanding of basic antenna property definitions, antenna design fundamentals and consideration, and RF propagation characteristics. In addition, this chapter also covers fractal antenna design and its advantageous characteristics, with focus on Sierpinski geometry.

Chapter 3, with main focus on the project methodology, describes the stages involved in doing this project in a step-by-step approach. Here, different processes, starting from finding the required information until the completion of the antenna design will be explained in detail. Various methods used during the implementation of the project will be stated clearly.

Chapter 4 is the results and analysis part. It contains all the data resulting from antenna simulations by using Microwave Office 2002. The simulation results will be properly arranged in table form for the ease of tracking and analyzing. Each result will be accompanied by clear and precise analysis. Besides, the performance and characteristics of the antenna designed will be explained. Comparisons will be made between the simulation results in this project and the experimental results in journal [2].

Finally, Chapter 5 concludes all the works done during the implementation of the project. All the results will be finalized to draw a clear conclusion. Limitation and problems faced in this project will also be stated. This chapter will also outline recommendations on improving the antenna design and performance in the last section.

# CHAPTER 2

## LITERATURE REVIEW

### 2.1 Fundamentals of Antenna

#### 2.1.1 Electric Field

The electric field is produced by stationary electric charges. Whenever charges are located in proximity to each other in free space or a dielectric medium, an electric field exists throughout the medium, originating from the positive charge and terminating on the negative charge. Figure 2.1 shows the field lines for a positive point charge and a negative point charge. The field lines flow out of the positive charge and into the negative charge.

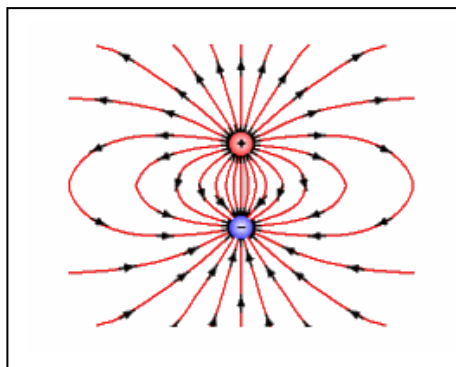


Figure 2.1 Electric Field Associated with Positive and Negative Charge [3]

The electric field strength is the amount of force exerted on a unit test charge and is equal to [4]:

$$E = \frac{F}{q} \quad (2.1)$$

where E = Electric field strength, V/m

F = force, N

q = test charge, C

### 2.1.2 Magnetic Field

The magnetic field is produced by moving electric charges. The magnetic field is the force on a moving charge, such as electron current flowing in a wire due to other moving charges. Whenever there is a net charge in motion in a specific direction, a magnetic field is established around that charge. Figure 2.2 shows the magnetic flux lines established around a wire with current flowing in the given direction. The direction of the magnetic field is perpendicular to the wire and is determined by the right-hand-rule. It is in the direction the fingers would curl when they are wrapped around the wire with the thumb in the direction of the current.

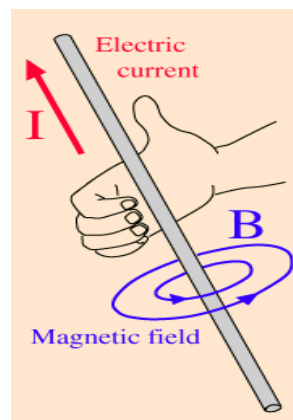


Figure 2.2 Magnetic Field Resulting From a Flowing Current [5]

The magnetic field strength is given by the following equation [4]:

$$H = \frac{m}{4\pi\mu r^2} \quad (2.2)$$

where H = magnetic field strength, A/m

m = magnetic charge, Wb

$\mu$  = permeability, H/m

r = distance to test pole, m

### 2.1.3 Electromagnetic Waves

Electromagnetic waves are the combination of electric and magnetic waves which propagate in a direction that is oriented at right angles to the vibrations of the electric (E) and magnetic (B) oscillating field vectors. Being the solutions to Maxwell's equations, electromagnetic waves transport energy from the radiation source to an undetermined final destination. The E and B fields are mutually perpendicular as shown in Figure 2.3 and vibrate in phase following the mathematical form of a sine wave through the space at the speed of light. The E and B fields are also perpendicular to the direction of wave propagation.

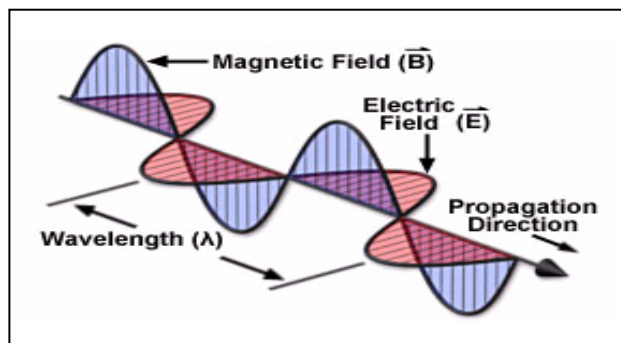


Figure 2.3 Electromagnetic Wave [6]

## 2.1.4 Basic Microwave System

Microwaves are desirable for communications and radar applications due to their high frequency and short wavelength. Ranging from 300MHz to 300GHz, the high frequency range of microwaves provides wide bandwidth capability. The range of frequency and wavelength occupied by microwaves are illustrated in Figure 2.4.

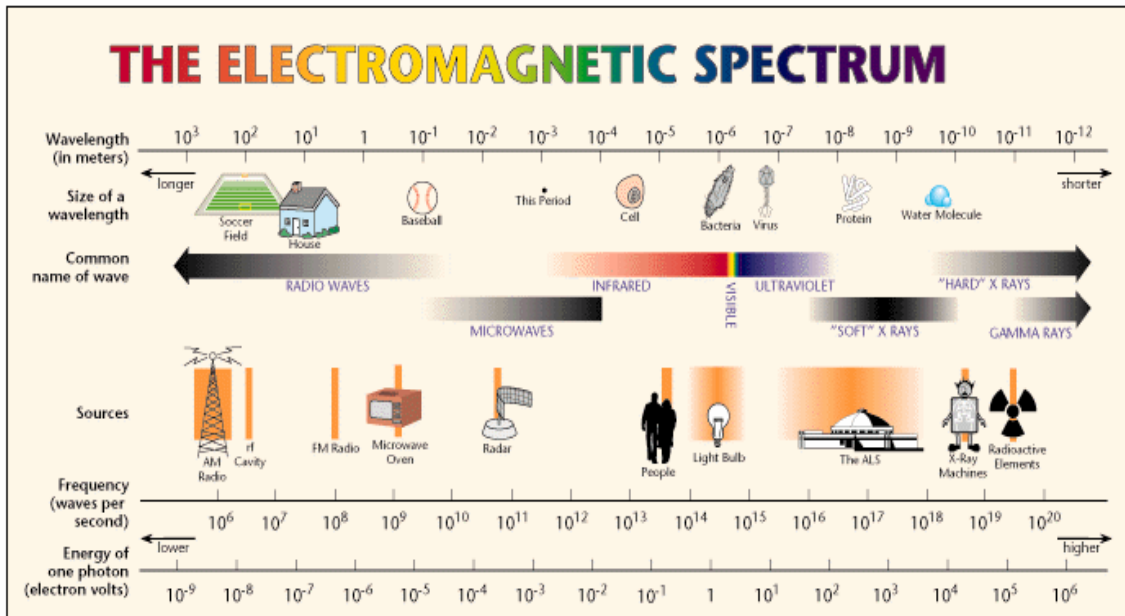


Figure 2.4 The Electromagnetic Spectrum [7]

The need to transmit and receive microwave signals makes antennas very important. Antennas are used as the first or last element in a system in which the antenna acts as a transducer between confined and unconfined electromagnetic energy. The block diagram of a basic microwave communication system is shown in Figure 2.5.

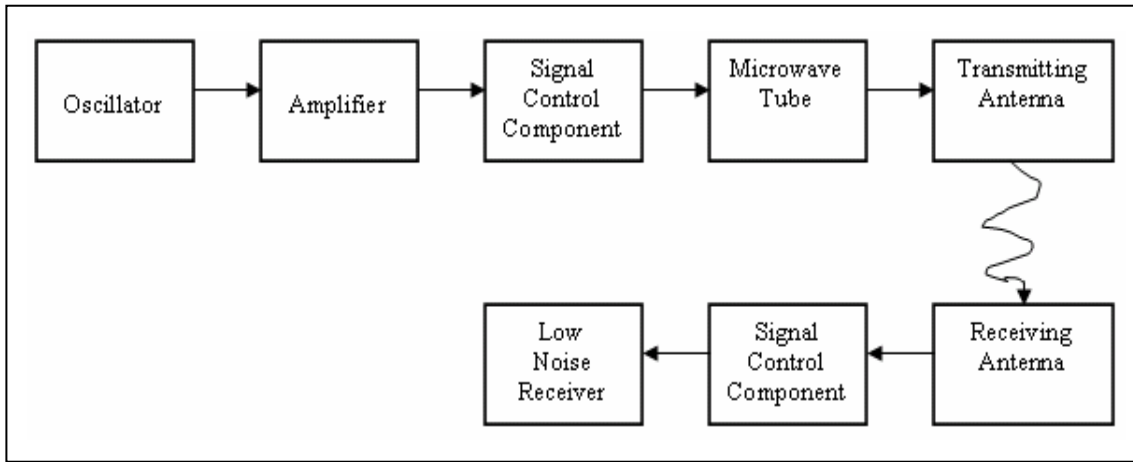


Figure 2.5 Basic Microwave Communication System

## **2.2 Antenna Design Parameters and Considerations**

Since the development and practical applications of log periodic and frequency independent antennas, a wide range of truly broadband antennas has been introduced to meet the varying demands imposed by specific requirements, such as area coverage and point-to-point circuits. Choosing the right type of antenna design for use in a specific link is very important if the best link performance is to be achieved. To differentiate among the various antennas available, an understanding of the basic parameters of antennas performance and the ways this information is presented is vital. The information of antenna parameters is also important for antenna design consideration in order to achieve the optimum outcome.

### **2.2.1 Radiation Pattern**

Radiation pattern of an antenna shows the power or field strength radiated in any direction relative to that in the direction of maximum radiation. All antennas have directional qualities. They do not radiate power equally in all directions. Therefore, antenna radiation patterns or plots are a very important tool to both the antenna designer and the end user [8].

The actual radiation pattern of an antenna is a three dimensional function. However, for the sake of simplicity, only cuts through the principles planes – the horizontal (azimuth) and vertical (elevation) planes are usually presented. Nowadays, many plotting formats or grids are in use. Rectangular grids as shown in Figure 2.6 and coordinate systems as shown in Figure 2.7 are in wide use. The principal objective is to

show a radiation plot that is representative of a complete  $360^\circ$  in either the azimuth or the elevation plane.

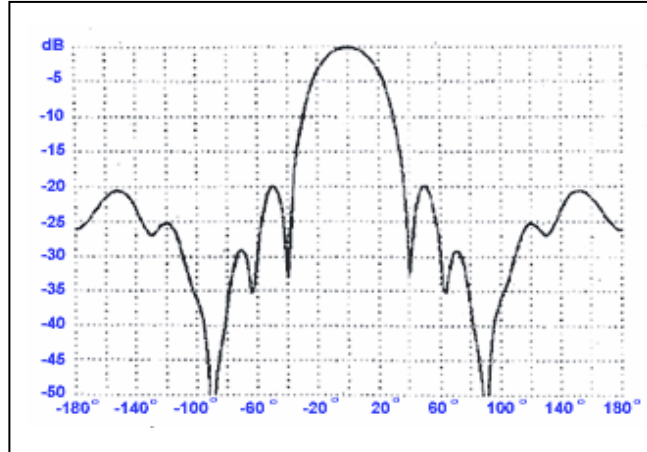


Figure 2.6 A Rectangular Azimuth Plot Presentation of a 10 Element Yagi Antenna [8]

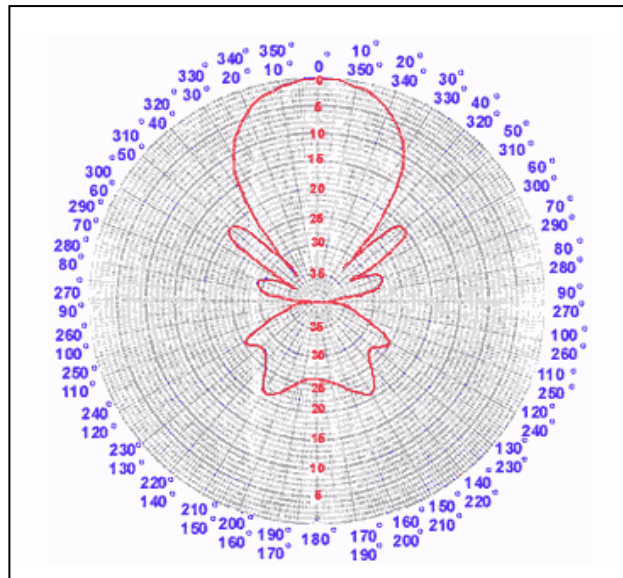


Figure 2.7 Polar Plot of a 10 Element Yagi Antenna [8]

For ease in use, clarity and maximum versatility, radiation plots are usually normalized to the outer edge of the coordinate system and expressed in dB (decibels) values. Antennas with high gain typically show side lobes in the radiation pattern. Side lobes are peaks in gain other than the main lobe. Side lobes cause undesirable impact to the antenna quality when the system is being used to determine the direction of a signal such as in radar systems. Figure 2.8 illustrates the main lobe and side lobe of a radiation pattern.

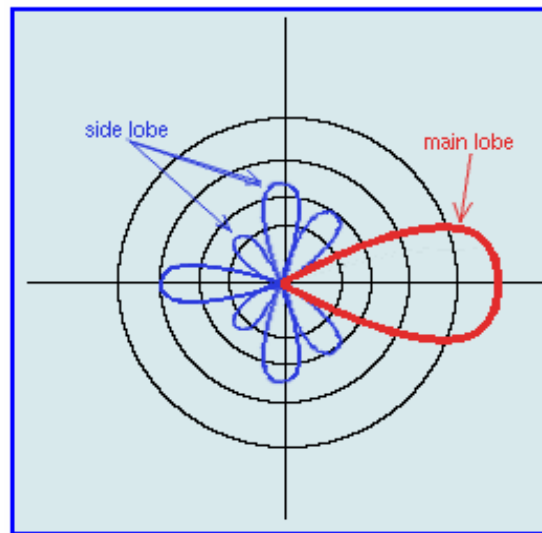


Figure 2.8 Main Lobe and Side Lobe in a Radiation Pattern [9]

### 2.2.2 Power Handling Capability

The power handling requirements coupled with the environment are instrumental factors in determining elements in antenna design. For example, if significant power levels are to be handled, then the choice of input connector, the separation between the feed points, the decision on whether to use waveguides or wire-type structures, and the avoidance of lossy materials are all important [10].

A trend exists towards increasing the transmitted power level in high frequency (HF) systems. This trend is not entirely unjustified in view of the usage of multi-channel or multimode transmission; the overall power capability of the transmission system must be sufficient to allow adequate power levels per channel [7]. Moreover, operation at high power levels increases reliability, especially in an emergency situation. Apart from cost, the main detraction from high power operation is the problem of interference. However, improvements in radiation pattern characteristics and frequency improvement have alleviated this situation.

### **2.2.3 Frequency Range and Bandwidth**

The frequency range and antenna bandwidth determine the antenna type because they relate wavelength directly to antenna size. Three categories of bandwidth classification exist:

- (i) Under half an octave
- (ii) On the order of half an octave
- (iii) Greater than an octave

To meet under half an octave requirement, the antenna structure is generally tuned to achieve optimum performance over the band. On the order of half an octave, the structure should be optimized to achieve the best average over-the-band performance. For requirements greater than an octave, frequency-independent antenna is generally used.

It is generally desirable to incorporate maximum bandwidth capability to prolong the operational lifetime of the antenna system. The logarithmically periodic antenna and the application of the “angle condition” (such as conical and equi-angular antennas) have been the principle developments in the field of broadband high performance antennas over the past few decades [7].

#### **2.2.4 Power Gain**

An antenna has gain if it radiates more strongly in one direction than in another. Gain is measured by comparing an antenna to a model antenna, typically the isotropic antenna which radiates equally in all directions [9]. Power gain indicates how well the radiated energy is directed through a selected surface area on the spherical surface enclosing the antenna. Gain is one-dimensional.

Antennas can be categorized into low, medium, and high gain. Maximum input power is determined by the following factors:

- (i) Dielectric losses causing overheating of insulators
- (ii) Ohmic losses caused by conductors carrying large currents
- (iii) Corona discharge from insulators, element tips or other parts

#### **2.2.5 Polarization**

Polarization refers to the electric field vector of a propagating electromagnetic wave. Horizontally polarized antennas are more versatile than vertically polarized antennas to some extent, as the elevation plane radiation pattern can be readily varied to

suit the path requirements by altering the height of the radiator above the ground plane. On the other hand, vertically polarized antennas tend to have maximum radiation at lower angles in theory towards the horizon when the ground is perfectly conducting. Elliptical polarization is a combination of the two fundamental planes. The ellipticity is determined by the ratio of horizontal to vertical components. If both are equal, the resultant wave would be circular.

### **2.2.6 Beamwidth**

A further characteristic of radiation pattern performance is the beamwidth, or properly the half power beamwidth. Beamwidth is the angle between the points on either side of the direction of maximum radiation at which the intensity of power radiated has fallen to half the maximum value [7]. Specifying the beamwidth as  $\pm$  degrees removes any ambiguity at times.

### **2.2.7 Coverage**

The coverage requirement uniquely classifies the antennas. As the spatial coverage decreases, the antenna's electrical size must increase [10]. For frequency-independent antenna such as fractal antenna, the antenna's structural pattern is repeated. Hence, for any particular frequency in the band, three to five elements are effective. As the frequency is moved to another value, the three to five elements are again effective and electrically identical to the first set of elements. This behavior pattern is repeated over and over to cover the full band, giving full band coverage.

### **2.2.8 Input Impedance**

The ability of an antenna to accept power from a source (such as an amplifier) is determined by the input impedance of the antenna. For maximum power transfer, the input impedance should exactly match the output impedance of the source.

As an electric wave travels through different parts of an antenna system (such as radio, feed line, antenna, free space) it may encounter differences in impedance. At each interface, some fraction of the wave's energy will reflect back to the source, thus forming a standing wave in the feed line. The ratio of maximum power to minimum power in the wave is called the standing wave ratio (SWR). SWR is measurable. A SWR of 1:1 is ideal. A SWR of 1.5:1 is considered to be marginally acceptable in low power applications where power loss occurs more critically. However, SWR of 6:1 may still be usable with the right choice of equipment. Minimizing impedance differences at each interface can reduce SWR and maximize power transfer through each part of the antenna system.

### **2.3 Microwave Transmission Line**

As the frequency of antenna application increases to the microwave region (typically with wavelengths from 1 meter to 1 millimeter), low frequency circuit theory analysis where resistance (R), capacitance (C), conductance (G) and inductance (L) are represented as lumped constant elements cannot be used. In the microwave frequency range, power is considered to be contained in electric and magnetic fields that are guided from place to place by transmission line. In this case, transmission line theory is used where the R, C, G, and L of microwave transmission lines are considered distributed parameters. Hence, the microwave transmission line is a distributed element circuit. In transmission-line theory, the magnitude and phase of voltage and current along a transmission line can vary as a function of position. The electrical length of the microwave transmission line is a function of the physical length and the velocity of propagation.

Many different types of microwave transmission lines have been developed over the years. In an evolutionary sequence from rigid rectangular and circular waveguide, to flexible coaxial cable, to planar stripline to microstrip line, microwave transmission lines have been reduced in size and complexity. The microstrip transmission line is the technology employed in the current hyperthermia applicator studied [11]. For fields having a sinusoidal time dependence and steady-state conditions, a field analysis of a terminated lossless transmission line results in the relations illustrated in Figure 2.9.

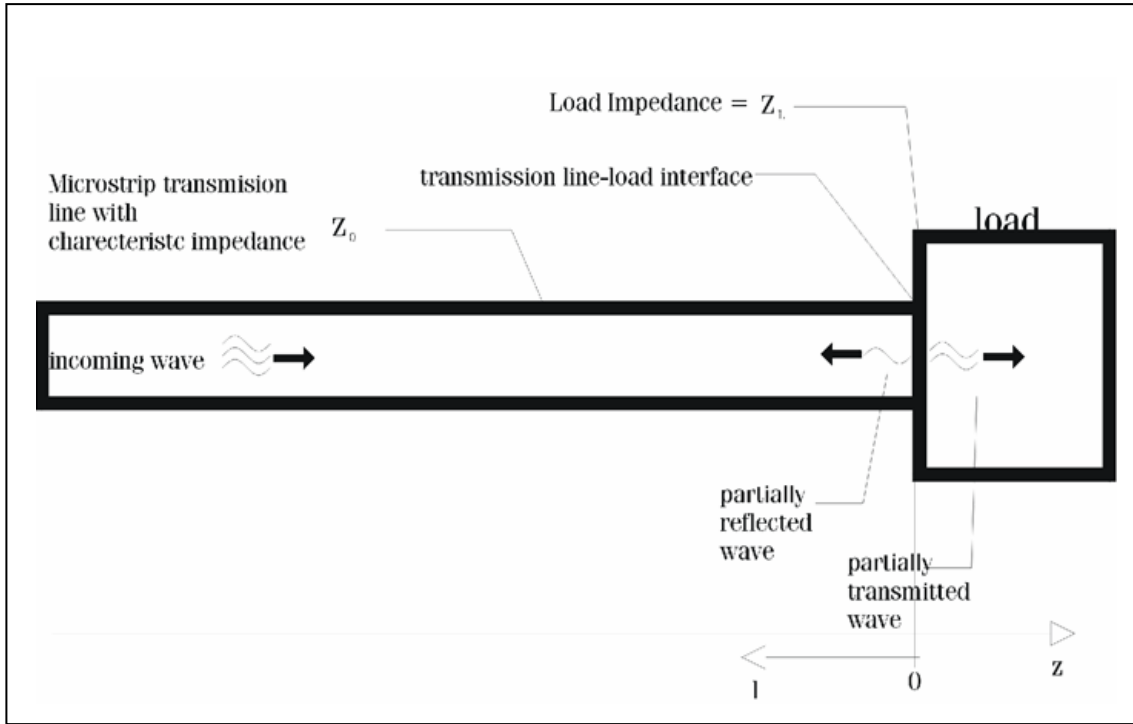


Figure 2.9 Diagram of Lossless Transmission Line with Load Showing Incident, Reflected-Transmitted Waves [11]

## **2.4 Types of Antenna**

An antenna is a transducer that transforms a high frequency electric current into radio waves and vice versa. An antenna is used to transmit and receive radio waves. There are numerous types of antenna, ranging from very small size (such as a monopoly antenna in a cordless telephone) to very large antenna reflectors of 100 meters in diameter for radio wave astronomy. Antennas can be classified in many different ways such as in frequency band of operation, physical structure, electrical/electromagnetic design, sizes, and shapes. Some common antenna types are elaborated in the following sections.

### **2.4.1 Dipole Antenna**

The dipole antenna consists of two wire feedlines pointed in opposite directions arranged either horizontally or vertically. Each feedline of the antenna extends at right angles for one quarter of wavelength, making the total length of the antenna to be half a wavelength. Thus, this type of antenna is also called halfwave dipole antenna. This length is chosen so that the dipole resonates at the operating wavelength. The resulting current and voltage pattern of a halfwave dipole antenna is illustrated in Figure 2.10.

Dipole is the common antenna building block for low frequency antennas, including AM and FM radio transmitting and receiving antennas, television transmitting and receiving antennas, and mobile radio antennas [12]. Variations of the dipole include the folded dipole and the whip antenna. Generally, the dipole is considered to be omnidirectional in the plane perpendicular to the axis of the antenna, but it has deep

nulls in the directions of the axis. Figure 2.11 shows the power pattern of the halfwave dipole.

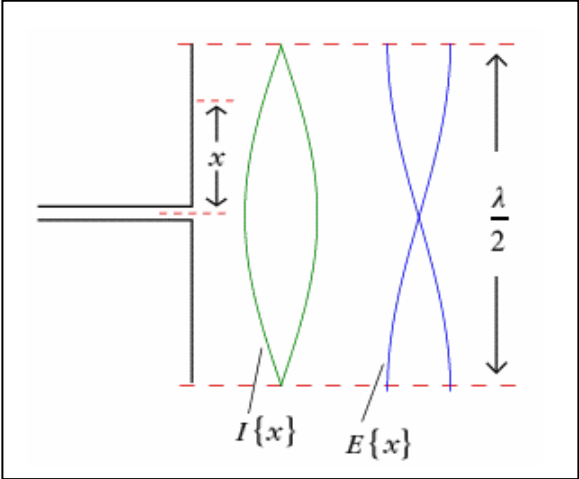


Figure 2.10 Current and Voltage Distribution on a Halfwave Dipole [13]

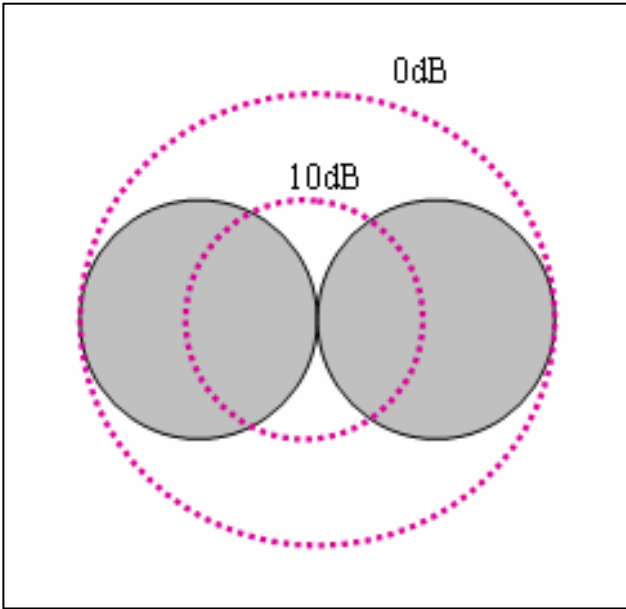


Figure 2.11 Power Pattern of a Halfwave Dipole

### 2.4.2 Horn Antenna

A horn antenna is formed as an extension of a waveguide, where one or both dimensions of the waveguide are tapered so that the microwave power can be transitioned from the waveguide into the radiating horn without mismatch. Figure 2.12 illustrates a horn antenna, showing that antenna resembles an acoustic horn and is usually fed with a waveguide.

Horn antennas come in different shapes, such as the conical horn, rectangular horn, and square horn. Normally, horn antennas are limited to approximately 20dB of gain, as the gain of horn antenna depends on the ratio of the horn opening to the square of the wavelength. Therefore, if the horn opening is increased significantly to get a large gain, the length of the horn becomes excessive. A good solution for higher gain requirements is to feed the horn antenna with a parabolic reflecting dish. The horn is pointed toward the center of the dish reflector. The use of a horn, rather than a dipole antenna or any other type of antenna, at the focal point of the dish minimizes loss of energy (leakage) around the edges of the dish reflector. It also minimizes the response of the antenna to unwanted signals not in the favored direction of the dish [14].

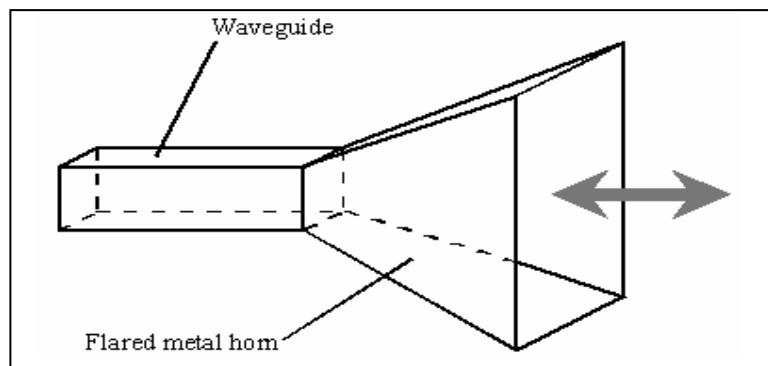


Figure 2.12 Horn Antenna [14]

### 2.4.3 Yagi Antenna

Yagi antenna design uses passive elements. It is inexpensive and effective. It can be constructed with one or two reflector elements and one or more director elements. Figure 2.13 illustrates a Yagi antenna with one reflector, a folded-dipole active element, and seven directors mounted for horizontal polarization.



Figure 2.13 A Typical Multiple Elements Yagi Antenna [15]

The typical horizontal plane pattern for a three-element (one reflector, one active element, and one director) Yagi antenna is shown in Figure 2.14. In general, the more elements a Yagi has, the higher the gain, and the narrower the beamwidth. Yagi antenna can be mounted to support either horizontal or vertical polarization. It is often used for point-to-point applications, such as between a base station and repeater-station sites.

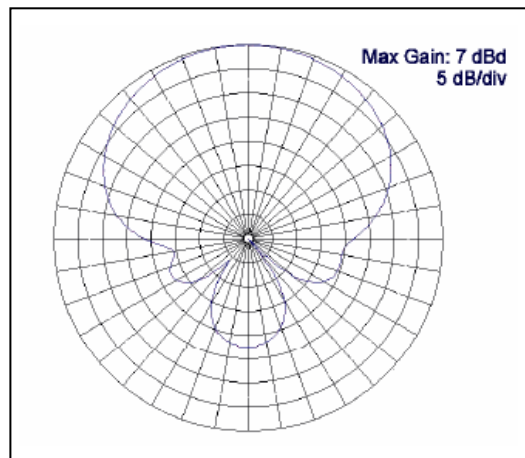


Figure 2.14 Horizontal Plane Pattern of a Yagi Antenna [15]

#### 2.4.4 Log-Periodic Antenna

Log-periodic antenna is usually constructed so the antenna terminals are located at the front (on the shortest dipole). Log-periodic antenna is directional and it possesses many similarities to the Yagi antenna as it exhibits forward gain and has a significant front to back ratio. The log periodic antenna exists in a number of forms. The most common is the log periodic dipole array (LPDA) as shown in Figure 2.15.



Figure 2.15 The Typical Log-Periodic Antenna [15]

The main characteristics of the log-periodic antenna are its broadband nature and its relatively high front-to-back gain ratio. The latter feature is proven in the typical radiation pattern shown in Figure 2.16. The log-periodic antenna can be used in a number of applications where a wide bandwidth is required along with directivity and modest level of gain. Sometimes, it is utilized on the high frequency (HF) portion of the spectrum where operation is required on a number of frequencies to enable communication to be maintained.

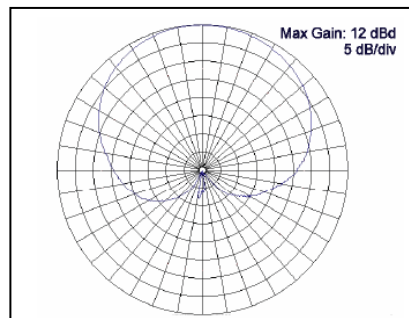


Figure 2.16 Horizontal Plane Pattern of Log-Periodic Antenna [15]

### 2.4.5 Loop Antenna

The loop antenna is an antenna primarily for the amplitude modulation (AM) broadcast. There are two different types of loop antennas, one is the ferrite bar (as in the AM radio), the other is wound on an air core form. A loop antenna is very directional. The loop will allow signals on opposite sides to be received, while off the sides of the loop the signal will decrease or be nulled out. Air core loop antennas come in many sizes. The larger the loop the more gain there is [16].

The magnetic loop antenna is an efficient short wave antenna. Consisting of a loop radiator made of copper or aluminium tubing and a tuning capacitor, the diameter of the loop is in the range of 1/10 to 1/100 of the wavelength. Figure 2.17 shows a magnetic loop antenna. Loop antenna works with the magnetic component of the electromagnetic field, which extends to both the electromagnetic components on larger distance.



Figure 2.17 Magnetic Loop Antenna [17]

### 2.4.6 Helical Antenna

Helical antenna consists of a conducting wire coiled in the form of a helix or spiral. The direction of the coil determines its polarization whereas the space and diameter between the coils determine its wavelength. Figure 2.18 shows three variations of helix antenna.

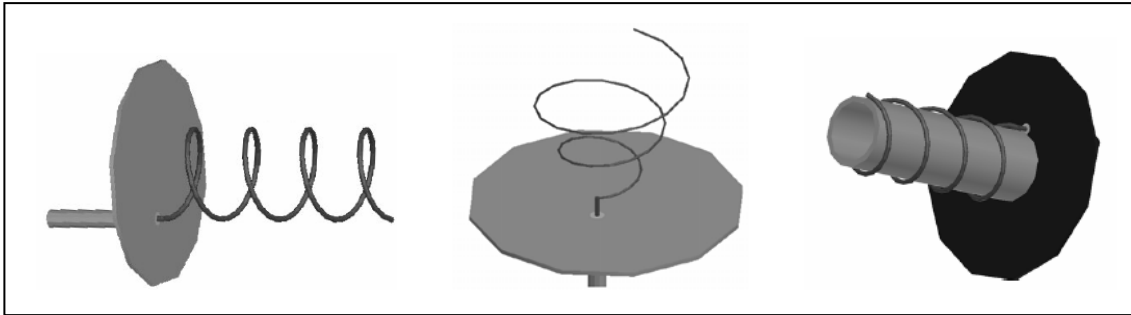


Figure 2.18 Variations of Helix Antenna [18]

Helical antennas can operate in normal (broadside) mode or axial (endfire) mode. In normal mode, the dimensions of the helix are relatively small if compared to the wavelength. The far field radiation pattern is similar to an electrically short dipole or monopole. In axial mode, helical antenna produces circular polarization which is best suited for space communications where the polarization of signal may vary.

Helical antennas can have clockwise (right-handed) or counter-clockwise (left-handed) polarization. Signals with any type of polarization such as horizontal or vertical polarization, can be received by helical antennas. However, clockwise polarized antennas suffer severe gain loss when receiving counter-clockwise signals, and vice versa.

### 2.4.7 Microstrip Antenna

Microstrip antennas are also known as printed antennas. There are several types of microstrip antennas in which the most common one is the patch antenna. A patch antenna is a narrowband, wide-beam antenna fabricated by etching the antenna element pattern in metal trace bonded to an insulating substrate [19]. Figure 2.19 shows an aperture-coupled patch antenna.

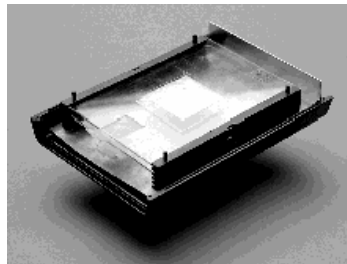


Figure 2.19 Aperture-Coupled Patch Antenna [20]

Patch antennas incorporate the ability to have polarization diversity. With a single feedpoint, patch antennas can easily be designed to have vertical, horizontal, right hand circular (RHCP) or left hand circular (LHCP) polarizations. This unique property allows patch antennas to be used in many areas of communication links with varied requirements. Patch antennas have a very low profile, are mechanically rugged and can be conformable. Hence, they are often mounted on the exterior of aircraft and spacecraft, and are incorporated into mobile radio communications devices.

Microstrip antennas are relatively inexpensive to manufacture and design due to the simple 2-dimensional physical geometry. They are usually utilized at ultra-high frequency (UHF) and higher frequencies because the size of the antenna is directly tied to the wavelength at the resonant frequency.

### 2.4.8 Corner-Reflector Antenna

The corner reflector antenna as illustrated in Figure 2.20 consists of one or more dipole elements in front of a corner reflector.

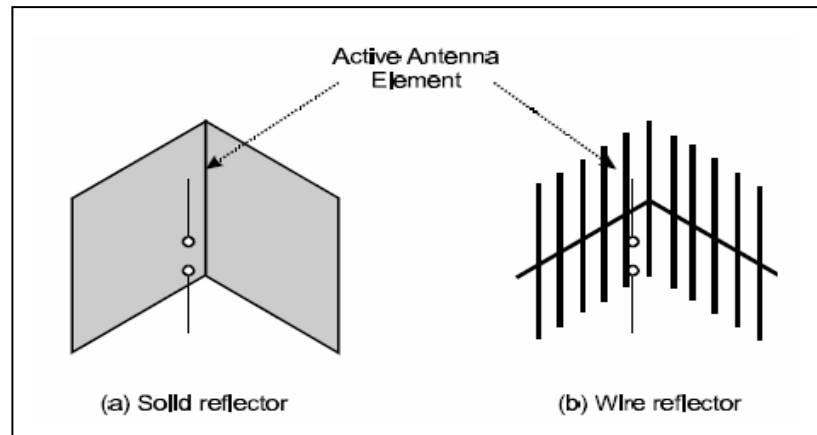


Figure 2.20 Corner-Reflector Antennas [15]

The corner-reflector antenna has moderately high gain. Its forward (main beam) gain, called the front-to-back ratio is much greater than the gain in the opposite direction. This important pattern feature of the corner-reflector antenna is shown in the horizontal plane pattern in Figure 2.21.

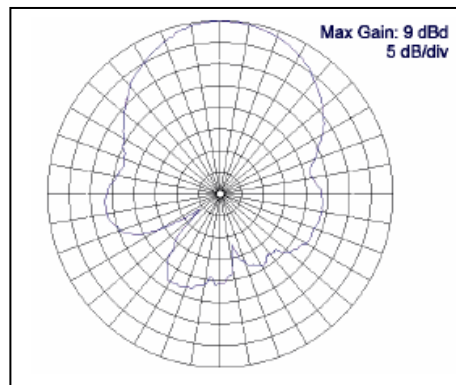


Figure 2.21 Horizontal Plane Pattern of Corner-Reflector Antenna [15]

### 2.4.9 Array Antenna

An array antenna consists of several elements interconnected and arranged in a regular structure to form an individual antenna. Nowadays, many antennas are formed of arrays of various antenna elements. Array antennas exhibit higher gain, larger receiving areas, and greater bandwidth than individual elements would do.



Figure 2.22 A Typical Vertical Array Using Folded Dipoles [15]

A stacked dipole array, as shown in Figure 2.22, is comprised of vertical dipole elements. Having an omnidirectional pattern like the element dipole does, this dipole array has higher gain and a narrower main lobe beamwidth in the vertical plane. Figure 2.23 shows how the vertical-plane gain of the dipole element can be enhanced and improved by making an array of them.

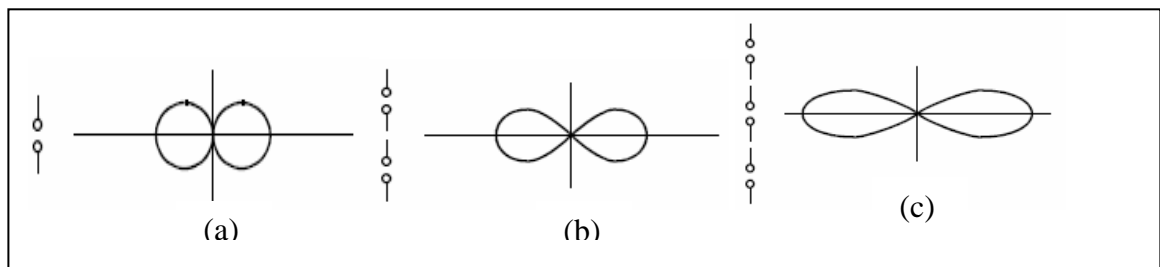


Figure 2.23 Vertical-Plane Radiation Patterns: (a) Single Half-Wave Dipole, (b) Two-Element Array, and (c) Three-Element Array [15]

#### 2.4.10 Parabolic Dish

The parabolic dish is the most common type of microwave antenna. A satellite dish is a type of parabolic antenna designed for transmitting signals to and/or receiving from satellites. Parabolic dishes come in varying sizes and designs, and are most commonly used to receive satellite television. Figure 2.24 shows a parabolic dish antenna.



Figure 2.24 Parabolic Dish Antenna [21]

The parabolic antenna consists of an antenna feed, which radiates its power into a parabolic-shaped reflecting surface. The parabolic reflector concentrates the microwave power back along the antenna axis. The parabolic shape has the unique property that all rays from the feed to any point on the parabolic surface travel an equal length from the feed to a plane at right angles to the direction of propagation. This feature gives the parabolic reflecting surface its focusing characteristics and allows it to concentrate the microwave power from the feed horn along the antenna axis. The gain, receiving area, and beamwidth are determined by the parabolic reflector. Antenna polarization and bandwidth are determined by the feed [12].

### 2.4.11 Smart Antenna

A smart antenna is an array of antenna elements connected to a digital signal processor as shown in Figure 2.25. Such configuration dramatically enhances the capacity of a wireless link through a combination of diversity gain, array gain, and interference suppression [22]. This increased capacity results in higher data rates for more users for a given data rate per user.

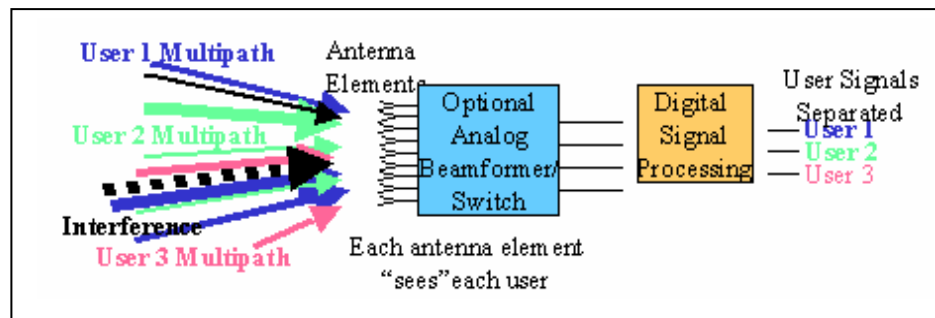


Figure 2.25 Configuration of Smart Antenna [22]

There are two basic types of smart antennas. The first type is the phased array or multibeam antenna, which consists of either a number of fixed beams with one beam turned on towards the desired signal or a single beam (formed by phase adjustment only) that is steered toward the desired signal. The other type is the adaptive antenna array, which is an array of multiple antenna elements, with the received signals weighted and combined to maximize the desired signal to interference plus noise power ratio. This essentially puts a main beam in the direction of the desired signal and nulls in the direction of the interference. A smart antenna is therefore a phased or adaptive array that adjusts to the environment. That is, for the adaptive array, the beam pattern changes as the desired user and the interference move; and for the phased array the beam is steered or different beams are selected as the desired user moves [23].

## **2.5 Fractal Antenna**

### **2.5.1 Definition of Fractal Antenna**

A fractal antenna is an antenna that uses a fractal design to maximize the length of material that transmits or receives electromagnetic signals within a given total surface area. Due to this reason, fractal antennas are very compact and hence are anticipated to have useful applications in cellular telephone and microwave communications.

Fractal antenna's response differs markedly from traditional antenna designs, in the sense that it is capable of operating optimally at many different frequency ranges simultaneously. This makes the fractal antenna an excellent design for broadband applications.

### **2.5.2 Fractal Theory**

A fractal is a geometrical shape or pattern constructed of identical parts, which are in turn identical to the overall pattern. A fractal possesses self-similar structure that occurs at different levels of magnification. A fractal can be generated by a repeating pattern, in a typically recursive or iterative process.

Fractals of many kinds were originally studied as mathematical objects. Fractal geometry is the branch of mathematics which studies the properties and behaviour of fractals. It describes many situations which cannot be explained easily by classical geometry, and has often been applied in science, technology, and computer-generated

art. The conceptual roots of fractals can be traced to attempts to measure the size of objects for which traditional definitions based on Euclidean geometry or calculus fail [24].

### 2.5.3 Fractal Geometry

Over the years, various fractal geometries have been developed by mathematicians and scientists. Some common types of fractal geometry (in which some are used for antenna design) are illustrated and explained in the following sections.

#### 2.5.3.1 Sierpinski Gasket

The Sierpinski gasket is recursively constructed by starting with a solid equilateral triangle and removing the inner triangle formed by its three midpoints, as shown in Figure 2.26. Now there are three smaller triangles. The process is continued by removing the smaller triangle formed in each by connecting its midpoints. Then, the nine resulting smaller triangles are cut in the same way, and so on, indefinitely.

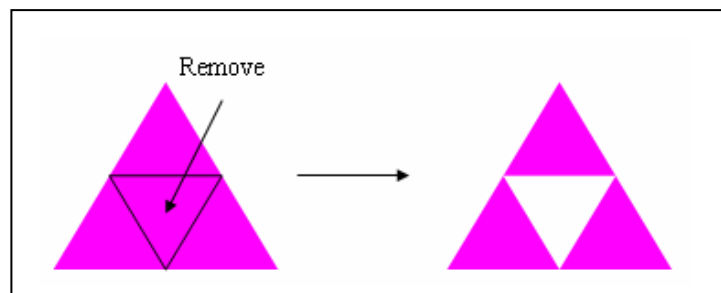


Figure 2.26 Removal of Inner Triangle to Form Sierpinski Gasket

Figure 2.27 shows the number of iteration along with the resulting Sierpinski gasket geometry. The gasket is perfectly self similar, an attribute of many fractal images. Any triangular portion is an exact replica of the whole gasket.

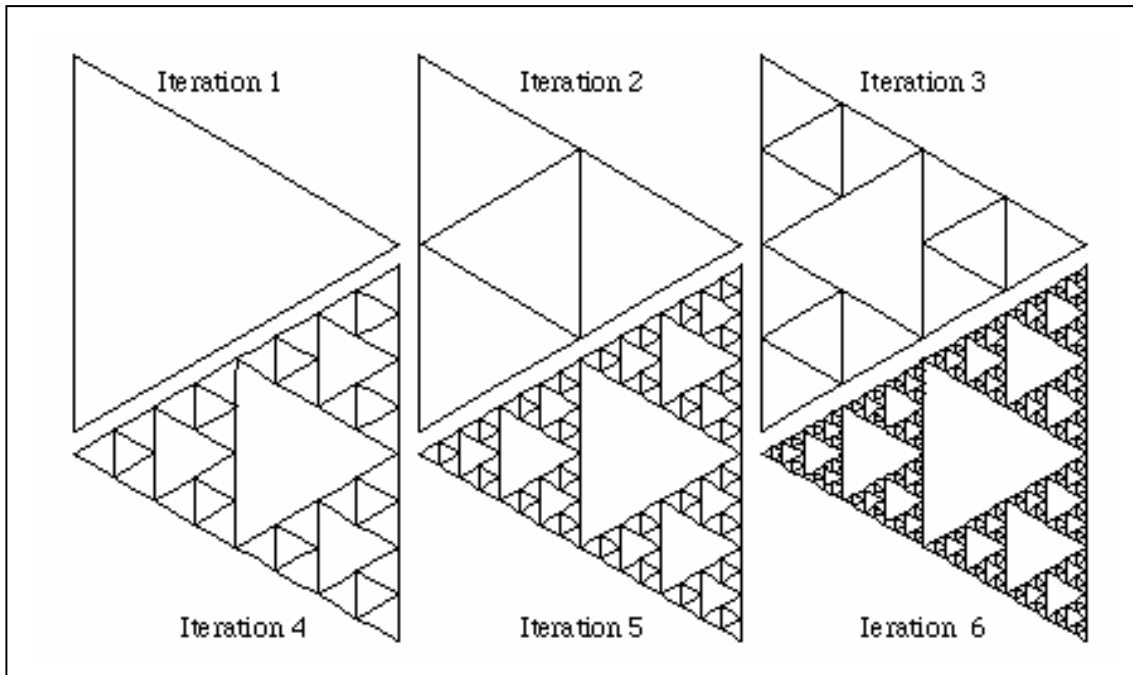


Figure 2.27 Sierpinski Gasket with Different Numbers of Iteration [25]

### 2.5.3.2 Sierpinski Carpet

As shown in Figure 2.28, Sierpinski carpet can be constructed by starting with a solid (filled) square  $C(0)$  and divide it into 9 smaller congruent squares. The interior of the center square is removed to get  $C(1)$ . Then, each of the eight remaining solid squares is subdivided into 9 congruent squares and the center square from each is removed to obtain  $C(2)$ . The construction is repeated to obtain a decreasing sequence of sets

$$C(0) \supseteq C(1) \supseteq C(2) \supseteq C(3) \supseteq \dots$$

The Sierpinski carpet is the intersection of all the sets in this sequence, that is, the set of points that remain after the construction is repeated infinitely. Figure 2.28 shows the first four iterations. The squares in red denote some of the smaller congruent squares used in the construction.

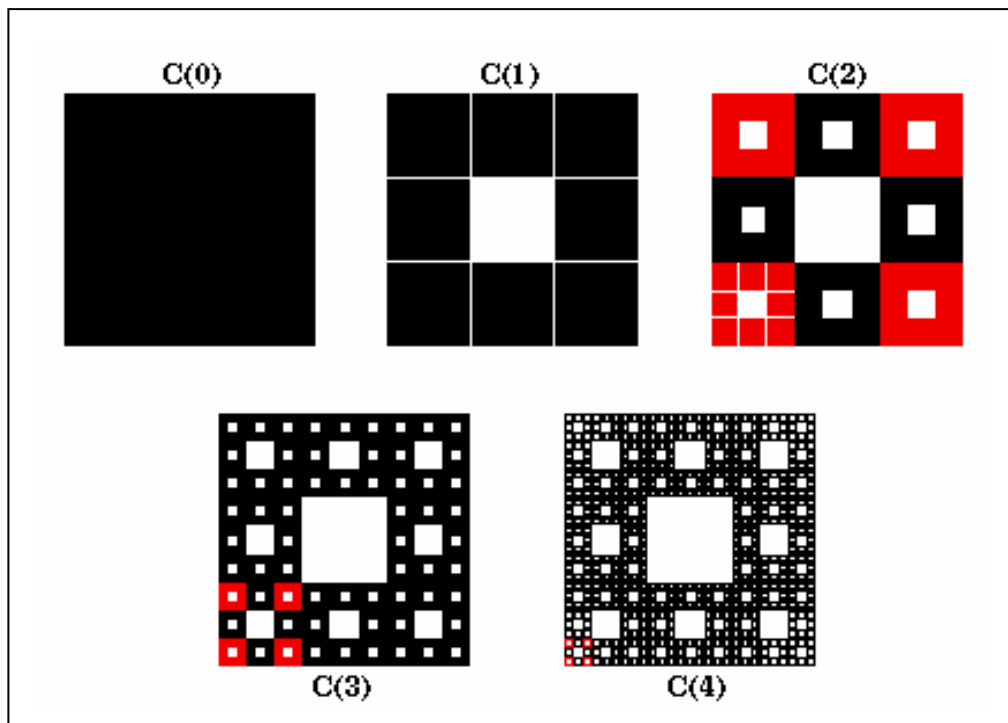


Figure 2.28 First Four Iterations of Sierpinski Carpet [26]

### 2.5.3.3 Koch Curve

A Koch curve is constructed by starting with a straight line. The line is then divided into three equal segments and the middle segment is replaced by the two sides of an equilateral triangle of the same length as the segment being removed. Then the process is repeated, taking each of the four resulting segments, dividing them into three equal parts and replacing each of the middle segments by two sides of an equilateral triangle. The process of Koch curve construction is shown in Figure 2.29.

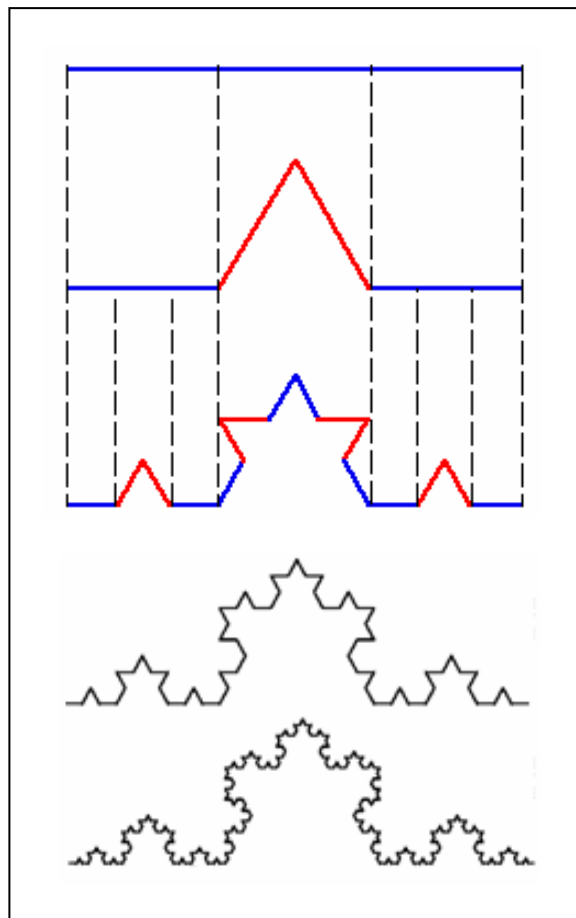


Figure 2.29 Construction of Koch Curve [27]

### 2.5.3.4 Koch Snowflake

The basic unit of the Koch snowflake is the equilateral triangle which can be built up into a much larger but still similar pattern. Koch snowflake is constructed by starting with an equilateral triangle. The equilateral triangle is scaled by a factor of  $1/3$  and 3 copies are placed along each of the three sides of the equilateral triangle 1 as illustrated in Figure 2.30 to form a new image 2. Next, the equilateral triangle is scaled by a factor of  $1/9=(1/3)^2$  and  $12=4 \times 3$  copies are placed along the sides of 2 as illustrated to form the image 3. For the next iteration,  $48=4 \times 12$  copies of 1 scaled by a factor of  $1/27=(1/3)^3$  are taken and placed around the sides of 3 to form the image 4. The construction is continued on.

As shown in Figure 2.30, any part of the snowflake is equally crinkly, whatever scale it is viewed at [28].

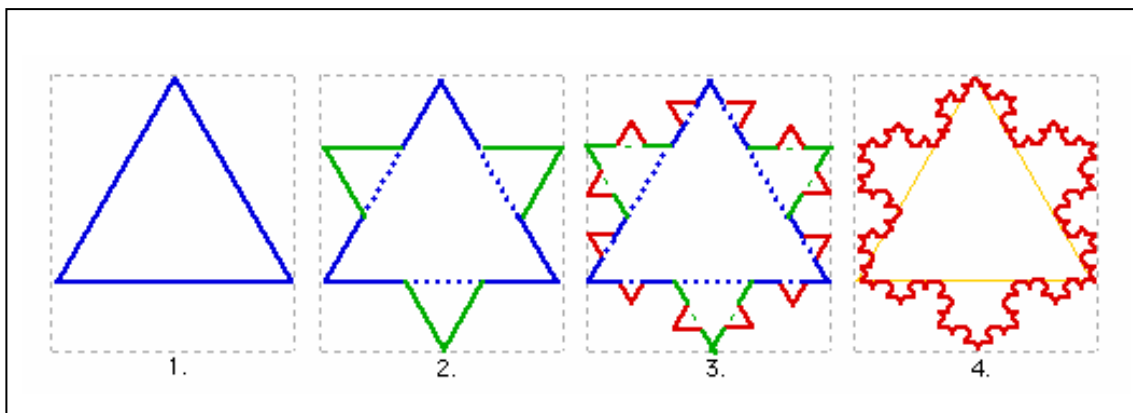


Figure 2.30 Koch Snowflake [28]

## **2.5.4 Advantageous Characteristics of Fractal Antenna**

### **2.5.4.1 Miniaturization and Space-Filling**

A fractal can fill the space occupied by an antenna in a more effective manner than other traditional antennas. This leads to more effective coupling of energy from feeding transmission lines to free space in less volume. The space filling and miniaturization properties of fractal lead to curves that are electrically very long, but fit into a compact physical space.

### **2.5.4.2 Multiband Performance**

To achieve frequency-independent characteristic, an antenna must be designed to have no characteristic size, or include many characteristic sizes for it to operate over many different frequency bands. Fractal structures with no characteristic size and possess self-similar geometry shape consisting of multiple copies of themselves on various different scales have the potential to be frequency-independent or multi-frequency antennas. For example, a bow-tie antenna based on the Sierpinski gasket can operate over different frequency bands that can be chosen by modifying the structure.

### **2.5.4.3 Input Impedance Matching**

Generally, small antennas are poor radiators with small input impedance and significant negative input reactance, resulting in difficulty and high expenses to match the antenna input impedance with a matching network. However, small fractal antennas have greater input resistance and smaller input reactance than small traditional antennas

[30]. Fractal antennas can even resonate with a size much smaller than other traditional antennas. Therefore, the cost associated with input impedance matching can be reduced.

#### 2.5.4.4 Efficiency and Effectiveness

Fractal antennas are convoluted. Uneven shapes, sharp edges, corners, and discontinuities of a fractal structure enhance radiation of electromagnetic energy from electric systems more efficiently. For example, it has been proven that a monopole Koch fractal curve is more efficient and effective than an ordinary monopole of the same size.

#### 2.5.4.5 Improved Directivity

The directivity of an antenna can be improved by shaping the antenna in fractal geometry. It has been shown that Vee dipoles with their arms replaced by the Koch fractal curve can outperform the conventional Vee dipole in terms of directivity and small side-lobes, as illustrated in Figure 2.31.

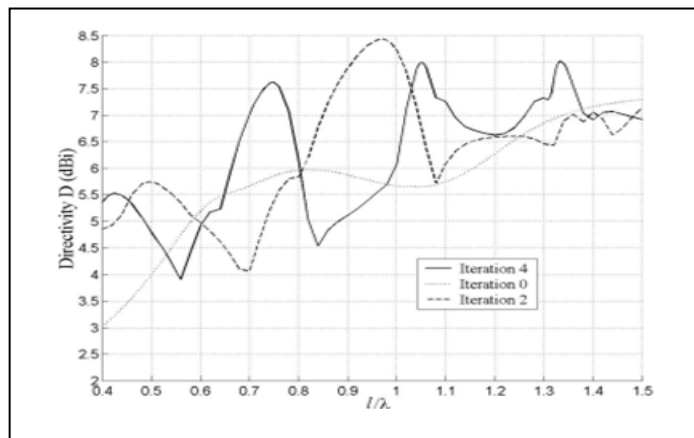


Figure 2.31 Directivity Versus Projected Arm Length for a Koch Fractal-Vee Dipole at Different Fractal Iterations [29]

## **2.5.5 Fractal Antenna Applications**

### **2.5.5.1 Mobile Devices**

Nowadays, wireless devices ranging from PDAs to cellular phones to mobile computing require high-performance multiband antennas. Fractal antennas are available in multiband and wideband configurations, allowing them to operate effectively with all existing and future wireless communication standards. Along with frequency versatility and excellent gain, fractal antennas are also small enough to be embedded into virtually any device on the market [30].

### **2.5.5.2 Radio Frequency Identification (RFID)**

Fractal antennas provide compact, low-cost performance solution for a multitude of RFID applications. As fractal antennas are small and versatile, they are ideal for creating compact RFID equipment – both tags and readers [31]. Fractal antennas contribute to various design opportunities for both active and passive RFID labels and tags, including Electronic Product Code (EPC) technology and handheld RFID reader enhancements.

### **2.5.5.3 Wireless Network**

Fractal antennas technology now enables emerging wireless networking protocols such as MIMO and WiMAX to deliver their maximum potential. Fractal antennas are suited for compact single and multiband applications. In array

configurations of closely packed elements, fractal geometry dramatically reduces mutual coupling and improves aperture efficiency. Superior beam characteristics and lower sidelobes result in better link budget [32].

#### **2.5.5.4 Telematics**

Telematic is the branch of information technology which deals with long distance transmission of computerized information, such as vehicle-based communications. Today's automobile can have dozens of antennas that provide everything from emergency notification and navigational services to satellite radio and TV [33]. With approximately one quarter the size of conventional antennas, fractal antennas can be manufactured on flat, conformal, and even transparent substrates with a host of new design, performance options and concealment enhancement. They conform to all major telecommunications standards, including GSM, CDMA, and PCS.

#### **2.5.5.5 Military Defense and Intelligence Applications**

Fractal antenna has successfully tackled the defense and intelligence community's most vexing antenna challenges, from signal intelligence and tactical communications applications to electronic warfare. Fractal antennas have been utilized in numerous real world environments, operating under the most demanding military conditions. Inherently wideband with 50 Ohm impedance, low noise fractal antennas offer higher potential for military monitoring over a wide frequency range without being detected. With extreme wideband frequency range, fractal antennas are uniquely suited to enable new software-defined tactical communications architectures such as JTRS.

# CHAPTER 3

## METHODOLOGY

### 3.1 Design and Simulation

The broad-band dual-frequency fractal antenna in this project is designed based on [2] with similar modified Sierpinski geometry, but with different design parameters such as the material's dielectric constant, thickness, size, and using different simulation software. In this project, Microwave Office 2002 is used to design and simulate the antenna. Mathematical operations such as bandwidth calculation are performed by using Mathcad v.12.

#### 3.1.1 Antenna Design

For a microstrip antenna based on the Sierpinski gasket, it is difficult to obtain a multifrequency behavior unless some modifications are made. One of the simple modifications is to perturb the scale factor [2]. The modified Sierpinski fractal geometry used for the antenna design in this project has been obtained through a perturbation of the classic Sierpinski fractal based on a reduction of the fractal iteration and a modification of the scale properties, as shown in Figure 3.1 and Figure 3.2. In this project, simulations will be done up to the second stage iteration.

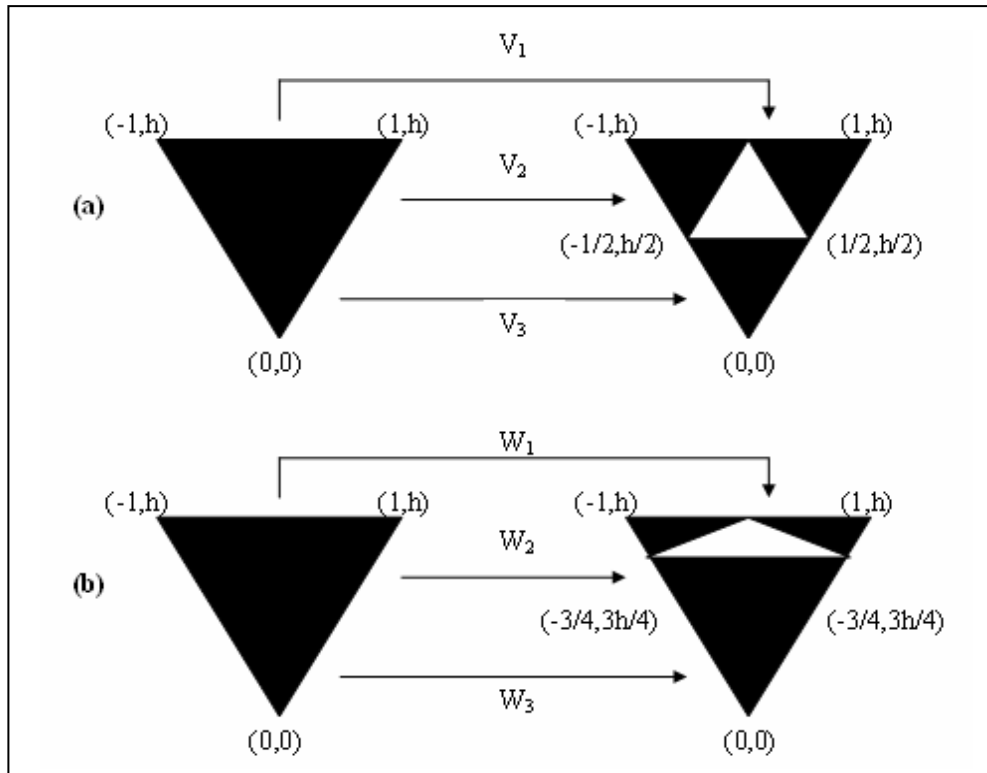


Figure 3.1 Iteration Function Process to Generate: (a) First Stage of the Classic Sierpinski Gasket and (b) Perturbed Sierpinski Gasket

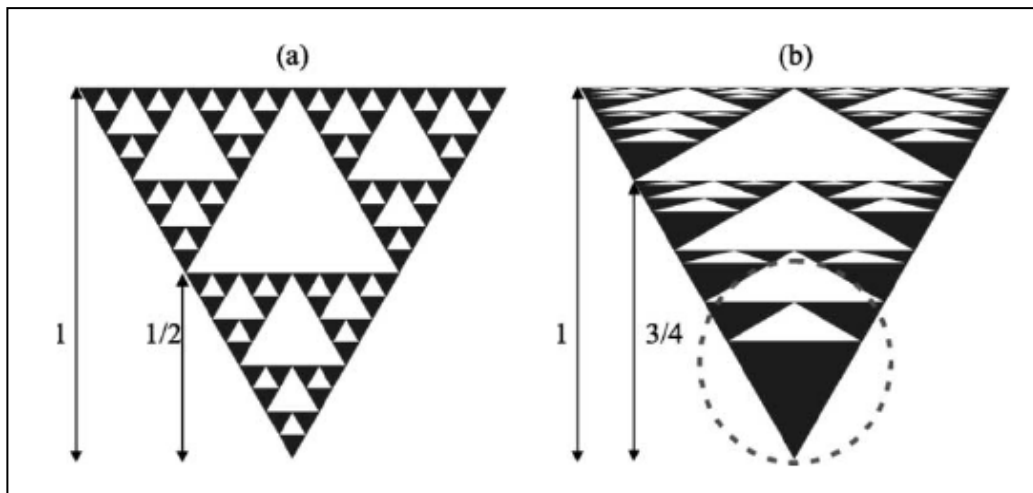


Figure 3.2 Iteration Function System Attractors: (a) Classic Sierpinski Gasket at Fourth Stage and (b) Perturbed Sierpinski Gasket at Fourth Stage [2]

### 3.1.2 Design and Simulation Process

The main part of this project consists of antenna design and simulation which involves a number of procedures. First, the shape and geometry of the patch antenna is determined, with focus on the frequency range obtainable from the size and geometry. Then, a dimension and cell calculation algorithm is written in Mathcad in order to find the triangular patch antenna's dimension and cell size to be used in Microwave Office simulation. Figure 3.3 shows the calculation performed by the algorithm written in Mathcad v.12.

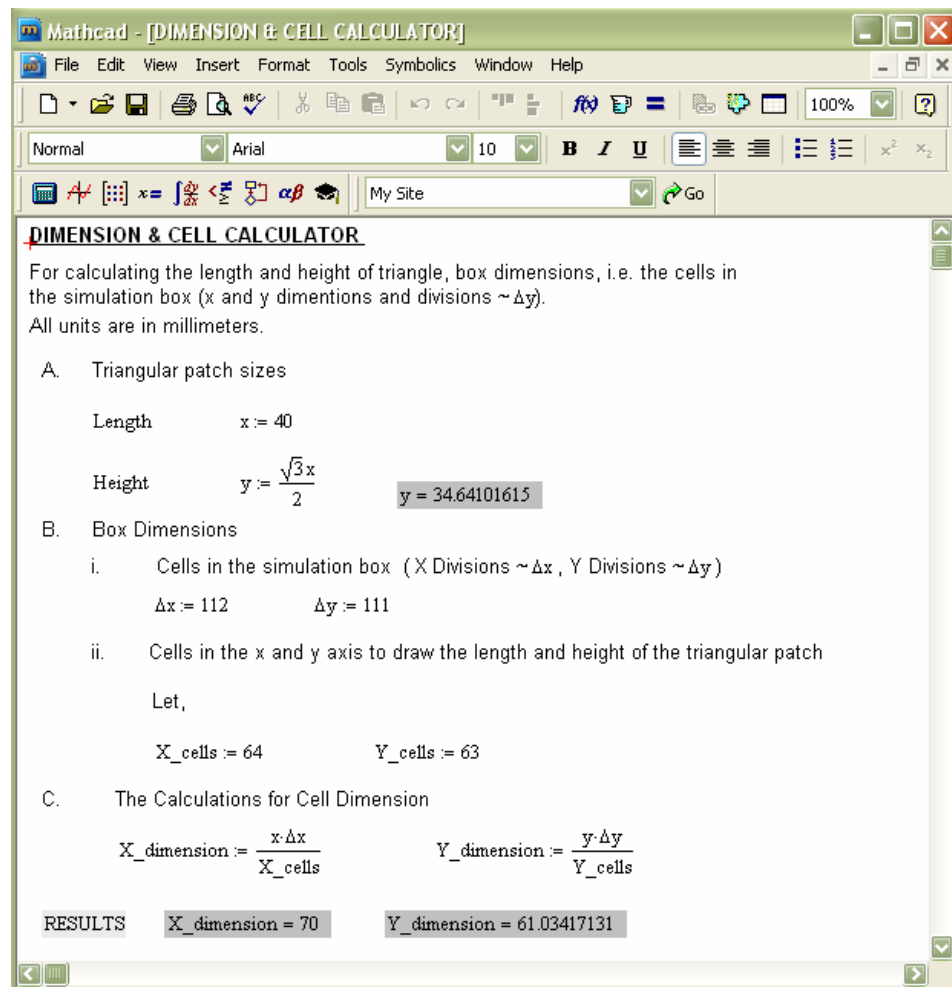


Figure 3.3 Dimension and Cell Calculation in Mathcad

Next, the patch antenna is drawn in Microwave Office 2002 according to the exact geometry and size. Parameters such as the dielectric constant, thickness, and probe position are carefully chosen. The frequency range and graphs to be displayed from the simulation are then selected. All necessary parameters are set and defined before the simulation starts, as shown in Figure 3.4.

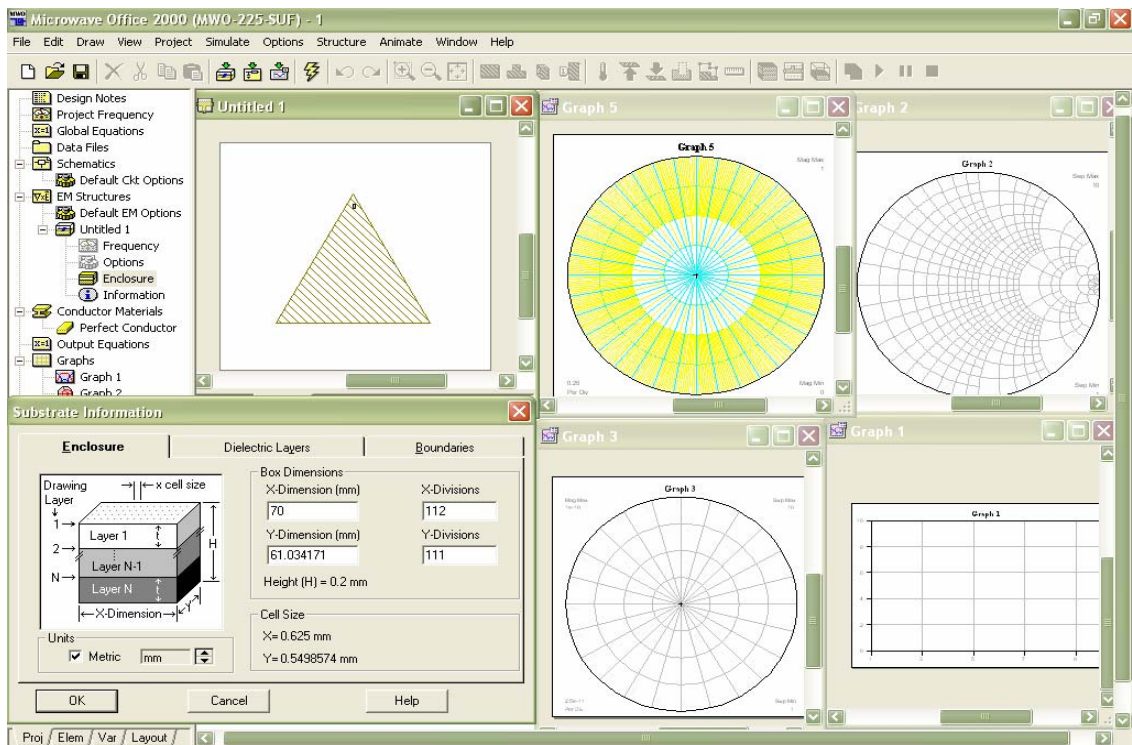


Figure 3.4 Setting Parameters and Graphs in Microwave Office Simulation

After the simulation, results are analyzed from various graphs such as the VSWR graph and Smith chart. The resonant frequency and bandwidth of the antenna are calculated using the bandwidth calculation algorithm written in Mathcad. Numerous simulations are to be done until the objective of the project is fulfilled. The flow chart for the antenna design and simulation process in a step-by-step approach is summarized in Figure 3.5.

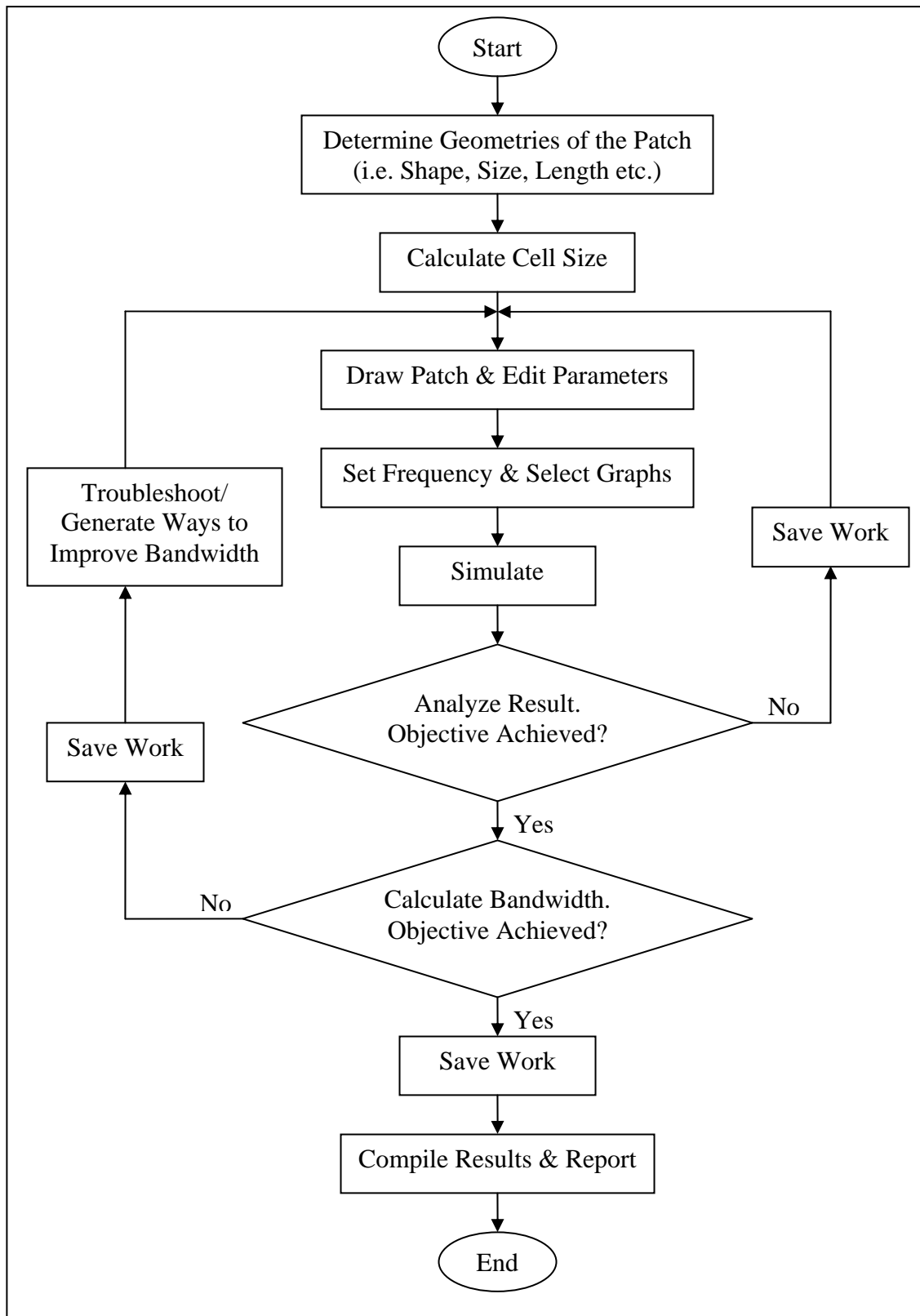


Figure 3.5 Design and Simulation Process Flow Chart

### 3.1.3 Microwave Office

Microwave Office is a simulation software that enables the design of circuits composed of schematics and electromagnetic (EM) structures from an extensive electrical model database. It generates layout representations of these designs. Simulations can be performed by using one of Microwave Office's simulation engines - a linear simulator, an advanced harmonic balance simulator, a 3D-planar EM simulator (EMsight.), or an optional HSPICE simulator. In Microwave Office, the design output can be displayed in a wide variety of graphical forms based on the analysis needed. The designs can then be tuned or optimized and the changes are automatically and immediately reflected in the layout. The snapshot in Figure 3.6 shows the interface of Microwave Office.

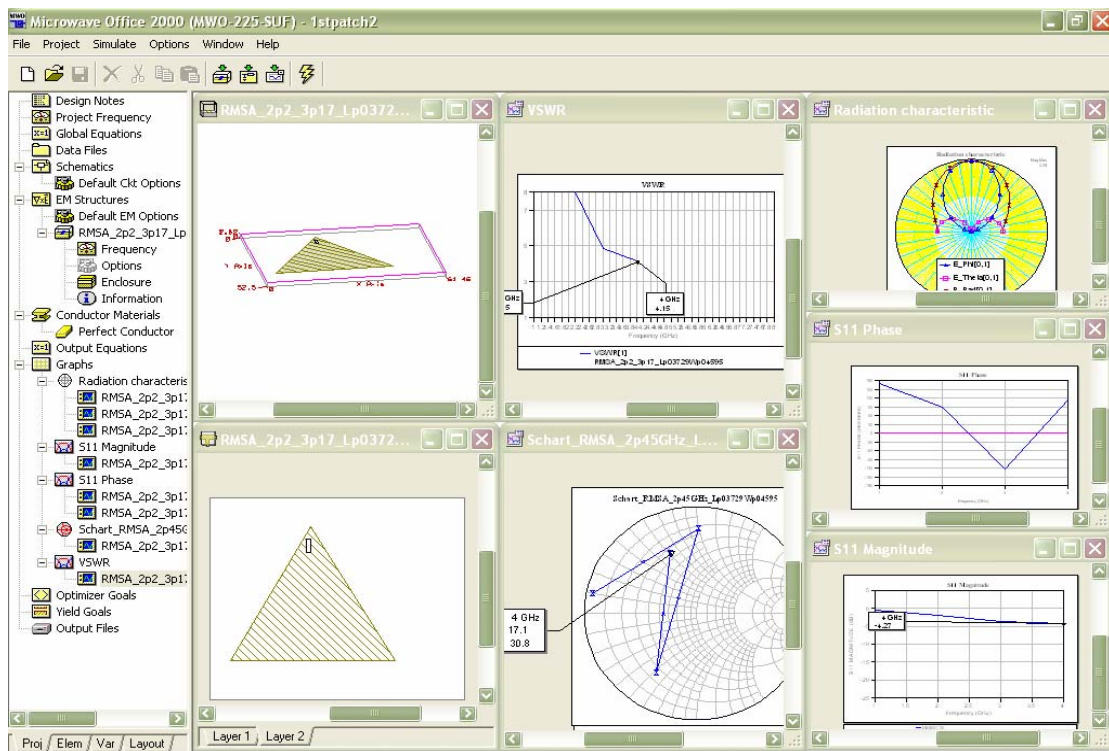


Figure 3.6 The Layout of Microwave Office

### **3.2 Analysis and Validation of Result**

The next stage after design and simulation is the analysis and validation of the results obtained from various simulations performed. Normally for each simulation, graphs such as the VSWR graph, polar graph, and Smith chart will be plotted. These graphs are analyzed to validate the simulation results. Mathcad will be used to perform mathematical analysis, such as frequency and bandwidth calculations.

The analysis from the simulation results will be properly done and arranged in table form, with design parameters such as the dielectric constant and thickness of the patch antenna being the variables. However, if there is insufficient result or the result is inaccurate, the design and simulation stage should be repeated in order to get the optimum outcome.

#### **3.2.1 Smith Chart**

Smith chart is a polar plot of the complex reflection coefficient (called gamma), or also known as the 1-port scattering parameter  $s$  or  $s_{11}$ , for reflections from a normalized complex load impedance  $z = r + jx$ . The normalized impedance is a complex dimensionless quantity obtained by dividing the actual load impedance  $Z_L$  in ohms by the characteristic impedance  $Z_0$  (also in ohms, and is a real quantity for a lossless line) of the transmission line [34]. Figure 3.7 shows an example of Smith chart.

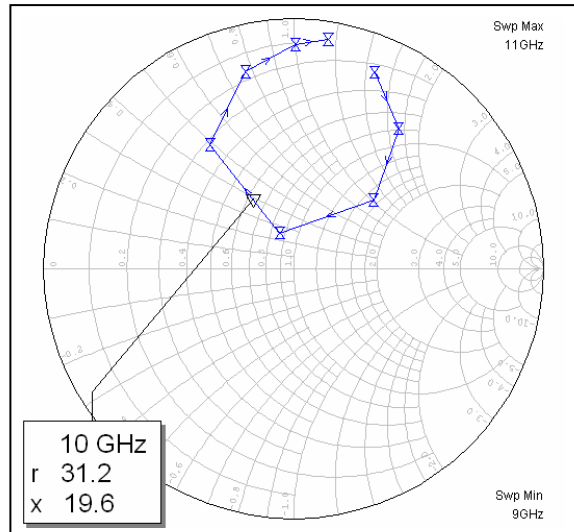


Figure 3.7 Example of a Smith Chart

The contours of  $z = r + jx$  (dimensionless) are plotted on top of this polar reflection coefficient (complex gamma) and two orthogonal sets of intersecting circles are formed. The centre of the Smith chart is at  $\text{gamma} = 0$  which is where the transmission line is matched, and where the normalized load impedance  $z = 1 + j0$ ; that is, the resistive part of the load impedance equals the transmission line impedance, and the reactive part of the load impedance is zero [34].

The complex variable  $z = r + jx$  is related to the complex variable gamma by the formula [34]:

$$z = r + jx = \frac{1 + \text{gamma}}{1 - \text{gamma}} \quad (3.1)$$

and the inverse of this relationship is [34]:

$$\text{gamma} = \frac{z - 1}{z + 1} = \frac{(r - 1) + jx}{(r + 1) + jx} \quad (3.2)$$

From Smith chart, the value of gamma for a given  $z$ , or the value of  $z$  for a given gamma can be read off. The modulus of gamma, written  $|\text{gamma}|$ , is the distance out from the centre of the chart. The phase angle of gamma, written  $\arg(\text{gamma})$ , is the angle around the chart from the positive  $x$  axis. There is an angle scale at the perimeter of the chart [34].

Once around the Smith chart is a half wavelength VSWR, or voltage standing wave ratio, which is depicted as a circle around the chart. The smaller this circle is, the lower the VSWR, the better the impedance match.

### **3.3 Discussion and Conclusion**

After all the simulation results are validated and finalized, the project shall proceed to the discussion section. Each analysis of the simulation result will be accompanied by clear and precise explanation. The performance and characteristics of the antenna designed will be discussed. Comparisons will be made between the simulation results in this project with the results from the method of moment commercial code and experimental setup in journal [2]. Finally, all the works done during the implementation of the project, including the difficulties and limitations faced will be concluded. All the results and analysis will be finalized to draw a clear conclusion.

### **3.4 Compile of Report**

After conducting all the stages in the methodology flow chart, all the information, data, design and simulation results are finalized and organized in order to compile an informative report. This marks the end of the Final Year Project.

# CHAPTER 4

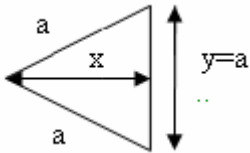
## RESULTS AND ANALYSIS

### 4.1 Equilateral Triangular Single Patch Antenna with Length 5cm

#### 4.1.1 Antenna Design

A single patch antenna with equilateral triangular shape is to be designed. The side length of the antenna is 5cm. Other important parameters of the antenna are outlined in Table 4.1.

Table 4.1 Parameters of Patch Antenna with Side Length of 5cm

<b>Geometry</b>	Equilateral Triangle 
<b>Size</b>	Length, $a = 5\text{cm}$ Thickness, $h = 0.159\text{cm}$
<b>Material of Patch</b>	RT Duroid 5870 with relative dielectric constant, $\epsilon_r = 2.32$
<b>Feeding Technique</b>	Single via port connected from the antenna patch to a $8.75000 \times 8.45406\text{cm}$ ground plane

Mathcad is used to compute the calculations of box dimensions and cell size in order to draw the 5cm antenna patch accurately in Microwave Office. A simple mathematical algorithm is written in Mathcad to perform the computation, as shown in Figure 4.1.

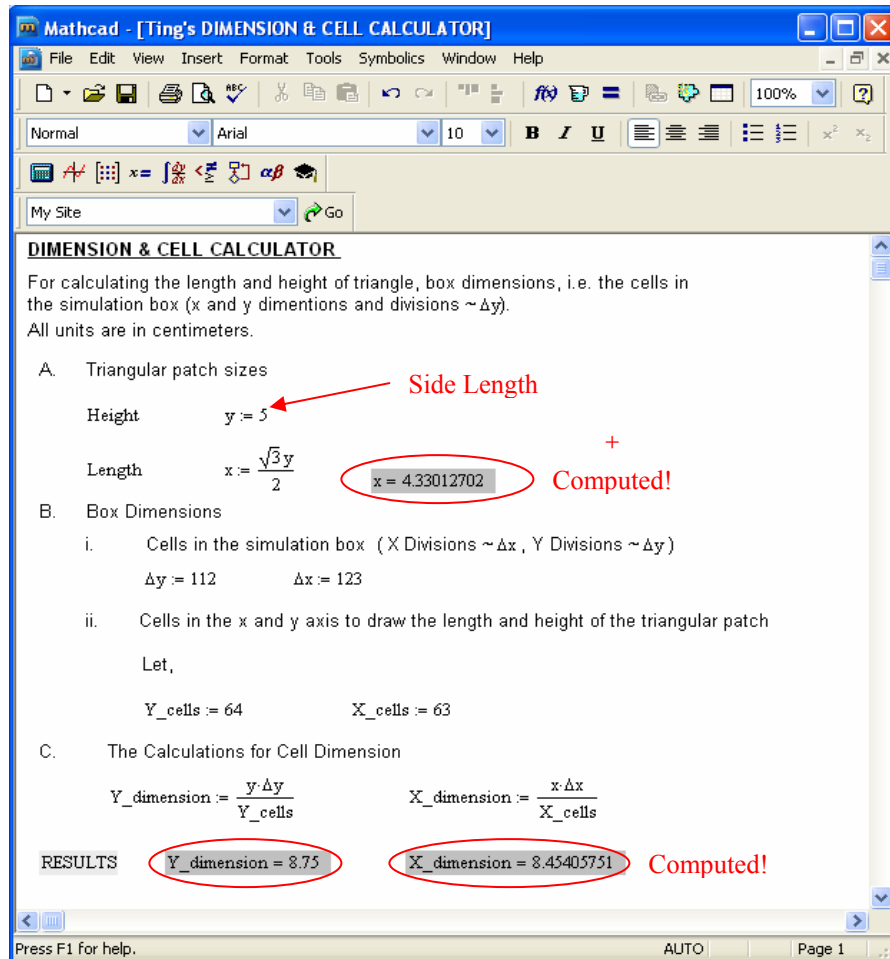


Figure 4.1 Computation of Cell Size and Dimension by Using Mathcad

By referring to Table 4.1, the side length of the patch antenna, y, is 5cm. This value is entered in the Mathcad algorithm. The value of x is automatically computed. The number of cells in the simulation box and number of cells in the x and y axes to draw the patch antenna are set to be 123 x 112 and 63 x 64 respectively. Calculations

are automatically performed to compute the size of X-dimension and Y-dimension which need to be entered in Microwave Office in order to draw the antenna patch of the desired shape and size accurately, as shown in Figure 4.2.

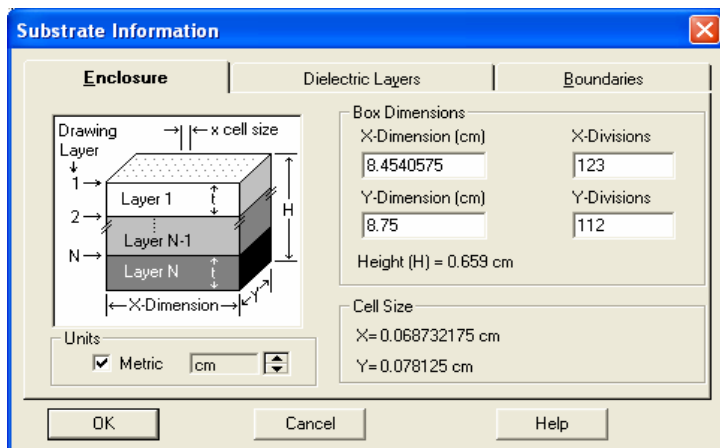


Figure 4.2 Entering Values of X-Dimension, Y-Dimension, X-Division, and Y-Division in Microwave Office

By referring to Table 4.1, the thickness and relative dielectric constant of the patch are set to 0.159cm and 2.32 respectively in Microwave Office's substrate information section, as shown in Figure 4.3. A layer of air with thickness of 0.5cm and relative dielectric constant of 1 is added above the antenna patch.

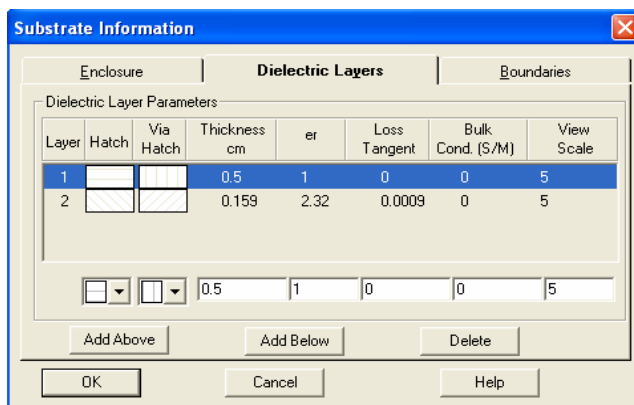


Figure 4.3 Information of Dielectric Layers

An equilateral triangular patch antenna with side length,  $a = 5\text{cm}$  enclosed by a box with dimension  $8.75\text{cm} \times 8.45406\text{cm}$  is drawn in Microwave Office, as shown in Figure 4.4 and Figure 4.5. A via port with the smallest possible size is added in a suitable position. The via port serves the purpose as a transmission line. The determination of a suitable position of via port requires several testing of different positions within the antenna patch in order to get the best location.

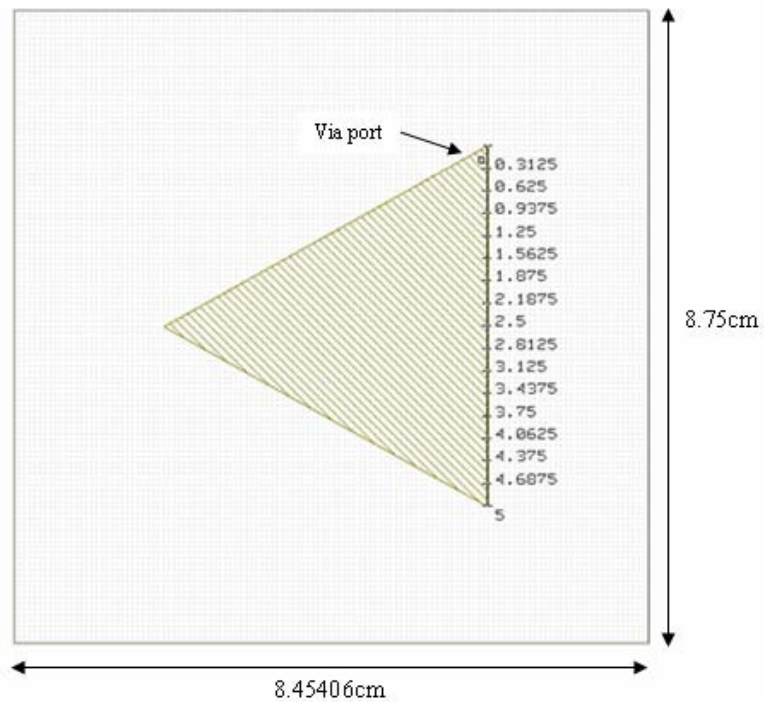


Figure 4.4 2D View of the 5cm Triangle Patch Antenna

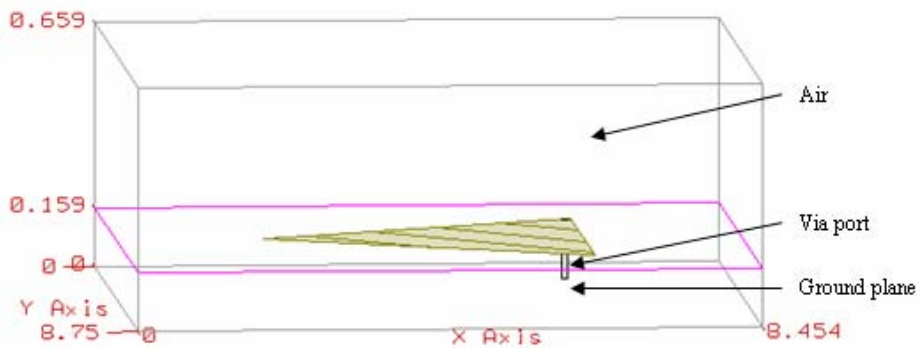


Figure 4.5 3D View of the 5cm Patch Antenna

## 4.1.2 Simulation Results

### (i) Return Loss Graph

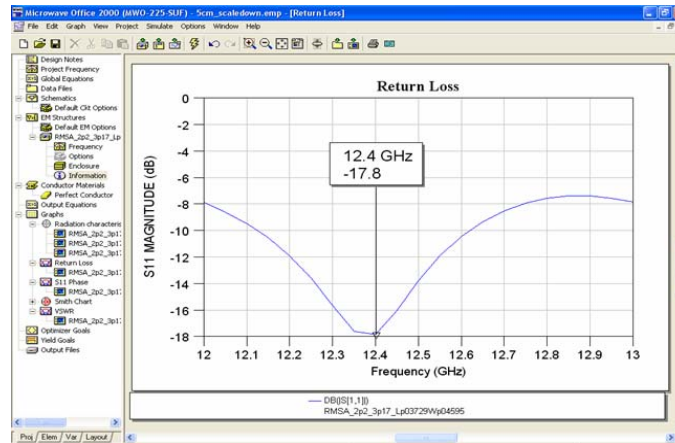


Figure 4.6 Return Loss Graph for 5cm Triangular Patch Antenna

The return loss indicates how much of the incident power is reflected from the antenna. It is measured in decibel (dB) unit. If 50 % of the signal is absorbed by the antenna and 50 % is reflected back, the return loss is -3dB. A good antenna might have a value of -10dB (90 % absorbed & 10 % reflected). The equation to calculate the return loss of an antenna is:

$$\text{Return Loss (dB)} = 10 \log_{10} Pr \dots\dots(4.1)$$

where Pr = Fraction of reflected power

From the simulation result as shown in Figure 4.6, the return loss of the patch antenna is -17.8dB. From equation 4.1, it can be calculated that 98.34% of the power is absorbed by the antenna and only 1.66% is reflected. The resonant frequency of the

patch antenna designed is the frequency when the magnitude of the antenna's return loss reaches the minimum value. In this case, resonant frequency,  $f_R = 12.4\text{GHz}$  which falls into the microwave region defined by the Institute of Electrical and Electronics Engineers (IEEE). In the return loss graph shown in Figure 4.6, the deep and wide dip of the curve is good since this shows that the antenna has good bandwidth (spreadband).

## (ii) VSWR Graph

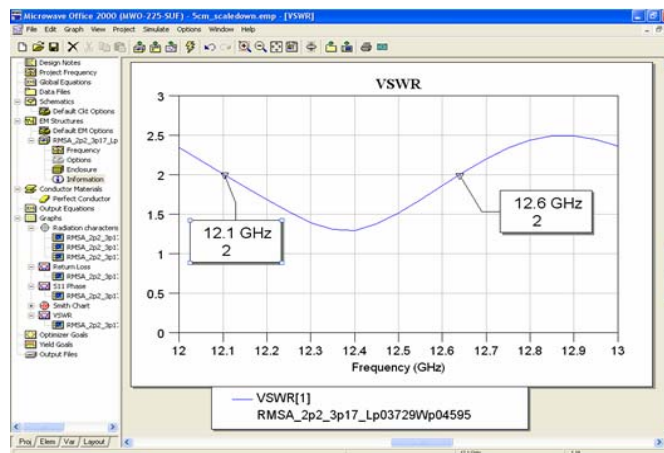


Figure 4.7 Finding Bandwidth from VSWR Graph

VSWR (Voltage Standing Wave Ratio) is a measure of impedance mismatch between a transmission line and its load. The VSWR graph is used to find the bandwidth of the antenna. Bandwidth is a measure of frequency range in which the antenna operates. It is measured in hertz (Hz). Typically, bandwidth is measured by looking at Standing Wave Ratio (SWR) - by finding the frequency range over which the VSWR is less than 2. The value of VSWR 2:1 is considered as a good bandwidth measurement

for small antennas. Figure 4.7 shows the VSWR graph for the 5cm triangular patch antenna.

From Figure 4.7, the frequency in which the VSWR is less than 2 ranges from 12.1 GHz to 12.6 GHz. In this case,

Low frequency,  $f_L = 12.1$  GHz; and

High frequency,  $f_H = 12.6$  GHz.

These frequency values are used to calculate the bandwidth of the patch antenna.

Bandwidth,  $BW = f_H - f_L$

$$= 12.6 \text{ GHz} - 12.1 \text{ GHz}$$

$$= 0.5 \text{ GHz}$$

Centre frequency,  $f_C = \frac{f_L + f_H}{2}$

$$= \frac{12.1 + 12.6}{2}$$

$$= 12.35 \text{ GHz}$$

Percentage of Bandwidth,  $\% BW = \frac{f_H - f_L}{f_C} \times 100\%$

$$= \frac{12.6 - 12.1}{12.35} \times 100\%$$

$$= 4.05\%$$

Thus, the 5cm equilateral triangular patch antenna occupies a bandwidth percentage of 4.05%.

**(iii) Phase Graph**

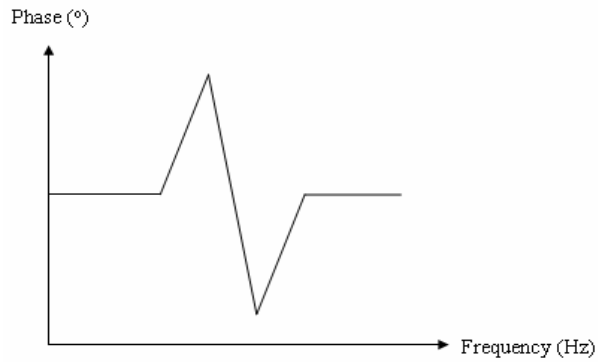


Figure 4.8 An Ideal Phase Graph

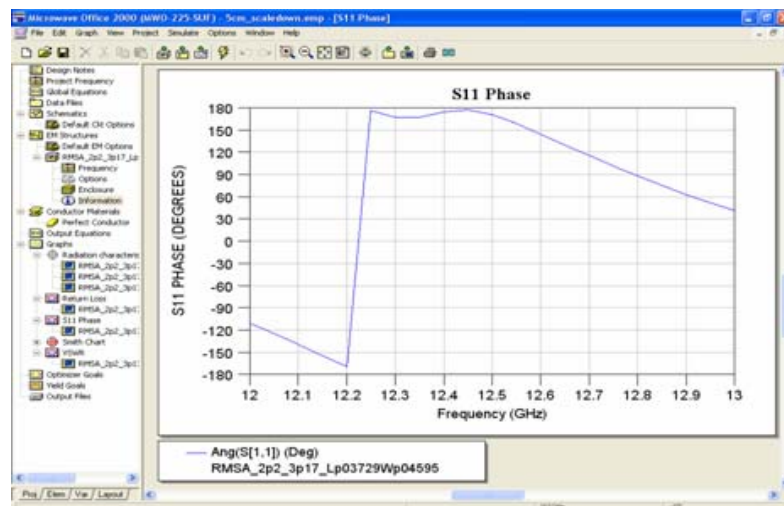


Figure 4.9 Phase Graph of 5cm Triangular Patch Antenna

The phase graph of an antenna illustrates the phase position in degree for a predefined frequency range. In ideal case, the phase graph of a patch antenna has the shape as shown in Figure 4.8. However, graph similar to that such as the one obtained from 5cm patch antenna simulation results as shown in Figure 4.9 is acceptable.

(iv) **Smith Chart**

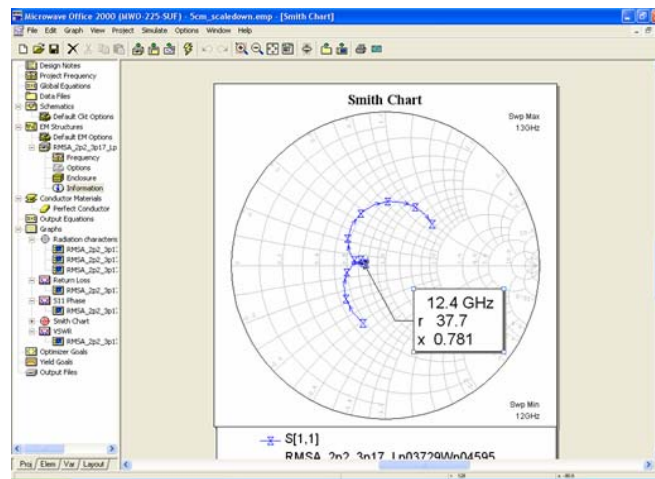


Figure 4.10 Finding Impedance from Smith Chart

Upon the completion of simulation, Smith chart displays a sequence of normalized impedance, admittance or reflection coefficient in a circle of unity radius. It is often used to simplify the impedance matching of a transmission line with its load.

Impedance of the patch antenna at resonant frequency can be found from Smith chart. In ideal case, the resonant frequency should be located at or near the middle point of the chart. Smith chart also shows the characteristic of the antenna being inductive or capacitive.

Figure 4.10 shows the Smith chart resulted from the simulation of the equilateral triangular patch antenna with side length 5cm. In this case, at the point where resonant

frequency  $f_R = 12.4$  GHz, resistance  $r = 37.7$  and reactance  $x = 0.781$ . Small value of  $x$  is desirable.

Impedance,  $z = r + jx$

$$= 37.7 + j0.781$$

Magnitude of total impedance,  $|z| = \sqrt{37.7^2 + 0.781^2}$

$$= 37.71 \Omega$$

As the resonant frequency falls near the middle of the Smith chart, the antenna is neither inductive nor capacitive. The total impedance approximates the resistance value. These features make the antenna a near-ideal antenna.

**(v) Radiation Characteristic Chart**

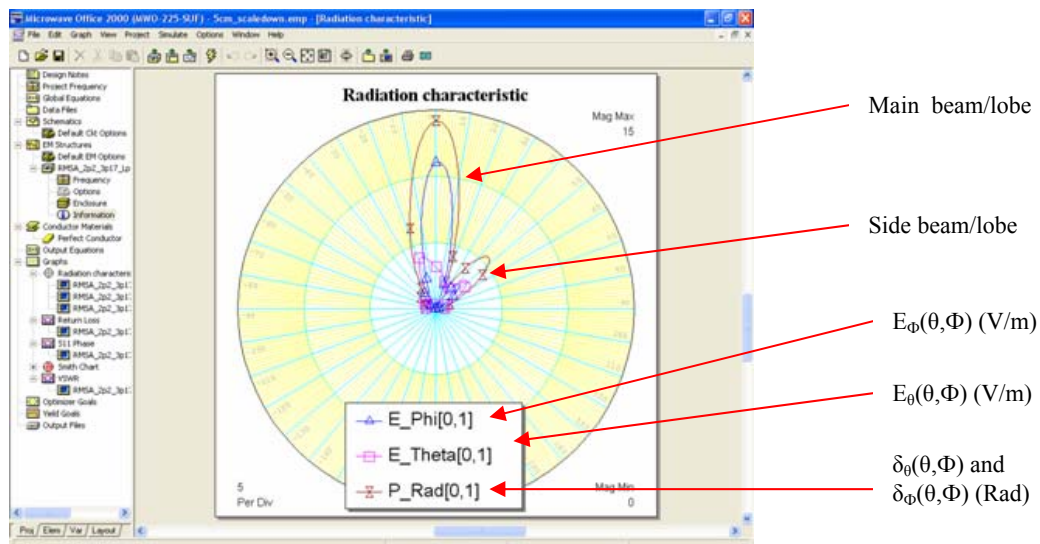


Figure 4.11 Radiation Pattern of the 5cm Triangular Patch Antenna

Radiation characteristic chart shows the patterns involving the variation of field or power as a function of spherical coordinates  $\theta$  and  $\Phi$ . The three elements of the radiation pattern with respect to field intensity and polarization of the 5cm triangular patch antenna as shown in Figure 4.11 are:

$E_{\Phi}[0,1] \rightarrow E_{\Phi}(\theta, \Phi)$  (V/m): The  $\Phi$  component of the electric field as a function of the angles  $\theta$  and  $\Phi$

$E_{\theta}[0,1] \rightarrow E_{\theta}(\theta, \Phi)$  (V/m): The  $\theta$  component of the electric field as a function of the angles  $\theta$  and  $\Phi$

$P_{\text{Rad}}[0,1] \rightarrow \delta_{\theta}(\theta, \Phi)$  and  $\delta_{\Phi}(\theta, \Phi)$  (Rad): The phases of these fields as a function of the angles  $\theta$  and  $\Phi$

### 4.1.3 Comparison of Simulation Results and Calculations

From the return loss graph in Section 4.1.2(i), Resonant Frequency,  $f_R = 12.4$  GHz

By using the formulas developed in [35],

Resonant frequencies of the equilateral triangular patch,

$$f_{m,n,l} = \frac{2c}{3a(\epsilon_r)^{1/2}}(m^2 + mn + n^2)^{1/2} \dots\dots (4.2)$$

where the integers satisfy the condition  $m+n+l=0$

$a$  = length of equilateral triangular patch

$$\text{Effective side length, } a_{\text{eff}} = a + h(\epsilon_r)^{-1/2} \dots\dots (4.3)$$

where  $h$  = thickness of patch

$$\text{Effective dielectric constant, } \epsilon_{\text{eff}} = \frac{1}{2}(\epsilon_r + 1) + \frac{1}{4}(\epsilon_r - 1)\left(1 + \frac{12h}{a}\right)^{-1/2} \dots\dots (4.4)$$

where  $\epsilon_r$  = relative dielectric constant

In this case,

$$\begin{aligned} a_{\text{eff}} &= a + h(\epsilon_r)^{-1/2} \\ &= 5 + 0.159(2.32)^{-1/2} \\ &= 5.1044 \text{ cm} \end{aligned}$$

$$\begin{aligned} \epsilon_{\text{eff}} &= \frac{1}{2}(\epsilon_r + 1) + \frac{1}{4}(\epsilon_r - 1)\left(1 + \frac{12h}{a}\right)^{-1/2} \\ &= \frac{1}{2}(2.32 + 1) + \frac{1}{4}(2.32 - 1)\left(1 + \frac{12 \times 0.159}{5}\right)^{-1/2} \\ &= 1.94075 \end{aligned}$$

$$\text{Resonant frequency, } f_{m,n} = \frac{2c}{3a_{\text{eff}}(\epsilon_{\text{eff}})^{1/2}}(m^2 + mn + n^2)^{1/2} \dots\dots (4.5)$$

When the antenna is radiating at mode  $m,n = 3,2$ ,

$$\begin{aligned} \text{Resonant frequency, } f_{3,2} &= \frac{2(3 \times 10^8)}{3(5.1044 \times 10^{-2})(1.94075)^{1/2}}(3^2 + 3(2) + 2^2)^{1/2} \\ &= 12.26 \text{ GHz} \end{aligned}$$

Table 4.2 Comparison of Frequencies from Simulation and Calculation

<b>Simulated Resonant Frequency</b>	$f_R = 12.4 \text{ GHz}$
<b>Calculated Resonant Frequency</b>	$f_{3,2} = 12.26 \text{ GHz}$

$$\begin{aligned} \text{Deviation of simulated frequency from calculated frequency} &= \frac{12.4 - 12.26}{12.26} \times 100\% \\ &= 1.14\% \end{aligned}$$

which is very small and is accepted

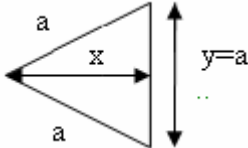
## 4.2 Equilateral Triangular Single Patch Antenna with Length 8cm

### 4.2.1 Antenna Design

A single patch equilateral triangular antenna with side length 8cm is designed.

Other important parameters of the antenna are outlined in Table 4.3.

Table 4.3 Parameters of Patch Antenna with Side Length of 8cm

<b>Geometry</b>	Equilateral Triangle 
<b>Size</b>	Length, $a = 8\text{cm}$ Thickness, $h = 0.159\text{cm}$
<b>Material of Patch</b>	RT Duroid 5870 with relative dielectric constant, $\epsilon_r = 2.32$
<b>Feeding Technique</b>	Single via port connected from the antenna patch to a $14.0000 \times 13.5265\text{cm}$ ground plane

Similar to Section 4.1.1, Mathcad is used to compute the calculations of box dimensions and cell size in order to draw the 8cm antenna patch accurately in

Microwave Office. Mathcad computation for the 8cm patch antenna is shown in Figure 4.12.

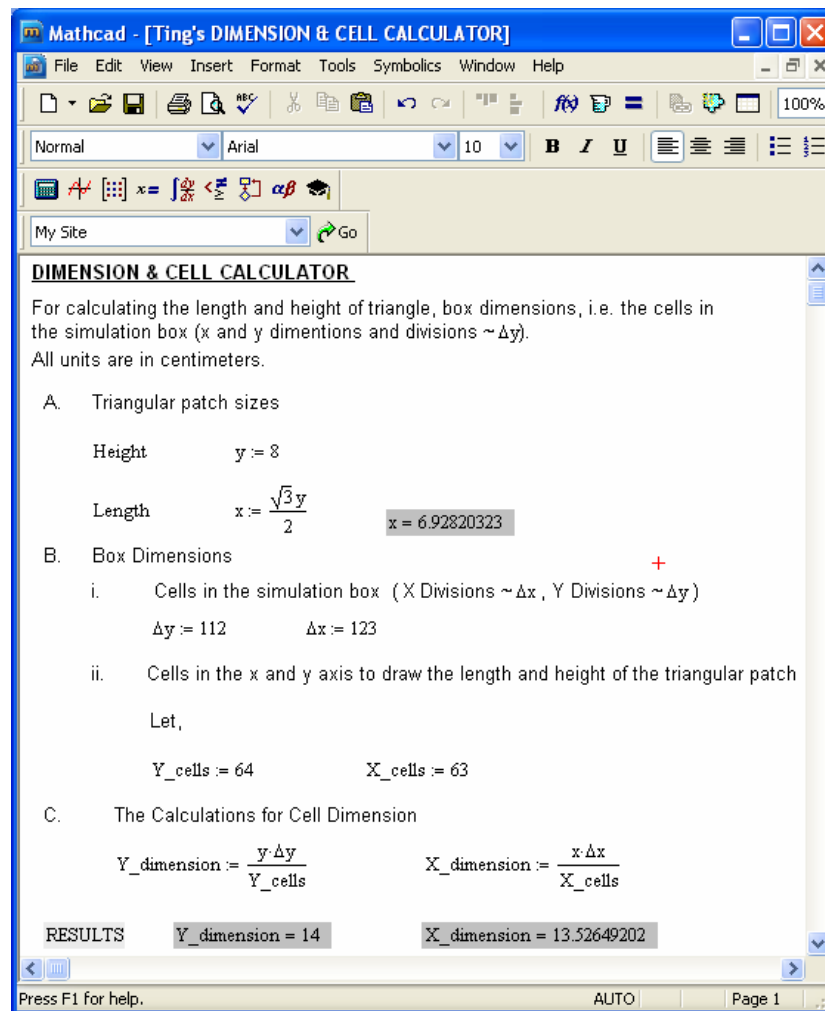


Figure 4.12 Mathcad Computation of Cell Size and Dimension

The enclosure information is then entered in Microwave Office as shown in Figure 4.13. By referring to Table 4.3, the thickness and relative dielectric constant of the patch are set to 0.159cm and 2.32 respectively in Microwave Office's substrate information section, as shown in Figure 4.14. A layer of air with thickness of 0.5cm and relative dielectric constant of 1 is added above the antenna patch.

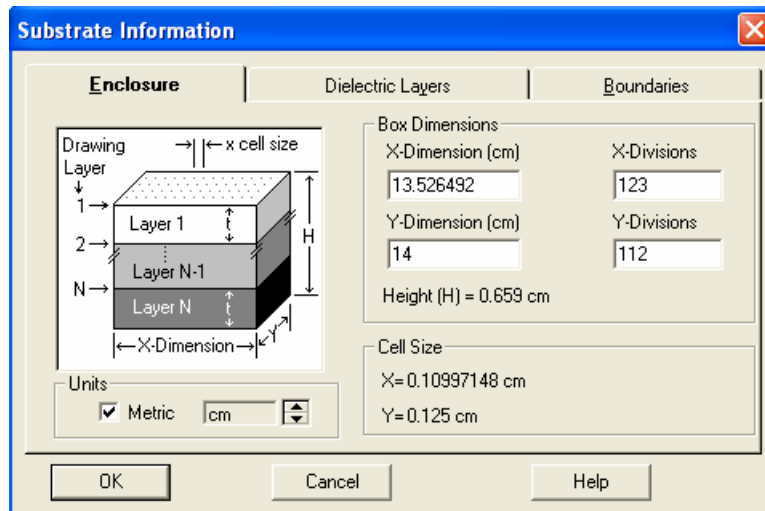


Figure 4.13 Enclosure Information in Microwave Office

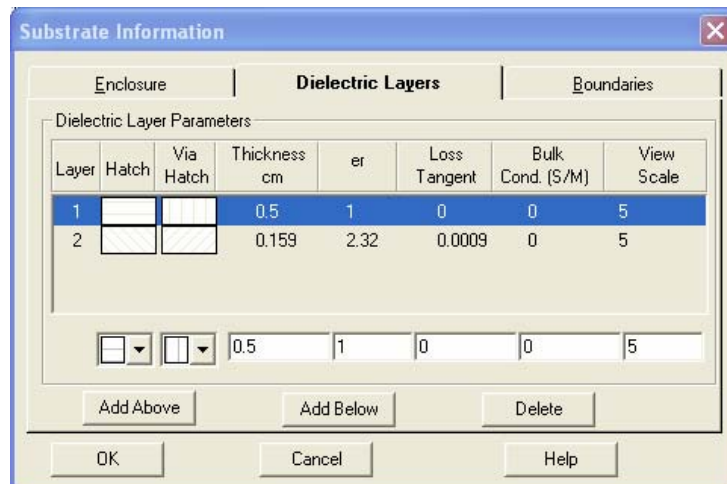


Figure 4.14 Substrate Information

An equilateral triangular patch antenna with side length,  $a = 8\text{cm}$  enclosed by a box with size  $14.0000 \times 13.5265\text{cm}$  is drawn in Microwave Office, as shown in Figure 4.15 and Figure 4.16. The patch antenna is fed by a single via port that is connected to the ground plane.

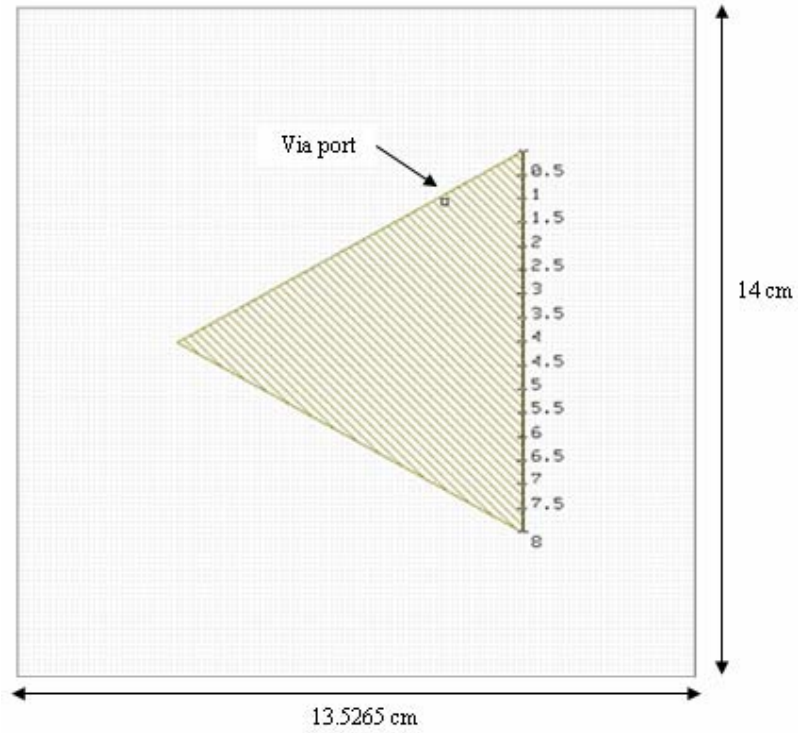


Figure 4.15 2D View of 8cm Triangular Patch Antenna

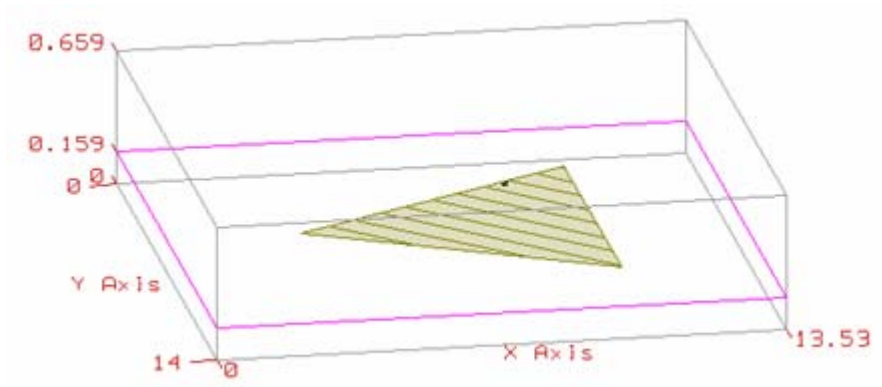


Figure 4.16 3D View of 8cm Triangular Patch Antenna

## 4.2.2 Simulation Results

### (i) Return Loss Graph

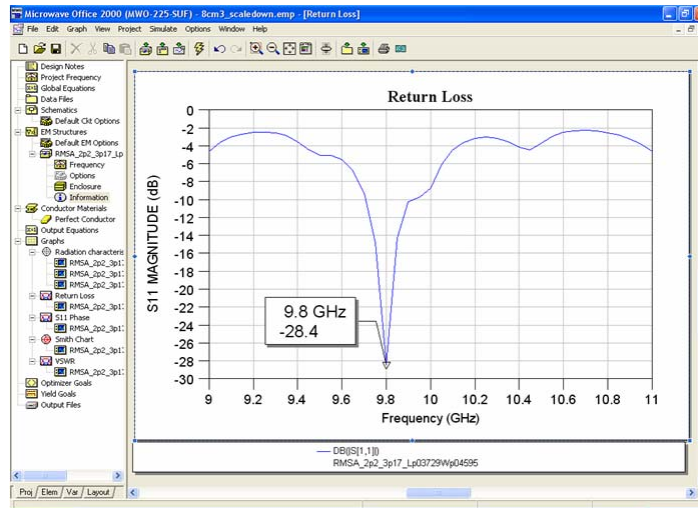


Figure 4.17 Return Loss Graph for 8cm Triangular Patch Antenna

By referring to the simulation result in Figure 4.17, the return loss of the patch antenna is -28.4dB. From equation 4.1, this implies that 99.86% of the power is absorbed by the antenna and only 0.14% is reflected. The resonant frequency of the patch antenna designed is the frequency when the magnitude of the antenna's return loss reaches the minimum value. In this case, resonant frequency,  $f_R = 9.8\text{GHz}$ . The deep and wide dip of the curve in the return loss graph shows that the antenna has good bandwidth (spreadband).

## (ii) VSWR Graph

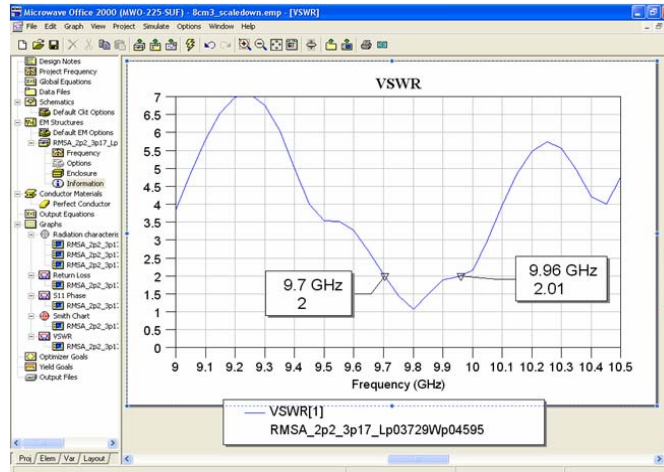


Figure 4.18 VSWR Graph of 8cm Triangular Patch Antenna

From the VSWR graph obtained from the simulation of equilateral triangular patch antenna with side length of 8cm as shown in Figure 4.18, bandwidth can be measured by looking at Standing Wave Ratio (SWR) - by finding the frequency range over which the VSWR is less than 2. The value of VSWR 2:1 is considered as a good bandwidth measurement for small antennas.

From Figure 4.18, the frequency in which the VSWR is less than 2 ranges from 9.7 GHz to 9.96 GHz. In this case,

Low frequency,  $f_L = 9.7$  GHz; and

High frequency,  $f_H = 9.96$  GHz.

These frequency values are used to calculate the bandwidth of the patch antenna.

Bandwidth,  $BW = f_H - f_L$

$$= 9.96 \text{ GHz} - 9.7 \text{ GHz}$$

$$= 0.26 \text{ GHz}$$

$$\begin{aligned} \text{Centre frequency, } f_c &= \frac{f_L + f_H}{2} \\ &= \frac{9.7 + 9.96}{2} \\ &= 9.83 \text{ GHz} \end{aligned}$$

$$\begin{aligned} \text{Percentage of Bandwidth, \% BW} &= \frac{f_H - f_L}{f_c} \times 100\% \\ &= \frac{9.96 - 9.7}{9.83} \times 100\% \\ &= 2.64\% \end{aligned}$$

Therefore, the 8cm equilateral triangular patch antenna occupies a bandwidth percentage of 2.64%.

### (iii) Phase Graph

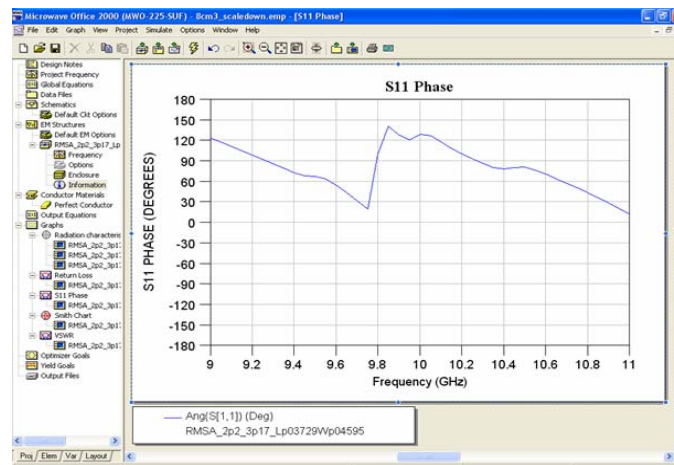


Figure 4.19 Phase Graph of 8cm Triangular Patch Antenna

Figure 4.19 shows the phase graph from the simulation of the 8cm triangular patch antenna. It has a shape similar to the ideal shape of a phase graph for an antenna.

#### (iv) Smith Chart

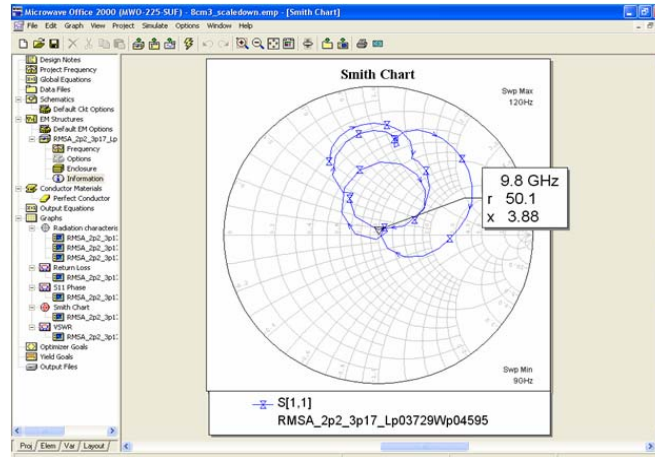


Figure 4.20 Finding Impedance from Smith Chart

Smith chart as shown in Figure 4.20 displays a sequence of normalized impedance, admittance or reflection coefficient in a circle of unity radius. Impedance of the patch antenna at resonant frequency can be found from Smith chart.

From Figure 4.20, at the point where resonant frequency  $f_R = 9.8$  GHz, resistance  $r = 50.1$  and reactance  $x = 3.88$ .

Impedance,  $z = r + jx$

$$= 50.1 + j3.88$$

Magnitude of total impedance,  $|z| = \sqrt{50.1^2 + 3.88^2}$

$$= 50.25 \Omega$$

As the resonant frequency falls in the middle of the Smith chart, the antenna is neither inductive nor capacitive. The total impedance approximates the resistance value. These features make the antenna a near-ideal antenna.

(v) Radiation Characteristic Chart

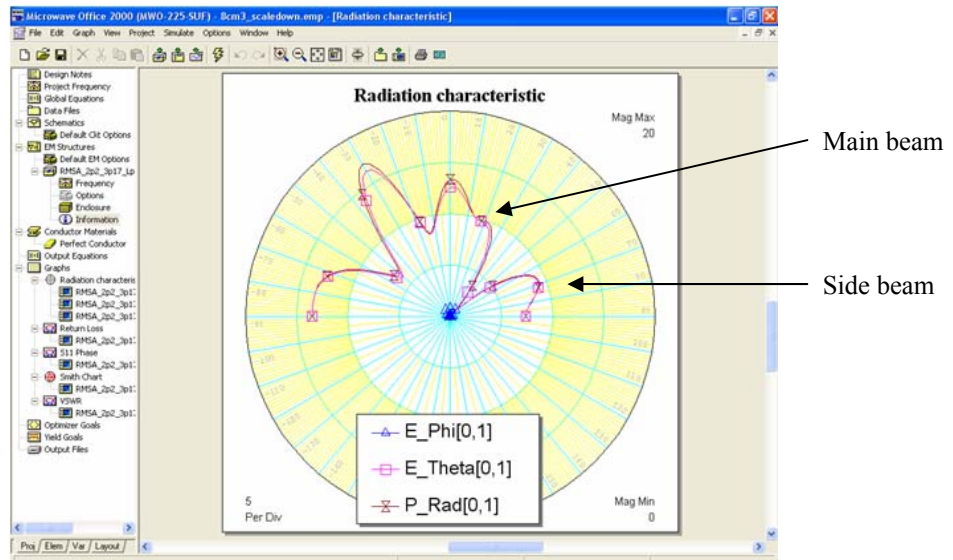


Figure 4.21 Radiation Characteristic Chart

The radiation characteristic chart in Figure 4.21 shows the radiation patterns involving the variation of field or power as a function of spherical coordinates  $\theta$  and  $\Phi$  for the 8cm triangular patch antenna. The main beam and side beam of the radiation have been labeled clearly.

### 4.2.3 Comparison of Simulation Results and Calculations

From the return loss graph in Section 4.2.2(i), Resonant Frequency,  $f_R = 9.8$  GHz

By using the formulas and similar calculations as in Section 4.1.2,

$$\begin{aligned} a_{\text{eff}} &= a + h(\epsilon_r)^{-1/2} \\ &= 8 + 0.159(2.32)^{-1/2} \\ &= 8.1044 \text{ cm} \end{aligned}$$

$$\begin{aligned} \epsilon_{\text{eff}} &= \frac{1}{2}(\epsilon_r + 1) + \frac{1}{4}(\epsilon_r - 1)\left(1 + \frac{12h}{a}\right)^{-1/2} \\ &= \frac{1}{2}(2.32 + 1) + \frac{1}{4}(2.32 - 1)\left(1 + \frac{12 \times 0.159}{8}\right)^{-1/2} \\ &= 1.95653 \end{aligned}$$

When the antenna is radiating at mode  $m, n = 5, 1$ ,

$$\begin{aligned} \text{Resonant frequency, } f_{5,1} &= \frac{2c}{3a_{\text{eff}}(\epsilon_{\text{eff}})^{1/2}}(m^2 + mn + n^2)^{1/2} \\ &= \frac{2(3 \times 10^8)}{3(8.1044 \times 10^{-2})(1.95653)^{1/2}}(5^2 + 5(1) + 1^2)^{1/2} \\ &= 9.82 \text{ GHz} \end{aligned}$$

Table 4.4 Comparison of Frequencies from Simulation and Calculation

<b>Simulated Resonant Frequency</b>	$f_R = 9.8$ GHz
<b>Calculated Resonant Frequency</b>	$f_{5,1} = 9.82$ GHz

$$\begin{aligned} \text{Deviation of simulated frequency from calculated frequency} &= \frac{9.82 - 9.8}{9.82} \times 100\% \\ &= 0.204\% \end{aligned}$$

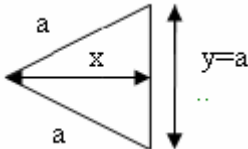
which is very small and can be neglected

### 4.3 Equilateral Triangular Single Patch Antenna with Length 10cm

#### 4.3.1 Antenna Design

A single patch equilateral triangular antenna with side length of 10cm is designed. The key parameters of the antenna are illustrated in Table 4.5.

Table 4.5 Key Parameters of Patch Antenna with Side Length of 10cm

<b>Geometry</b>	Equilateral Triangle 
<b>Size</b>	Length, $a = 10\text{cm}$ Thickness, $h = 0.159\text{cm}$
<b>Material of Patch</b>	RT Duroid 5870 with relative dielectric constant, $\epsilon_r = 2.32$
<b>Feeding Technique</b>	Single via port connected from the antenna patch to a $17.5000 \times 16.9081\text{cm}$ ground plane

The antenna is designed by using similar method as in Section 4.1.1 and 4.2.1. The cell size and dimension are computed using Mathcad and the values are entered in Microwave Office. After all parameters such as the substrate and enclosure information have been specified in Microwave Office, an equilateral triangular patch antenna with side length,  $a = 10\text{cm}$  enclosed by a box with size  $17.5000 \times 16.9081\text{cm}$  is drawn in Microwave Office.

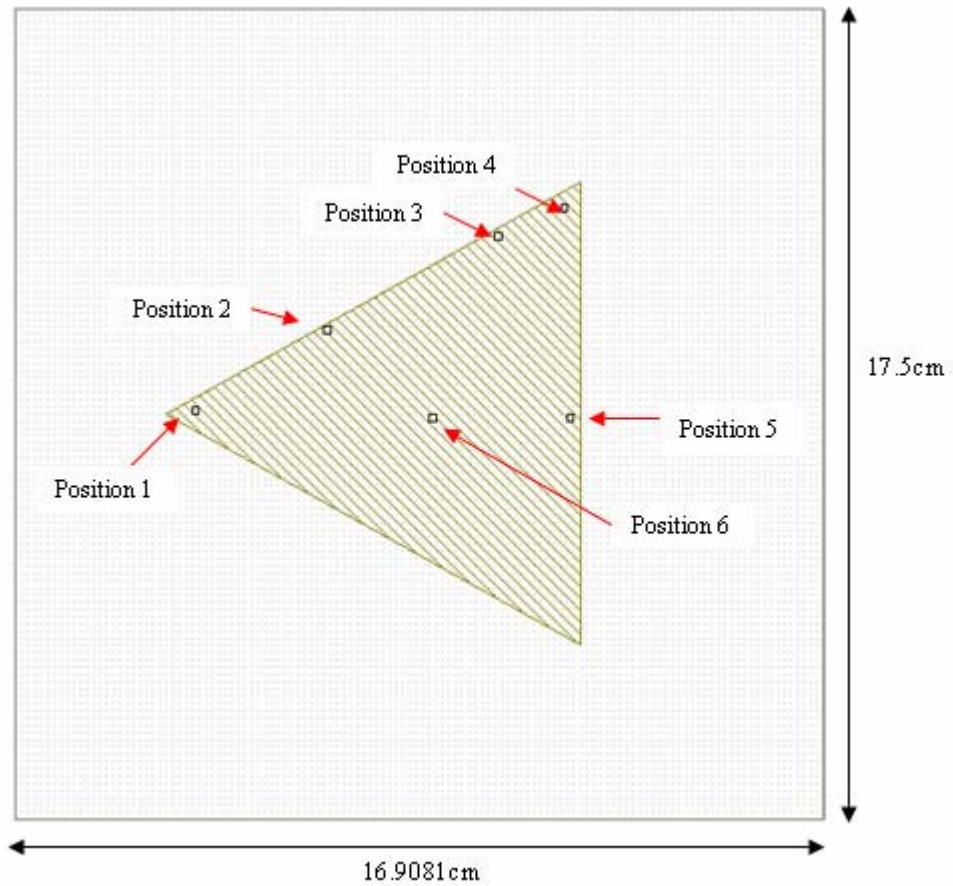


Figure 4.22 Different Positions of Via Port Tested

Simulations have been done on the patch with via port in different positions as shown in Figure 4.22. The best result is obtained when via port is placed in Position 3. Therefore, the simulation results of patch antenna with via port in position 3 as shown in Figure 4.23 and 4.24 are discussed in the following section.

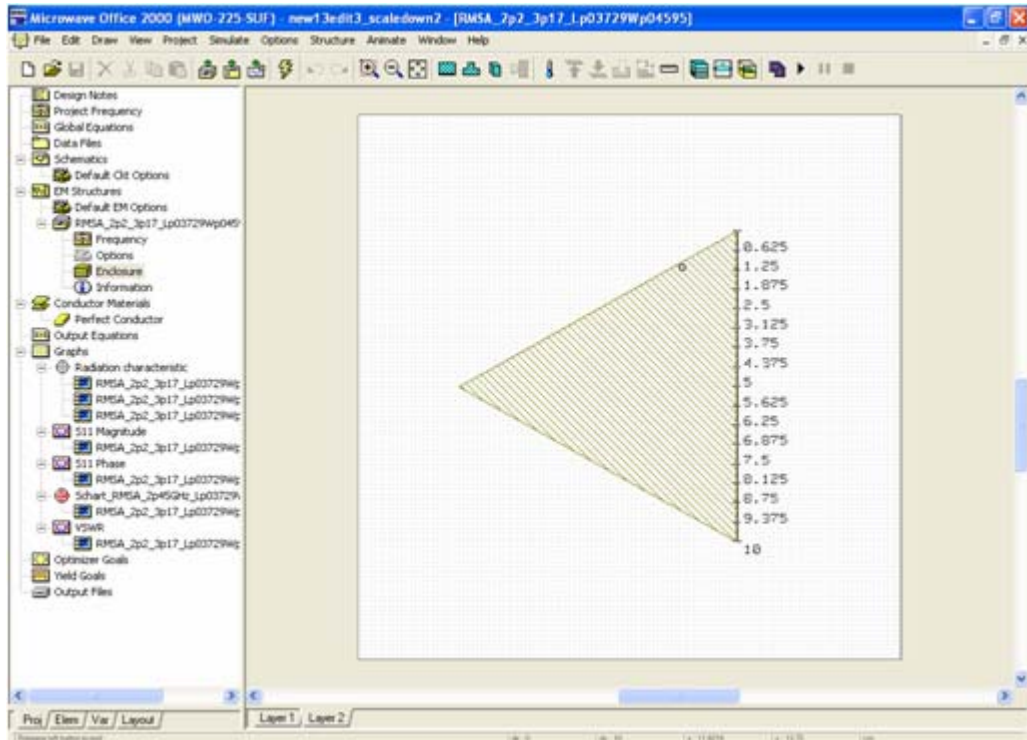


Figure 4.23 10cm Triangular Patch Antenna Design with Via Port in Best Position

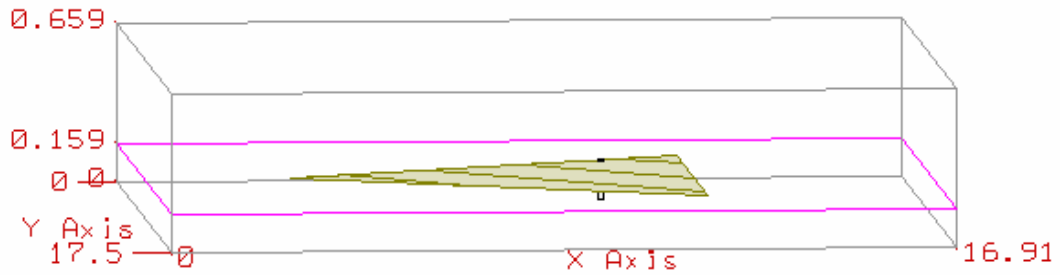


Figure 4.24 10cm Antenna Design in 3D View

### 4.3.2 Simulation Results

#### (i) Return Loss Graph

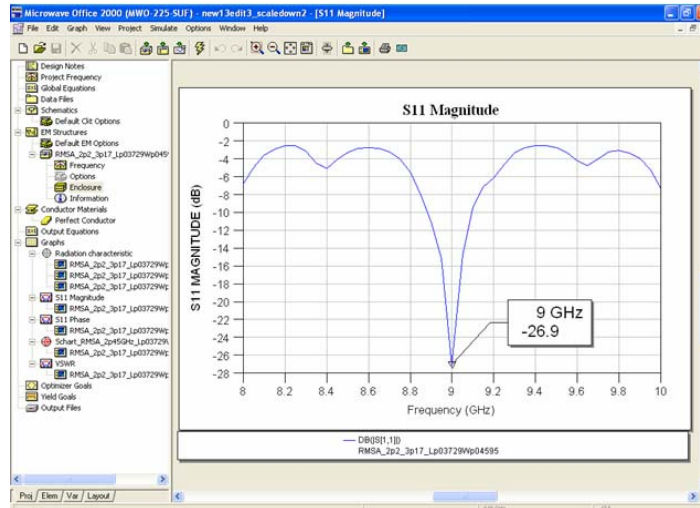


Figure 4.25 Return Loss Graph for 10cm Triangular Patch Antenna

From the graph in Figure 4.25, resonant frequency,  $f_R = 9.0$  GHz when the magnitude of return loss (in dB) reaches its minimum value. The resonant frequency of 9.0 GHz falls into the IEEE microwave region. The return loss of the patch antenna is observed to be -26.9dB. From formula 4.1, this implies that 99.8% of the power is absorbed by the antenna and only 0.20% is reflected. The deep and wide dip of the curve in the return loss graph shows that the antenna has good bandwidth (spreadband).

## (ii) VSWR Graph

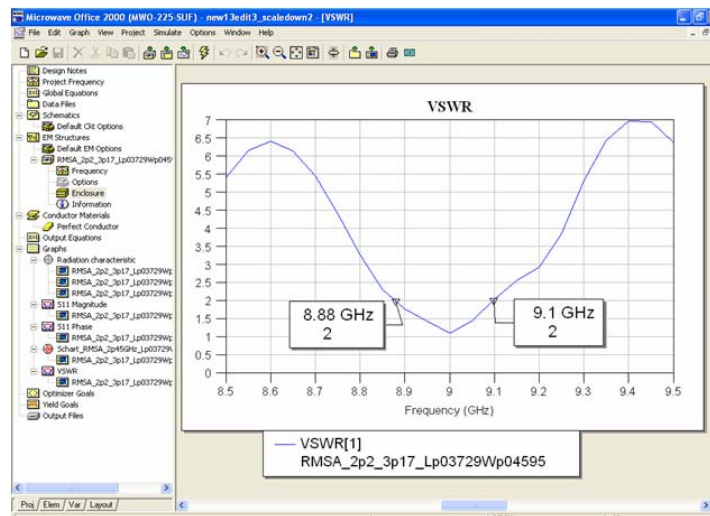


Figure 4.26 VSWR Graph of 10cm Triangular Patch Antenna

By referring to Figure 4.26, the bandwidth in which VSWR is less than 2 ranges from 8.88 GHz to 9.1 GHz. In this case,

Low frequency,  $f_L = 8.88$  GHz; and

High frequency,  $f_H = 9.1$  GHz.

These frequency values are used to calculate the bandwidth of the patch antenna.

$$\text{Bandwidth, } BW = f_H - f_L$$

$$= 9.1 \text{ GHz} - 8.88 \text{ GHz}$$

$$= 0.22 \text{ GHz}$$

$$\text{Centre frequency, } f_C = \frac{f_L + f_H}{2}$$

$$= \frac{8.88 + 9.1}{2}$$

$$= 8.99 \text{ GHz}$$

$$\begin{aligned} \text{Percentage of Bandwidth, \% BW} &= \frac{f_H - f_L}{f_c} \times 100\% \\ &= \frac{9.1 - 8.88}{8.99} \times 100\% \\ &= 2.45\% \end{aligned}$$

Thus, the 10cm equilateral triangular patch antenna occupies a bandwidth percentage of 2.45%.

### (iii) Phase Graph

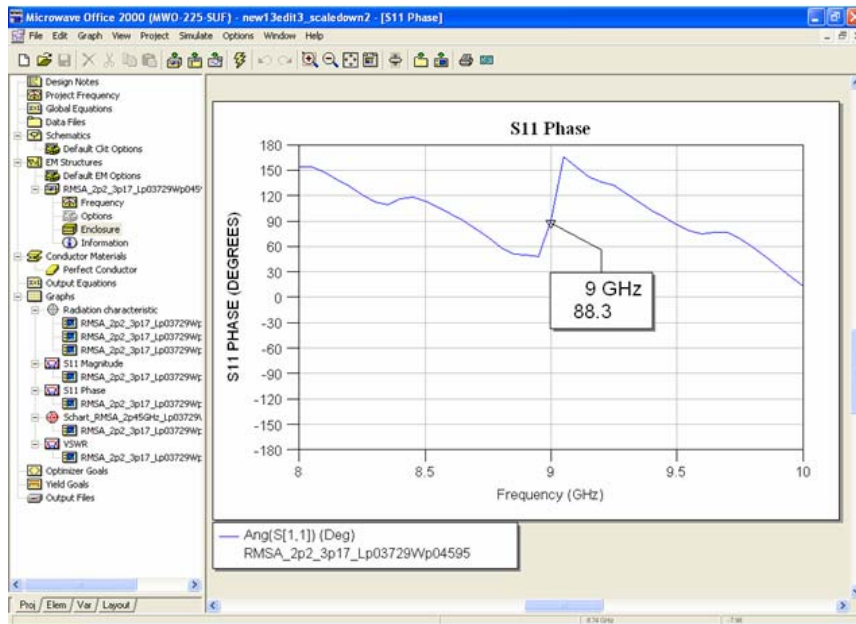


Figure 4.27 Phase Graph of 10cm Triangular Patch Antenna

Figure 4.27 shows the phase graph from the simulation of the 10cm triangular patch antenna. It has a shape similar to the ideal shape of a phase graph for an antenna.

(iv) Smith Chart

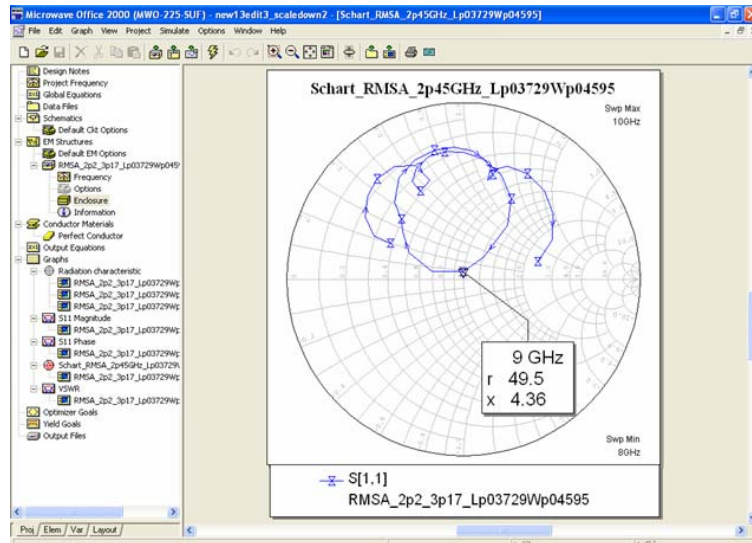


Figure 4.28 Smith Chart for 10cm Triangular Patch Antenna Radiating at 9 GHz

Smith chart of the 10cm equilateral triangular patch antenna simulation is shown in Figure 4.28. It displays a sequence of normalized impedance, admittance or reflection coefficient in a circle of unity radius. Resonant frequency of 9 GHz is displayed near the middle point of the chart. Thus, the antenna is neither inductive nor capacitive.

The chart in Figure 4.28 shows that when resonant frequency  $f_R = 9$  GHz, resistance  $r = 49.5$  and reactance  $x = 4.36$ .

Impedance,  $z = r + jx$

$$= 49.5 + j4.36$$

Magnitude of total impedance,  $|z| = \sqrt{49.5^2 + 4.36^2}$

$$= 49.69 \Omega$$

(v) Radiation Characteristic Chart

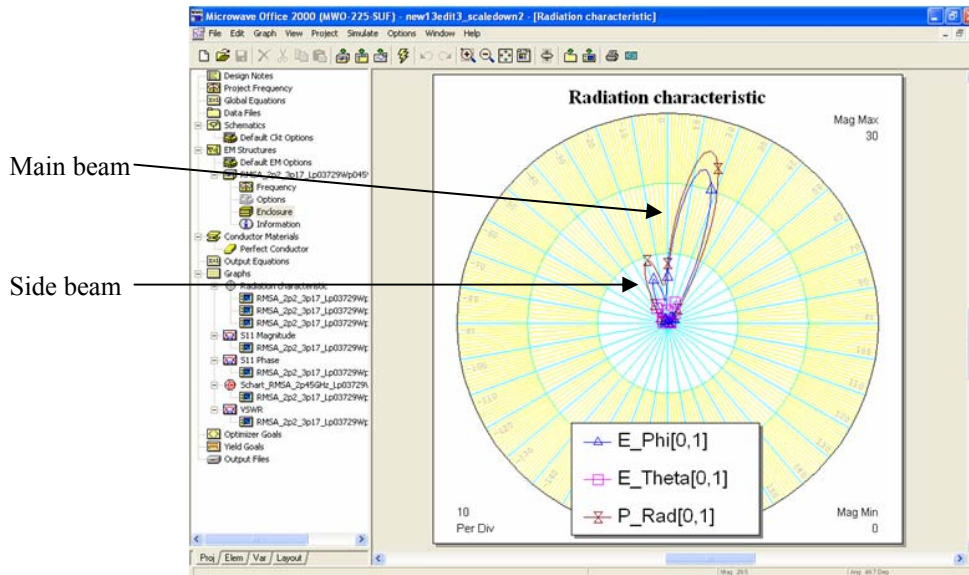


Figure 4.29 Radiation Characteristics Chart for 10cm Triangular Patch Antenna

The radiation patterns involving the variation of field or power as a function of spherical coordinates  $\theta$  and  $\Phi$  for the 10cm triangular patch antenna are shown in the radiation characteristic chart in Figure 4.29. The main beam and side beam of the radiation have been labeled accordingly.

### 4.3.3 Comparison of Simulation Results and Calculations

From the return loss graph in Section 4.3.2(i), Resonant Frequency,  $f_R = 9$  GHz

By using the formulas and similar calculations as in Section 4.1.2 and 4.2.2,

$$\begin{aligned} a_{\text{eff}} &= a + h(\epsilon_r)^{-1/2} \\ &= 10 + 0.159(2.32)^{-1/2} \\ &= 10.1044 \text{ cm} \end{aligned}$$

$$\begin{aligned} \epsilon_{\text{eff}} &= \frac{1}{2}(\epsilon_r + 1) + \frac{1}{4}(\epsilon_r - 1)\left(1 + \frac{12h}{a}\right)^{-1/2} \\ &= \frac{1}{2}(2.32 + 1) + \frac{1}{4}(2.32 - 1)\left(1 + \frac{12 \times 0.159}{10}\right)^{-1/2} \\ &= 1.96241 \end{aligned}$$

When the antenna is radiating at mode  $m, n = 5, 2$ ,

$$\begin{aligned} \text{Resonant frequency, } f_{5,2} &= \frac{2c}{3a_{\text{eff}}(\epsilon_{\text{eff}})^{1/2}}(m^2 + mn + n^2)^{1/2} \\ &= \frac{2(3 \times 10^8)}{3(10.1044 \times 10^{-2})(1.96241)^{1/2}}(5^2 + 5(2) + 2^2)^{1/2} \\ &= 8.82 \text{ GHz} \end{aligned}$$

Table 4.6 Comparison of Frequencies from Simulation and Calculation

<b>Simulated Resonant Frequency</b>	$f_R = 9.00$ GHz
<b>Calculated Resonant Frequency</b>	$f_{5,2} = 8.82$ GHz

$$\begin{aligned} \text{Deviation of simulated frequency from calculated frequency} &= \frac{9.00 - 8.82}{8.82} \times 100\% \\ &= 2.04\% \end{aligned}$$

which is very small and is acceptable

#### 4.3.4 Comparison of 5cm, 8cm, and 10cm Single Patch Antennas

Three single patch microstrip antennas of different sizes have been designed. The simulation results consisting of return loss graph, VSWR graph, phase graph, Smith chart, and radiation characteristics chart have been analyzed.

Table 4.7 Summary of Important Parameters for Microstrip Single Patch Antennas

Antenna Side Length, a (cm)	Comparison of Simulated & Calculated Resonant Frequency			Return Loss (dB)	Bandwidth (%)	Impedance,  z  ( $\Omega$ )
	Simulated Frequency (GHz)	Calculated Frequency (GHz)	Deviation (%)			
5	12.4	12.26	1.14	-17.8	4.05	37.71
8	9.8	9.82	0.204	-28.4	2.64	50.25
10	9	8.82	2.04	-26.9	2.45	49.69

Table 4.7 summarizes the important parameters of the three single patch antennas designed. Generally, the frequency obtained from simulation is only slightly deviated from the calculated frequency which is less than 3% and is acceptable. It is observed that when the size of the patch antenna is increased, the resonant frequency decreases. This proves that the frequency of antenna is inversely proportional to the antenna size.

In conclusion, all simulation results are satisfactory and acceptable.

#### **4.3.5 Causes of Inaccuracy in Simulation Results**

For the three microstrip single patch antennas designed in Section 4.1, 4.2, and 4.3, deviation of less than 3% exists between the resonant frequencies obtained from simulation results and calculation. Simulation results vary slightly from calculated value or results obtained from experimental setup due to the following factors:

##### **(i) Development of Equations Based on Other Simulation and Experimental Methods**

Equations used to calculate the resonant frequencies in this project such as equations 4.2, 4.3, 4.4, and 4.5 were developed mainly based on experimental results. Even if simulation results were used as references, most developers of the equations used simulation methods such as Method of Moment Commercial Code, but not Microwave Office. Thus, Microwave Office simulation results might slightly differ from the frequencies calculated from those equations.

##### **(ii) Inaccuracy of Triangular Antenna's Shape and Size**

In Microwave Office, antenna patches drawn are made up of small square grids. The size of the grid depends on the dimension and number of divisions set. One of the limitations faced when drawing triangular patches on Microwave Office is the inaccuracy of shape and size. Initially, an equilateral triangular antenna with smooth and straight sides as shown in Figure 4.30 is designed, but Microwave Office simulation only concerns grids contained within the drawing, hence causing two of the three sides of the triangle to become zigzag in shape, as shown in Figure 4.31. This results in deviation from the actual shape, geometry, and size. Figure 4.30 and 4.31 illustrate the

difference between the desired triangular patch designed and the simulated triangular patch.

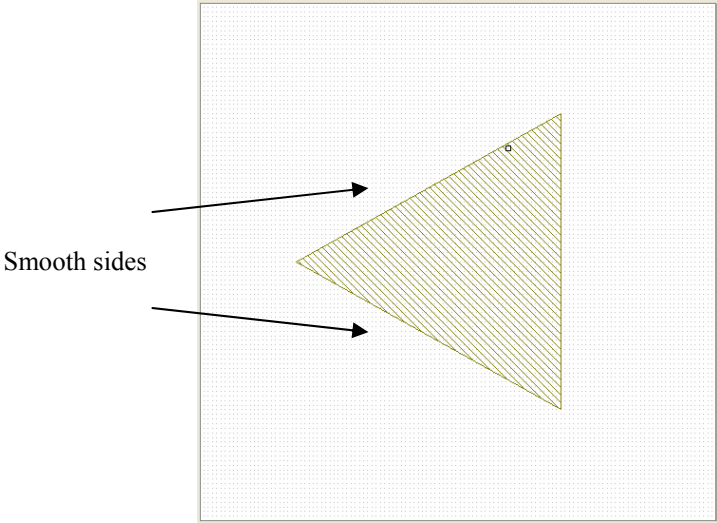


Figure 4.30 Actual Shape and Size of Antenna Patch

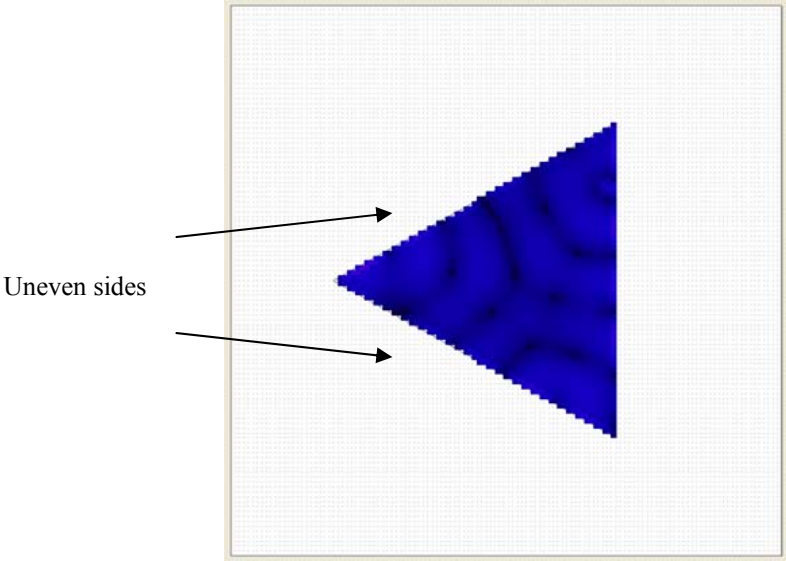


Figure 4.31 Antenna Patch Simulated By Microwave Office

### **(iii) Size of Via Port**

The size of feed point from the antenna patch to ground plane affects the overall performance of a patch antenna. The smaller the feed point, the better and more accurate the results will be. In Microwave Office, the minimum size of a via port (transmission line) connected from the antenna patch to the ground plane is the size of a grid, which is a square. The size of via port is relatively large if compared to the size of a coaxial feed line normally used in real case. For example, in Section 4.2.1, the size of via port is 0.13746435cm x 0.15625cm. This size is relatively large compared to a practical coaxial feed line. Via port (transmission line) of large size can act as an antenna by itself. It can create and produce spurious radiation, which is an unintentional emission. The interference of the spurious radiation and the desired radiation from the patch antenna will cause deviation and inaccuracy in the simulation results.

### **(iv) Transmission Line Loss and Other Losses**

Simulation processes normally consider ideal conditions. In Microwave Office, simulation results are based on ideal antenna without considerations of imperfection such as losses of transmission line.

Transmission line allows the mounting of antenna in a clear location for the lowest propagation loss. They are also the interface between an antenna and a receiver or transmitter. Therefore the transmission line is one of the most important considerations when designing antenna. Some of the power fed into a transmission line is lost because of its resistance, which is referred to as ohmic or resistive loss. Losses are also incurred in the soldering of transmission line to the antenna. Like the antenna selection, the

transmission line is in the receiver and the transmitter path. Hence, any loss in the transmission line is doubled. If 1 dB transmission line loss occurs, the overall system loss is really 2 dB, 1 dB on the receive side and 1 dB on the transmit side. However, in simulations, it is assumed that there is no transmission line loss, which can never be achieved in practical. This results in inaccuracy of simulation results.

At high frequencies, the effect of dielectric loss becomes significant, adding to the losses caused by resistance. Dielectric loss is incurred when the insulating material inside the transmission line absorbs energy from the alternating electric field and converts it to heat. In the simulation process of microwave frequency antennas, the assumption of no loss is made. Therefore, this inadvertently leads to inaccuracy of simulation results.

## 4.4 Microstrip Patch Antenna with Classical Sierpinski Fractal Geometry

### 4.4.1 Antenna Design and Power Radiation Pattern

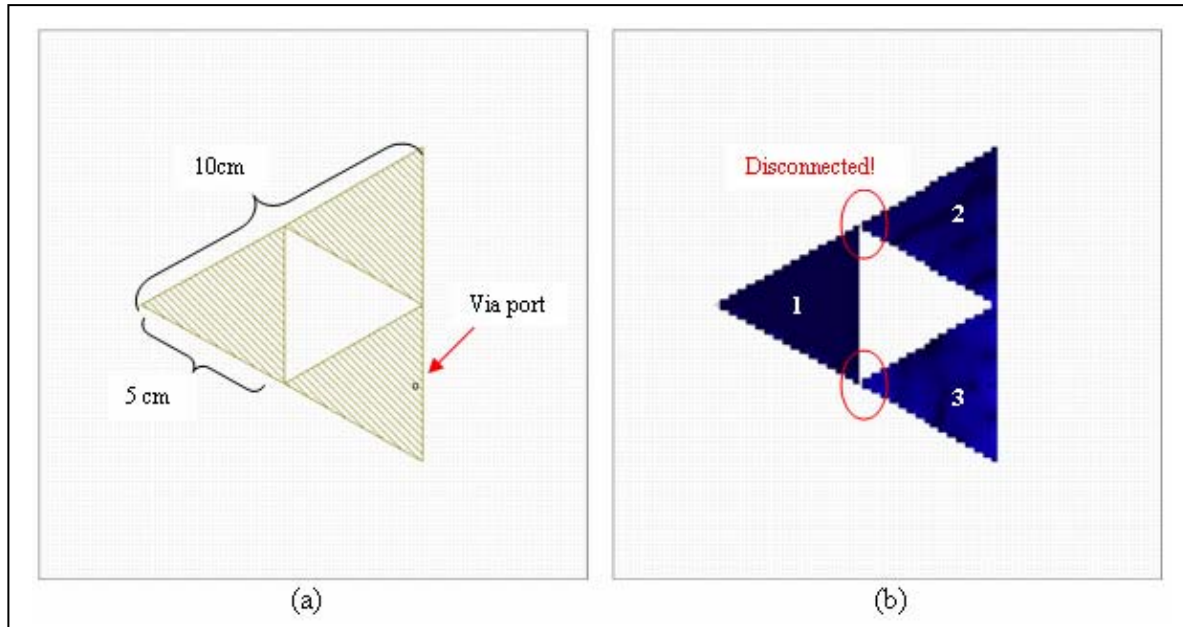


Figure 4.32

(a) Initial Design of Classic Sierpinski Antenna, (b) Corresponding Power Radiation

A microstrip patch antenna with Classic Sierpinski Fractal Geometry is designed in Microwave Office. The side length of the main antenna patch is 10cm and the sub patches have 5cm side length, as shown in Figure 4.32(a). The patch antenna has thickness,  $h = 0.159\text{cm}$  and relative dielectric constant,  $\epsilon_r = 2.32$ . It is fed by a single via port from the patch to ground plane. The power radiation as shown in Figure 4.32(b) implies that sub patches 2 and 3 are not properly connected to sub patch 1 due to the limitation of grids in Microwave Office, and the power is not radiated uniformly from

the via port to the three sub patches. As a consequence, an improved structure of the Classic Sierpinski fractal geometry must be designed in Microwave Office in order to achieve uniform power radiation and accurate results.

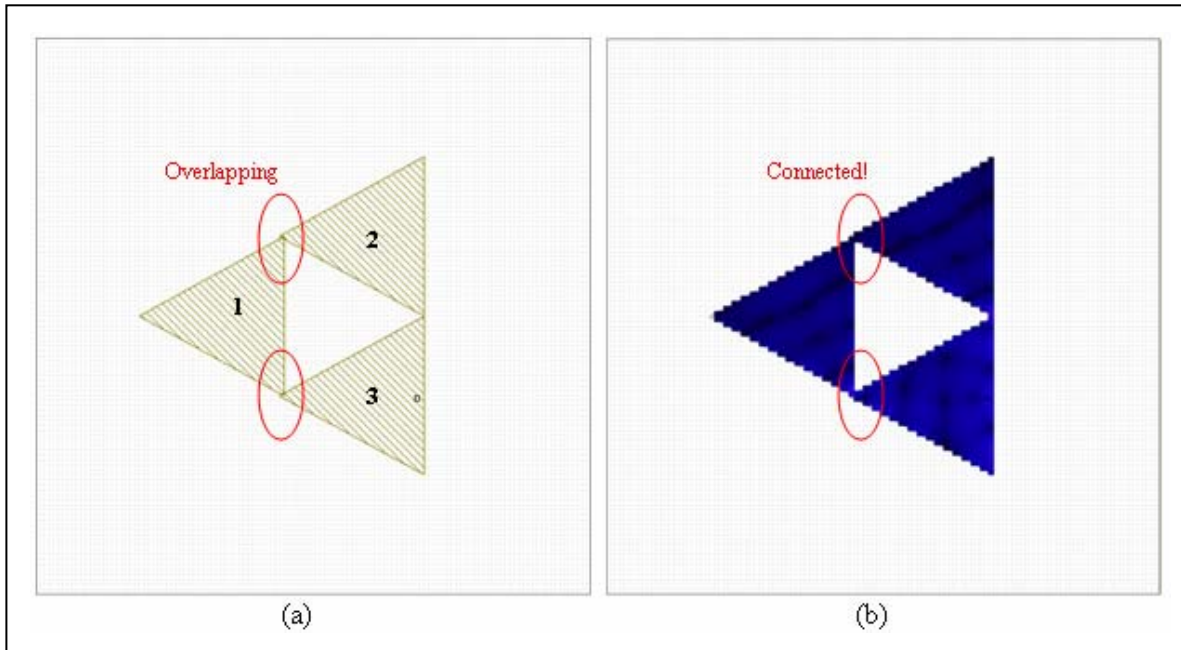


Figure 4.33

(a) Improved Design of Classic Sierpinski Antenna, (b) Corresponding Power Radiation

Figure 4.33(a) illustrates an improved drawing of Classic Sierpinski patch antenna in Microwave Office. Sub patches 2 and 3 are overlapped with sub patch 1. With this, the three sub patches are properly connected by square grids and power is radiated uniformly from via port to all the sub patches, as shown in Figure 4.33(b). Thus, in the following sections, the improved geometry of Classic Sierpinski antenna is used for simulation purpose.

#### 4.4.2 Determination of the Best Via Port Position

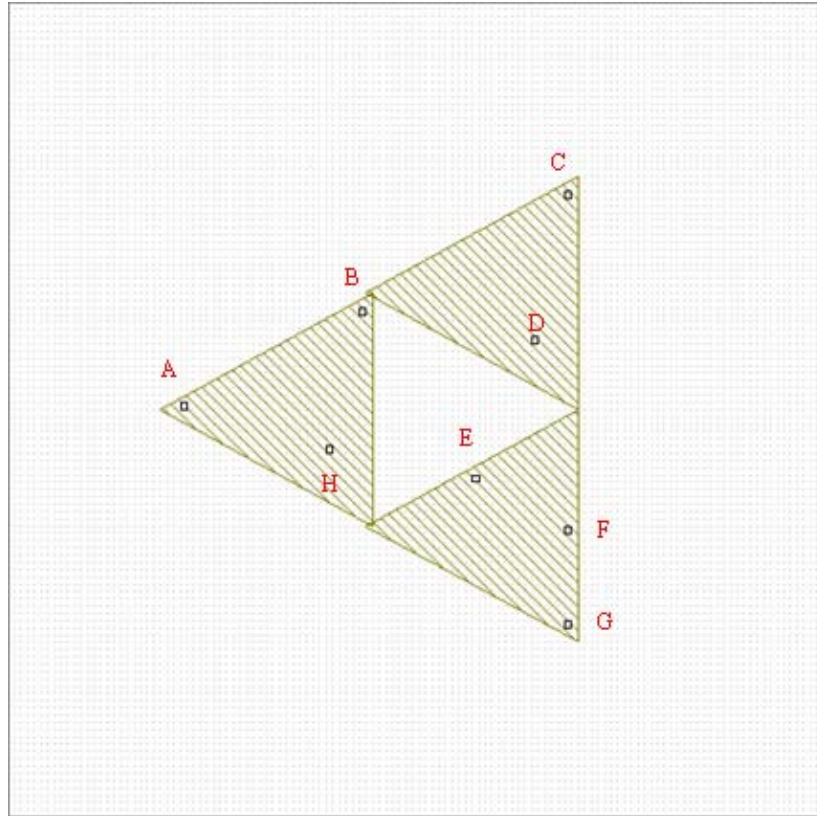


Figure 4.34 Different Positions of Via Port

Via port has been placed in different positions within the improved Classical Sierpinski patch antenna and the antenna simulated to get the average percentage of bandwidth. Figure 4.34 illustrates the positions of via port tested. This aims to determine the best position of via port to achieve the largest bandwidth.

Table 4.8 Average Bandwidth Corresponding to Different Via Port Position

<b>Via Port Position</b>	<b>Average Bandwidth (%)</b>
A	4.03
B	5.84
C	5.88
D	5.10
E	5.08
F	6.44
G	4.81
H	4.97

Table 4.8 summarizes the average bandwidth obtained within the frequency simulation range of 6GHz to 30GHz for the improved design of Classical Sierpinski antenna in Figure 4.33(a) with via ports in different positions as shown in Figure 4.34. It can be observed that the largest bandwidth is obtained when via port is placed in Position F.

The following section shows the detailed results of simulation for the Classical Sierpinski fractal antenna of second iteration with via port in position F. The antenna has been constructed through two iterations, so two-scaled versions of the Sierpinski gasket are found on the antenna. If the contribution of the center hole to the antenna performance is neglected and the current flowing from the feeder concentrates over a region that is comparable in size to the wavelength, a behavior similar to two-scaled bow-tie antennas (each one operating at its resonant frequencies) could be expected.

### 4.4.3 Simulation Results

This section illustrates the simulation results for the improved Classical Sierpinski antenna as shown in Figure 4.33(a) over a simulated frequency range of 6GHz to 26GHz.

#### (i) Return Loss Graph

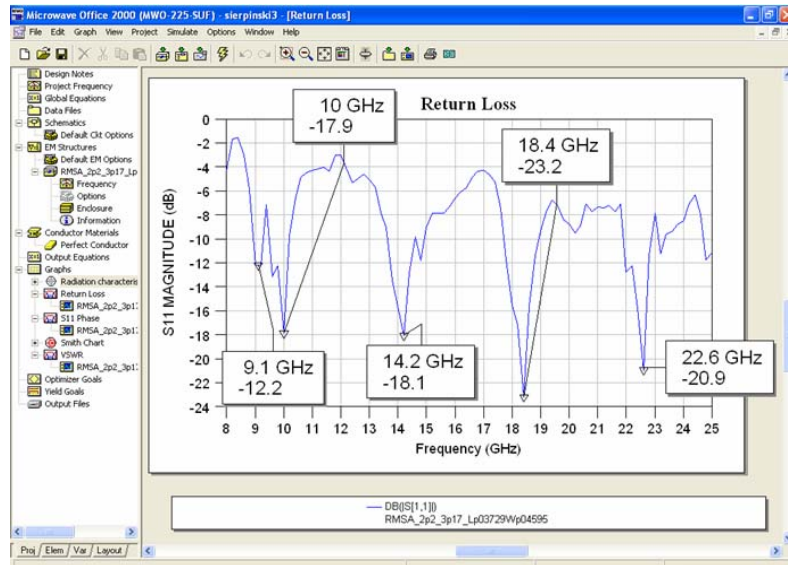


Figure 4.35 Return Loss Graph of Classical Sierpinski Antenna

By referring to Figure 4.35, the Classical Sierpinski antenna is operating at multiple resonant frequencies within the range of 8GHz to 25GHz – 9.1GHz, 10GHz, 14.2GHz, 18.4GHz, and 22.6GHz. With Sierpinski fractal geometry, the main triangular patch with 10cm length and sub patches with 5cm length are operating at more than one radiation mode each that contribute to multi-frequency behavior. This is desirable as one antenna is capable of radiating at multiple different frequency range, thus useful for transmitting and receiving microwave signals of different frequencies simultaneously.

(ii) VSWR Graph

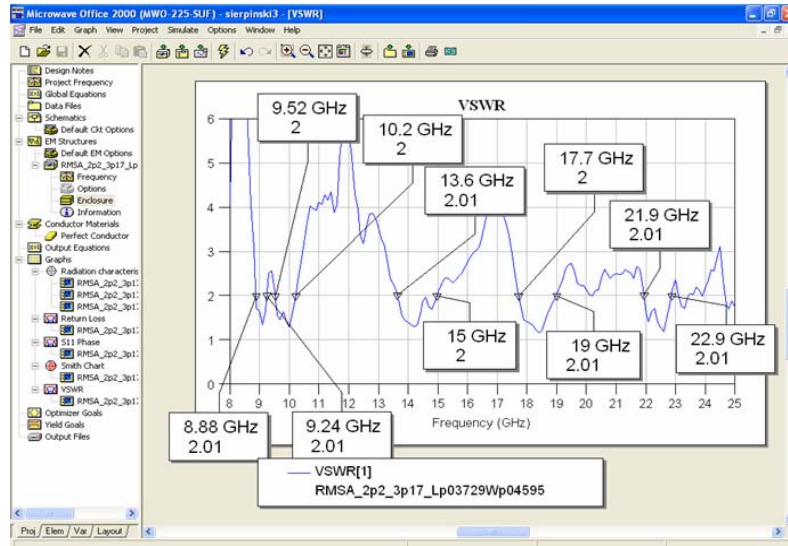


Figure 4.36 Return Loss Graph of Classical Sierpinski Antenna

By referring to Figure 4.36, the second iteration Classical Sierpinski fractal antenna occupies five bandwidths that correspond to its five resonant frequencies.

(iii) Smith Chart

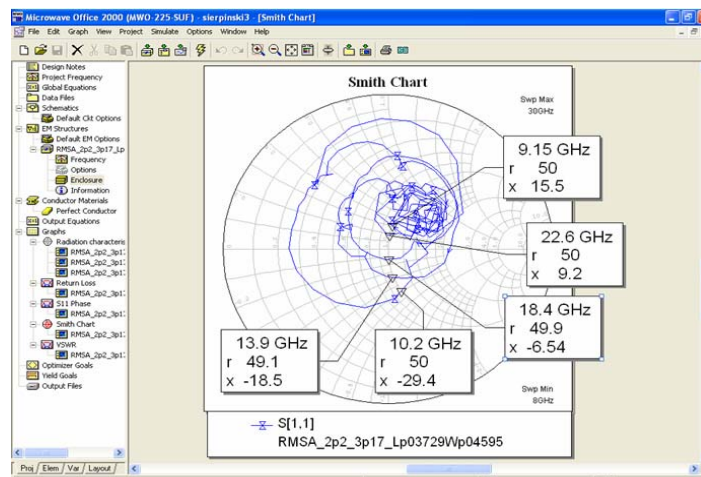


Figure 4.37 Smith Chart of Classical Sierpinski Antenna

Smith chart of the Classical Sierpinski antenna is shown in Figure 4.37. All the resonant frequency points are distributed near the center of the chart. Thus, the antenna is neither inductive nor capacitive.

Table 4.9 Main Parameters of the Simulated Classical Sierpinski Antenna

<b>Resonant Frequency, <math>f_R</math> (GHz)</b>	<b>Return Loss (dB)</b>	<b>Bandwidth Range (GHz)</b>	<b>Percentage of Bandwidth (%)</b>	<b>Impedance, <math>z = r + jx</math></b>	<b>Impedance Magnitude, <math> z </math> (<math>\Omega</math>)</b>
9.1	-12.2	8.88 – 9.24	3.97	$z = 50.0 + j15.5$	52.3
10.0	-17.9	9.52 – 10.20	6.90	$z = 50.0 - j29.4$	58.0
14.2	-18.1	13.60 – 15.00	9.80	$z = 49.1 - j18.5$	52.5
18.4	-23.2	17.70 – 19.00	7.08	$z = 49.9 - j6.54$	50.3
22.6	-20.9	21.90 – 22.90	4.46	$z = 50.0 + j9.2$	50.8

The five different resonant frequencies, return losses, bandwidths, and impedances of the fractal antenna derived from simulation results shown in Figures 4.35, 4.36, and 4.37 are summarized in Table 4.8.

$$\text{Average percentage of bandwidth} = \frac{3.97+6.90+9.80+7.08+4.46}{5} = 6.44\%$$

From the results displayed in Table 4.9, it is shown that the microstrip patch antenna designed based on the Classical Sierpinski fractal geometry is a multiband antenna that keeps a notable degree of similarity through the bands, with a moderate bandwidth at each one. It is possible to obtain more frequency band if the frequency range of simulation is enlarged as each iteration of the triangle is capable of radiating at more than one radiation mode, thus resulting in more than one resonant frequency and bandwidth.

#### (iv) Radiation Characteristics Chart

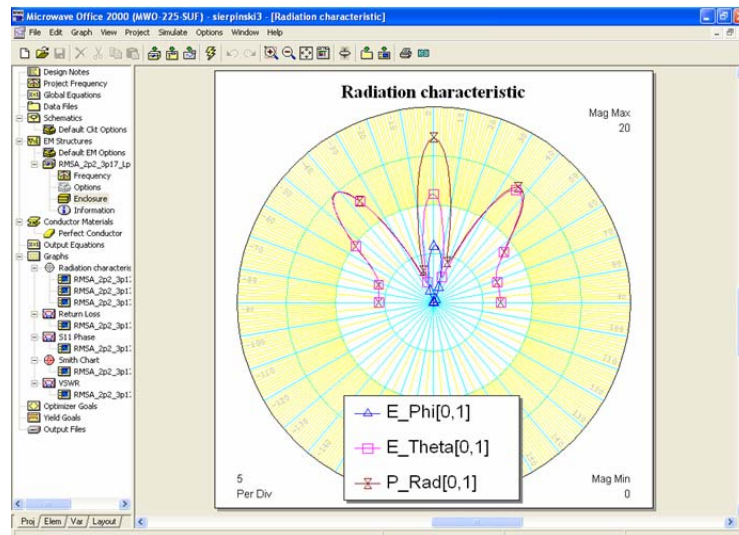


Figure 4.38 Radiation Characteristics of Classical Sierpinski Antenna

The radiation characteristic of the Classical Sierpinski antenna is illustrated in Figure 4.38. As shown by the chart, the power radiation only covers a relatively small area of region, and is sub-divided and contained in three major beams. In reality, radiation pattern with a wide coverage area contained within the minimal number (preferably one or two) of beam is desirable.

## 4.5 Microstrip Patch Antenna with Modified Sierpinski Fractal Geometry

### 4.5.1 P3/5SPK Geometry

#### 4.5.1.1 Antenna Design

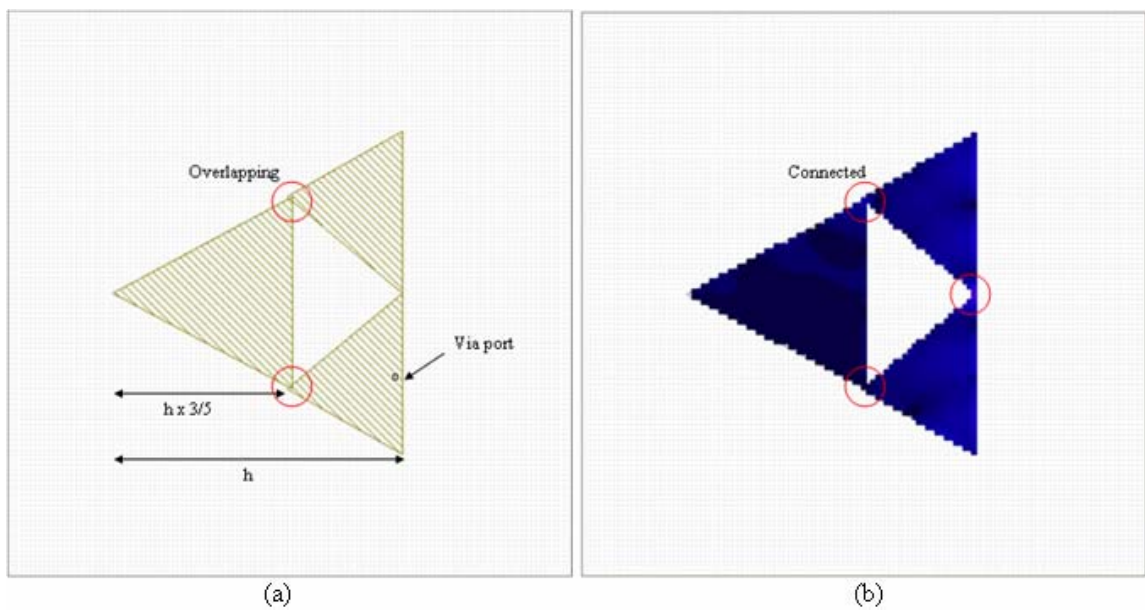


Figure 4.39 (a) P3/5SPK Antenna (b) Power Radiation

A microstrip patch antenna with modified Sierpinski fractal geometry is designed. The primary patch has a side length of 10cm and all other parameters similar to the antenna designed in Section 4.5, except that the geometry of the second iteration is perturbed. Apart from the geometry, all parameters are kept to be constant so that geometry is the only variable that affects the performance of the antenna. At second iteration stage, a reduction factor of  $3/5$  is found on the lower triangular cluster of the

first antenna, hereafter named P3/5SPK, which shorts for ‘Perturbed 3/5 Sierpinski’. The antenna design and power radiation pattern are shown in Figure 4.39.

#### 4.5.1.2 Simulation Results

##### (i) Return Loss Graph

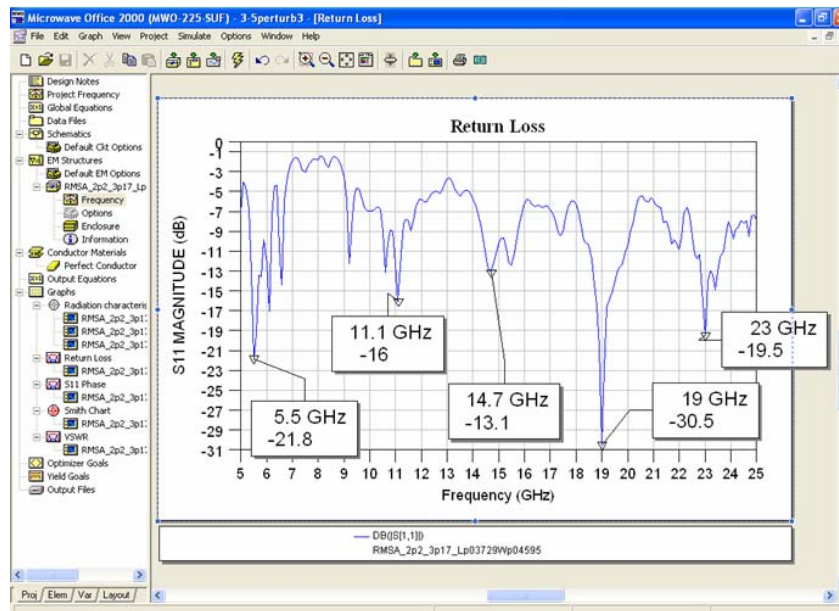


Figure 4.40 Return Loss Graph of P3/5SPK Antenna

By referring to Figure 4.40, the P3/5SPK antenna is operating at five resonant frequencies within the range of 8GHz to 25GHz – 5.5GHz, 11.1GHz, 14.7GHz, 19GHz, and 23GHz. With P3/5SPK fractal geometry, the main triangular patch with 10cm length and the three sub patches with two different sizes are operating at one or more radiation mode each that contribute to multi-frequency behavior.

## (ii) VSWR Graph

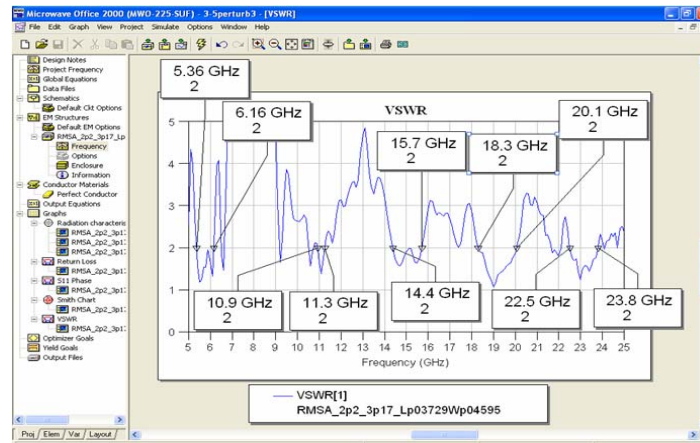


Figure 4.41 VSWR Graph of P3/5SPK Antenna

From Figure 4.41, it can be observed that by perturbing the characteristic scale factor of the fractal shape, the radiating bands of antenna can be shifted. However, the modified antenna still operates at five bandwidths corresponding to its five resonant frequencies.

## (iii) Smith Chart

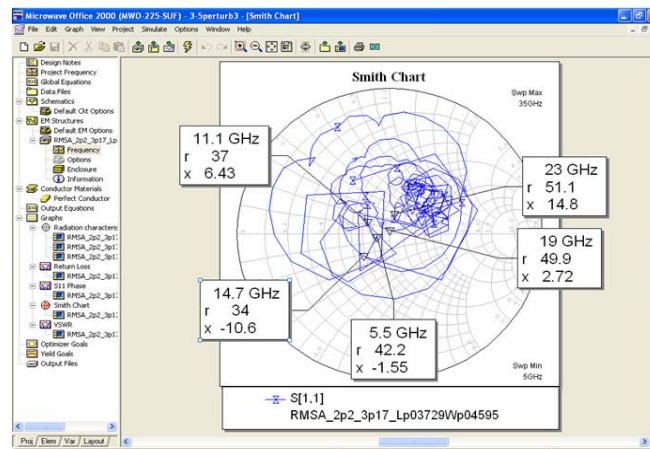


Figure 4.42 Smith Chart From P3/5SPK Antenna Simulation

Smith chart of the 3/5 perturbed Sierpinski antenna is shown in Figure 4.42. All the resonant frequency points are distributed near the center of the chart, which is desirable for a non-capacitive and non-inductive antenna.

Table 4.10 Main Parameters of the P3/5SPK Antenna

<b>Resonant Frequency, <math>f_R</math> (GHz)</b>	<b>Return Loss (dB)</b>	<b>Bandwidth Range (GHz)</b>	<b>Percentage of Bandwidth (%)</b>	<b>Impedance, <math>z = r + jx</math></b>	<b>Impedance Magnitude, <math> z </math> (<math>\Omega</math>)</b>
5.5	-21.8	5.36 – 6.16	13.89	$z = 42.2 - j1.55$	42.2
11.1	-16.0	10.90 – 11.30	3.60	$z = 37.0 + j6.43$	37.6
14.7	-13.1	14.40 – 15.70	8.64	$z = 34.0 - j10.6$	35.6
19.0	-30.5	18.30 – 20.10	9.38	$z = 49.9 + j2.72$	50.0
23.0	-19.5	22.50 – 23.80	5.62	$z = 51.1 + j14.8$	53.2

Table 4.10 summarizes all the resonant frequencies, return losses, bandwidths, and impedances of the P3/5SPK antenna derived from simulation results.

$$\text{Average percentage of bandwidth} = \frac{13.89 + 3.60 + 8.64 + 9.38 + 5.62}{5} = 8.23\%$$

From the results in Table 4.10, it is shown that the microstrip patch antenna designed based on the 3/5 perturbed Sierpinski fractal geometry is a multiband antenna. This antenna has an average bandwidth of 8.23%, which shows improvement from the Classic Sierpinski antenna with an average bandwidth of 6.44%.

(iv) Radiation Characteristics Chart

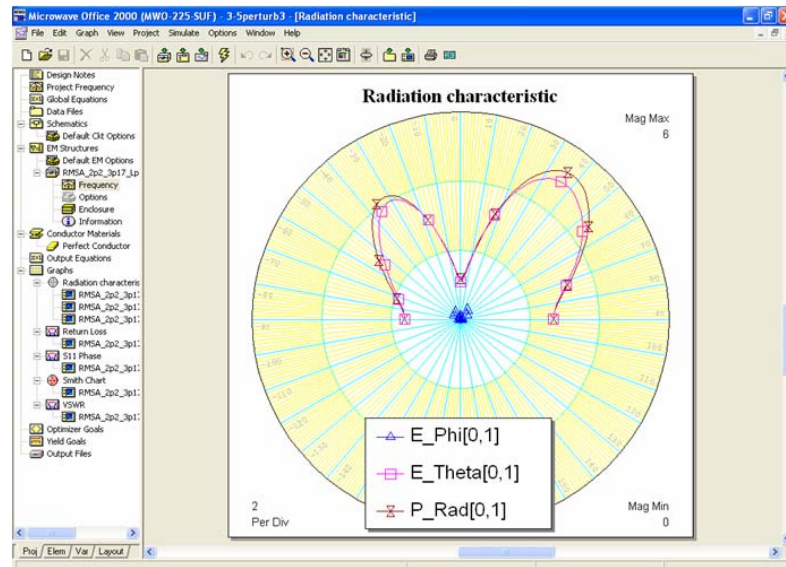


Figure 4.43 Radiation Characteristic of P3/5SPK Antenna

Figure 4.43 illustrates the radiation characteristic of the P3/5SPK antenna. As shown in the chart, the power radiation covers a moderate size of region, and is subdivided and contained in two major beams. It shows some improvements from the Classical Sierpinski antenna in Section 4.4.3 in term of coverage area size contained within reduced number of beams.

## 4.5.2 P3/4SPK Geometry

### 4.5.2.1 Antenna Design

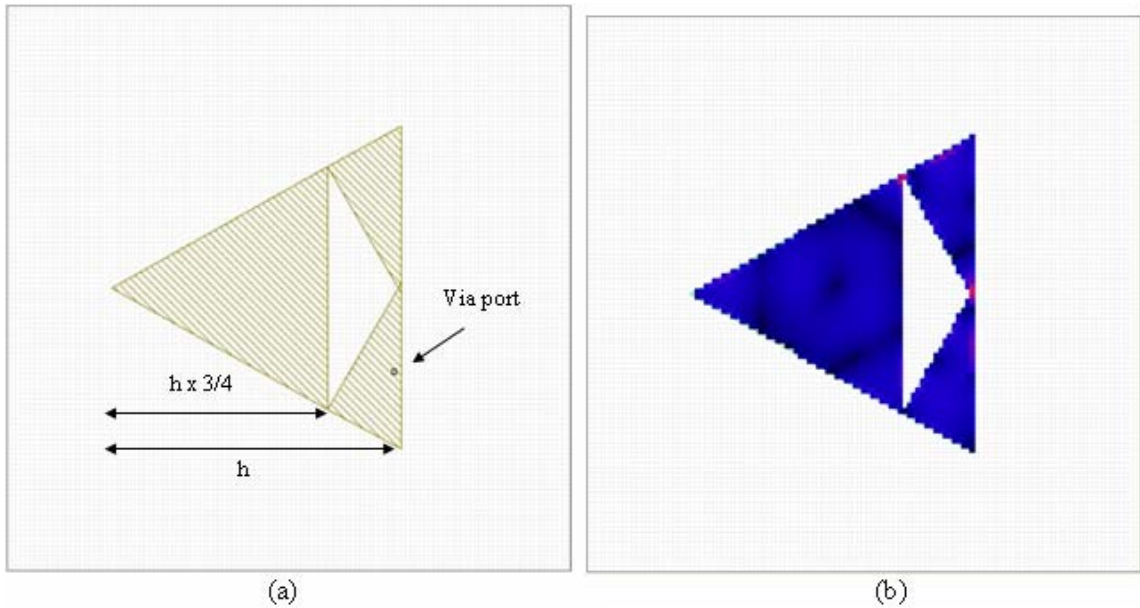


Figure 4.44 (a) P3/4SPK Antenna (b) Power Radiation

A microstrip patch antenna with P3/4SPK modified Sierpinski fractal geometry is designed. At second iteration stage, a reduction factor of  $3/4$  is found on the lower triangular cluster of the first antenna, hereafter named P3/4SPK. This antenna has a higher perturbation level than that designed in Section 4.5.1. All parameters are similar to the antennas designed in Sections 4.4 and 4.5.1, except the perturbed geometry so that geometry is the only variable that affects the performance of the antenna. The antenna design and power radiation pattern are shown in Figure 4.44.

## 4.5.2.2 Simulation Results

### (i) Return Loss Graph

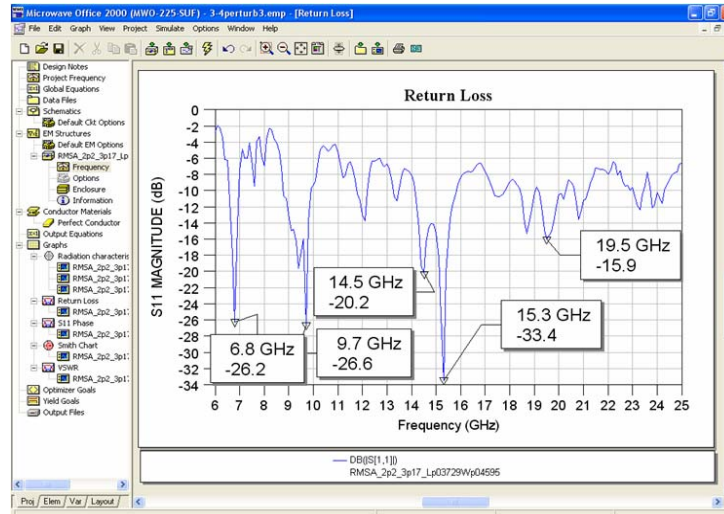


Figure 4.45 Return Loss Graph of P3/4SPK Antenna

### (ii) VSWR Graph

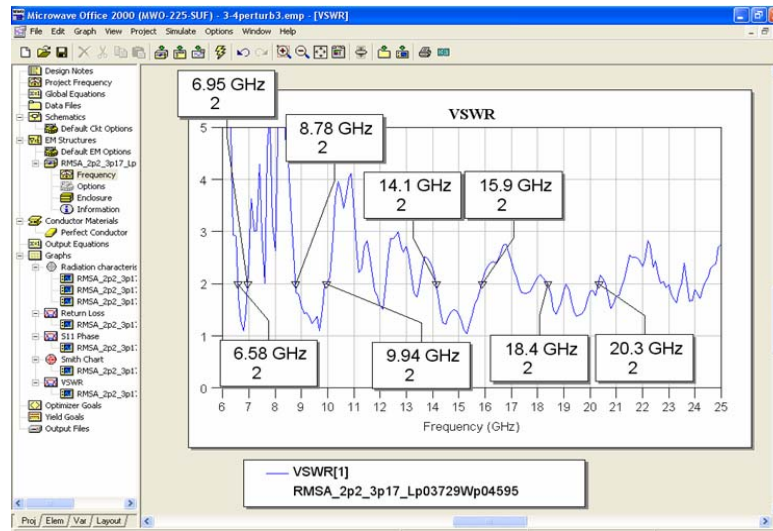


Figure 4.46 VSWR Graph of P3/4SPK Antenna

From Figures 4.45 and 4.46, it is observed that by perturbing the characteristic scale factor of the fractal shape, the radiating bands of antenna can be shifted. However, the modified antenna still operates at five bandwidths corresponding to its five resonant frequencies.

### (iii) Smith Chart

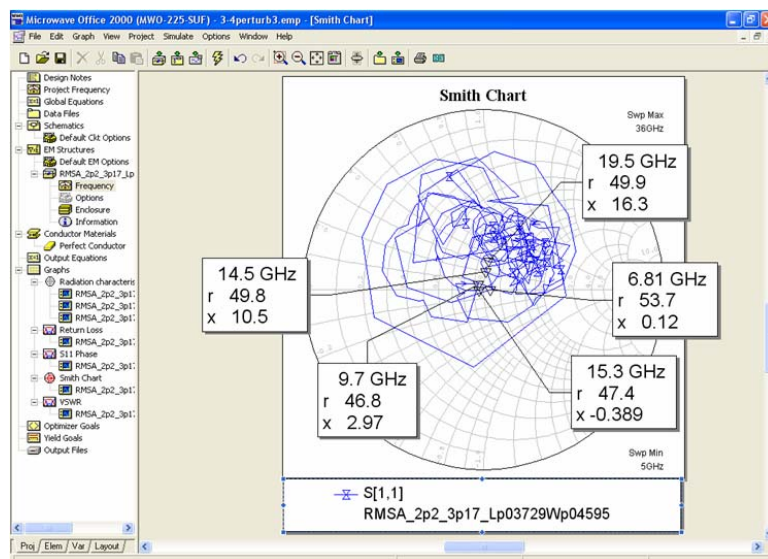


Figure 4.47 Smith Chart of P3/4SPK Antenna Simulation

Figure 4.47 shows the Smith chart of the 3/4 perturbed Sierpinski antenna. All the resonant frequencies are located near the center of the chart, which is desirable for a non-capacitive and non-inductive antenna.

Table 4.11 Main Parameters of the P3/4SPK Antenna

<b>Resonant Frequency, <math>f_R</math> (GHz)</b>	<b>Return Loss (dB)</b>	<b>Bandwidth Range (GHz)</b>	<b>Percentage of Bandwidth (%)</b>	<b>Impedance, <math>z = r + jx</math></b>	<b>Impedance Magnitude, <math> z </math> (<math>\Omega</math>)</b>
6.8	-26.2	6.58 - 6.95	5.47	$z = 53.7 + j0.12$	53.7
9.7	-26.6	8.78 - 9.94	12.39	$z = 46.8 + j2.97$	46.9
14.5	-20.2	14.10 - 15.90	12.00	$z = 49.8 + j10.5$	50.9
15.3	-33.4			$z = 47.4 - j0.389$	47.4
19.5	-15.9	18.4 - 20.3	9.82	$z = 49.9 + j16.3$	52.5

Table 4.11 summarizes all the resonant frequencies, return losses, bandwidths, and impedances of the P3/4SPK antenna derived from simulation results.

$$\text{Average percentage of bandwidth} = \frac{5.47 + 12.39 + 12.00 + 9.82}{4} = 9.92\% \approx 10\%$$

The results in Table 4.11 imply that the microstrip patch antenna designed based on the 3/4 perturbed Sierpinski fractal geometry is a multiband antenna. This antenna has an average bandwidth of approximately 10%, which shows vast improvement from the Classic Sierpinski antenna with an average bandwidth of 6.44% and P3/5SPK antenna with an average bandwidth of 8.23%. Thus, the higher the perturbation level of the Sierpinski geometry, the larger bandwidth the antenna will exhibit.

#### (iv) Radiation Characteristics Chart

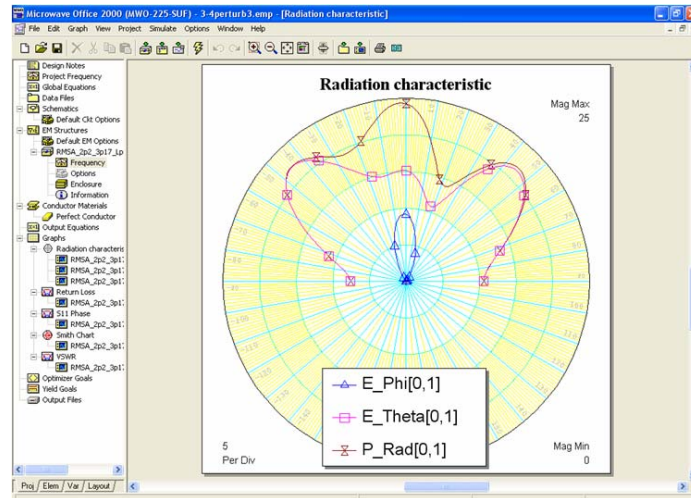


Figure 4.48 Radiation Characteristic of P3/4SPK Antenna

The radiation characteristic of the P3/4SPK antenna is shown in Figure 4.48. It is clearly shown on the chart that the power radiation exhibits a huge coverage of area, and the radiation is all contained within one major beam. It shows great improvements if compared to the Classical Sierpinski antenna in Section 4.5.3 which only has a narrow coverage area divided into three beams, and the P3/5SPK antenna which exhibits a moderate area of coverage divided into two beams.

### 4.5.3 Comparison of Classical Sierpinski, P3/5SPK, and P3/4SPK Antennas

Table 4.12 Comparison of Classical Sierpinski, P3/5SPK, and P3/4SPK Antennas

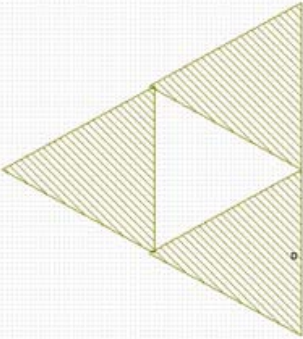
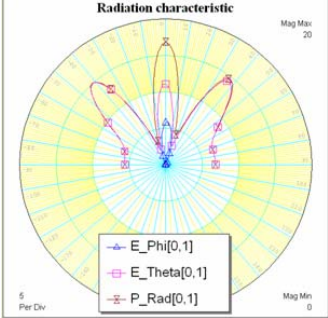
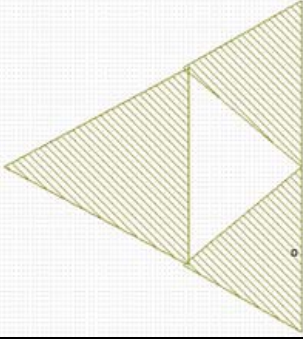
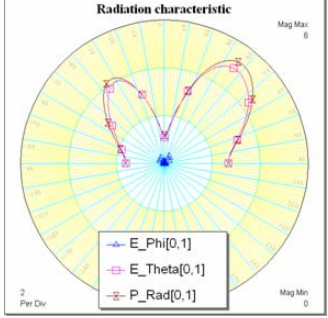
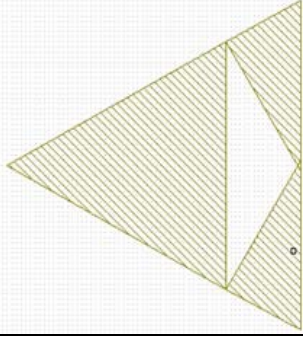
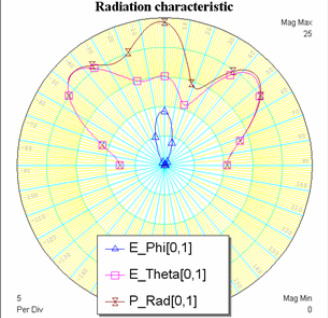
Antenna Geometry	Antenna 2D Design	Bandwidth (%)	Radiation Characteristics
Classic Sierpinski		6.44	
P3/5SPK Modified Sierpinski		8.23	
P3/4SPK Modified Sierpinski		9.92	

Table 4.12 compares the structure, bandwidth and radiation characteristics of the Classical Sierpinski, P3/5SPK, and P3/4SPK modified Sierpinski antennas. The results clearly prove that when the perturbation factor of the antenna geometry is gradually increased from the Classical Sierpinski to the P3/5SPK to P3/4SPK while setting all

other parameters as constant, the bandwidth of the antenna increases from 6.44% to 8.23% to 9.92%. Broadband (approximately 10% of bandwidth) is achieved when the perturbation factor reaches  $\frac{3}{4}$ .

The radiation characteristics column in Table 4.11 also proves that when perturbation factor of the Sierpinski geometry increases, the coverage area of the antenna radiation also increases, and the radiation is fully contained within one main beam when the perturbation factor reaches  $\frac{3}{4}$ . The microstrip patch antenna based on the P3/4SPK modified Sierpinski geometry is a broadband multi-frequency antenna that has a wide coverage region of radiation.

When an electromagnetic (EM) wave is fed through the via port of the antenna, it starts to propagate over the structure toward the flat end of the gasket. In this project, small size fractal antennas with high frequencies over the GigaHertz (GHz) range have been designed. As wavelength is inversely proportional to frequency, high frequencies denote small wavelengths which are comparable in size with the smaller sub patches of the perturbed structure of the modified Sierpinski antennas.

When the EM wave finds a cluster comparable in size to its wavelength, it becomes radiated. When this happens, the structure encounters discontinuities that enhance further radiation. As a result, the current can travel further over the patch and a large active region can be reached. As the geometry of the microstrip patch is modified from the Classical Sierpinski to modified Sierpinski of increasing perturbation scale, the size of the two smaller sub patches are decreasing. This causes the wavelength of the

antenna to become more comparable to the decreasing size of the sub patches. As a result, current travels further over the antenna and an increasing active region is achieved, which in turn enhances the bandwidth and enlarges the coverage region of the antenna.

Although it is difficult to precisely put bounds on the active region, it actually covers a wider area than the region of the antenna patch. Therefore, at least an additional scale level should be taken into account to properly model the antenna behavior.

# CHAPTER 5

## CONCLUSION AND RECOMMENDATION

### 5.1 Project Conclusion

Approximately two semesters have been spent on doing this project. Along the implementation of this project, three single patch microstrip antennas with side length of 5cm, 8cm, and 10cm that radiate at resonant frequencies 12.4GHz, 9.8GHz, and 9.0GHz respectively have been designed. Generally, numerous simulations have been done and adjustments been made before achieving every satisfactory result. The simulation results show high accuracy and the resonant frequency obtained from simulation is only slightly deviated from the calculated frequency which is less than 3% and is acceptable. It has been observed that when the size of the patch antenna is increased, the resonant frequency decreases. This proves that the frequency of antenna is inversely proportional to the antenna size.

Fractal antennas with Classical and modified Sierpinski geometries have also been designed to fulfill the objectives of this project. The simulation results clearly prove that when the perturbation factor of the antenna geometry is gradually increased from the Classical Sierpinski to the P3/5SPK to P3/4SPK modified Sierpinski structure, the bandwidth of the antenna increases from 6.44% to 8.23% to 9.92%. Broadband (approximately 10% of bandwidth) is achieved when the perturbation factor reaches  $\frac{3}{4}$ .

Simulation results also show that when perturbation factor of the Sierpinski geometry increases, the coverage area of the antenna radiation also increases, and the radiation with wide coverage region is fully contained within one main beam when the perturbation factor reaches  $\frac{3}{4}$ .

In conclusion, the microstrip patch antenna based on the P3/4SPK modified Sierpinski geometry is a broadband multi-frequency antenna that has a wide coverage region of radiation. Thus, the key objective of the project is achieved - a broadband multi-frequency microstrip patch antenna with modified Sierpinski fractal geometry has been successfully designed and investigated.

## 5.2 Limitations and Difficulties

Generally, this project goes on smoothly as planned. Satisfactory results are obtained from simulations, despite a few limitations which restrict the area of investigation and accuracy. Thus, proper methods have been taken to overcome the problems and minimize the difficulties.

From the simulation of microstrip patch antennas, it has been observed that the major limitation of microstrip single patch antenna is its inherently narrow bandwidth (approximately 2%~4%). Thus, in this project, simulations have been done to study the characteristics of microstrip patch antenna based on the Sierpinski fractal geometry. Results show that with Sierpinski fractal geometry, the bandwidth of microstrip antennas can be significantly improved to up to 10%.

Simulation process in Microwave Office is time-consuming. For instance, the simulation of antenna in Section 4.5.1 takes approximately 40 hours. In order to reduce simulation time, normally simulation for a specific set of parameters with large cell size and large frequency step which takes approximately 3-5 hours is run. If the simulation results are acceptable and fulfill the requirements, then a more detailed simulation with smaller cell size and frequency step will be run to obtain more precise results. This can save time and maximize the number of simulations done in a given time period.

Microwave Office software has its own limitations. For instance, the geometry of the antenna simulated by Microwave Office is not exactly the same as the geometry designed, with some variations limited by the design grids. The detail of this limitation

has been explained in Section 4.3.5. In addition, Microwave Office is unable to let user specify the desired radiation mode that the antenna will operate. It is also unable to display the mode. Therefore, the radiation mode has to be computed by user based on the results obtained. Furthermore, the size of transmission line (via port) limited by the area of a grid is relatively large, thus causing inaccuracy in the simulation results. To overcome this problem, small cell size needs to be used which in turn increases the simulation hours.

### **5.3 Recommendations**

For future works, the analysis of the microstrip patch antenna with modified Sierpinski fractal geometry can be extended to a higher level of iteration. The main idea is to investigate and differentiate the performance at each iteration level. Further analysis can also be performed for multistacked configuration of antenna based on the perturbed Sierpinski fractal gasket as proposed in [2]. However, this requires sophisticated understanding on the behavior of each layer of the microstrip patch antenna.

The broadband multi-frequency P3/4PSK modified Sierpinski antenna designed in this project is useful where integration of multiple services are required such as in mobile communication systems (GSM900, GSM1800, UMTS, PCS) where multiple bands having similar performance cooperate to provide integrated services. However, the antenna designed in this project has a relatively large size to be used in cell phones. Therefore, further investigation can be done on the antenna to reduce the size while maintaining its broadband, multi-frequency and wide coverage behavior so that it can be practically applied in mobile communication systems.

Simulations can be done by using multiple simulating tools such as CST (Computer Simulation Technology) and Zeland software in which both are FDTD (Finite-Difference Time-Domain) based Full-3D EM simulators. This is done to avoid over dependence on Microwave Office and to acquire a better understanding of the antenna performance by referring to the 3D radiation. The results given by different

simulating tools can be compared in order to acquire the most precise results. Furthermore, the antennas designed can be fabricated by using the standard printed circuit techniques to study fractal antenna based on the Classical and modified Sierpinski geometries in term of experimental measurement in real environment. The simulation and experimental results can then be compared to see the differences.

It is recommended that higher performance computers be used for the purpose of accelerating the simulation process. For instance, the use of high-end computers with dual-core processors and high capacity of RAM (Random Access Memory) can reduce simulation time and allow multiple simulation processes simultaneously.

# REFERENCES

- [1] Kraus, John Daniel. (2002). *Antenna for All Applications*. 3<sup>rd</sup> ed. New York: McGraw-Hill
- [2] J. Anguera (2004). "Broad-Band Dual-Frequency Microstrip Patch Antenna With Modified Sierpinski Fractal Geometry." IEEE Transactions on Antenna and Propagation, 52 (1); 1-6
- [3] *Irina Nelson, Physics Tutoring: Electric Fields*, [http://www.slcc.schools/hum\\_sci/physics/tutor/2220/e\\_fields/](http://www.slcc.schools/hum_sci/physics/tutor/2220/e_fields/), 10 September 2005.
- [4] John D. Kraus. (1991). *Electromagnetics*. 4<sup>th</sup> ed. Singapore: McGraw-Hill, Inc.
- [5] *Carl Rod Nave, Magnetic fields of currents*, <http://hyperphysics.phy-astr.gsu.edu/hbase/magnetic/magcur.html#c1>, 10 September 2005.
- [6] *Mortimer Abramowitz, Matthew J. Parry-Hill, Michael W. Davidson, Molecular Expressions Microscopy Primer: Light and Color - Electromagnetic Radiation: Interactive Java Tutorial*, <http://micro.magnet.fsu.edu/primer/java/electromagnetic/>, 10 September 2005.
- [7] *Lawrence Berkeley National Laboratory, Electromagnetic Spectrum*, <http://www.lbl.gov/MicroWorlds/ALSTool/EMSpec/EMSpec2.html>, 15 August 2005.
- [8] *Joseph H. Reiser, Understanding and Using Antenna Radiation Patterns*, [http://www.astronwireless.com/radiation\\_patterns.html](http://www.astronwireless.com/radiation_patterns.html), 10 August 2005.
- [9] *Wikipedia Foundation, Inc., Antenna (Radio)*, [http://en.wikipedia.org/wiki/Antenna\\_\(radio\)](http://en.wikipedia.org/wiki/Antenna_(radio)), 5 September 2005.
- [10] George J. Monser. (1996). *Antenna Design – A Practical Guide*. United States: McGraw-Hill.
- [11] *Microwave Theory*, <http://www.madmadscientist.com/html/Theory.htm>, 26 September 2005.
- [12] Allan W. Scott. (1993). *Understanding Microwaves*. New York: John Wileys & Sons, Inc.

- [13] *Jim Lesurf, Types of Antenna*, [http://www.st-andrews.ac.uk/~www\\_pa/Scots\\_Guide/RadCom/part7/page1.html](http://www.st-andrews.ac.uk/~www_pa/Scots_Guide/RadCom/part7/page1.html), 15 August 2005.
- [14] *Horn Antenna - a Whatis.com Definition*, [http://searchmobilecomputing.techtarget.com/sDefinition/0,,sid40\\_gci214327,00.html](http://searchmobilecomputing.techtarget.com/sDefinition/0,,sid40_gci214327,00.html), 25 September 2005.
- [15] *Antenna Types*, [www.ncjrs.gov/pdffiles1/nij/1850306.pdf](http://www.ncjrs.gov/pdffiles1/nij/1850306.pdf), 25 September 2005.
- [16] *MDXC, Loop Page*, <http://www.frontiernet.net/~jadale/Loop.htm>, 25 September 2005.
- [17] *MAGLoop Antenna / magnetic loop antenna*, <http://home.datacomm.ch/hb9abx/loop1-e.htm>, 25 September 2005.
- [18] *Paul Wade, Helical Feed Antennas*, [http://www.w1ghz.org/antbook/conf/Helical\\_feed\\_antennas.pdf](http://www.w1ghz.org/antbook/conf/Helical_feed_antennas.pdf), 20 September 2005.
- [19] *Wikipedia Foundation, Inc., Microstrip antenna*, [http://en.wikipedia.org/wiki/Microstrip\\_antenna](http://en.wikipedia.org/wiki/Microstrip_antenna), 18 August 2005.
- [20] *Research on Microstrip Antennas*, <http://www.elmagn.chalmers.se/elmagn/antenna/research93-95/research-ms-a.html#fig7>, 18 August 2005.
- [21] *Satellite dish - Wikipedia, the free encyclopedia*, [http://en.wikipedia.org/wiki/Satellite\\_dish](http://en.wikipedia.org/wiki/Satellite_dish), 20 September 2005.
- [22] *Kuo-Hui Li, Tutorial: What is a Smart Antenna?*, [http://users.ece.gatech.edu/~mai/tutorial\\_sa\\_def.htm](http://users.ece.gatech.edu/~mai/tutorial_sa_def.htm), 21 September 2005.
- [23] *Smart Antenna Description*, [http://www.wtec.org/loyola/wireless/06\\_02.htm](http://www.wtec.org/loyola/wireless/06_02.htm), 21 September 2005.
- [24] *Wikipedia Foundation, Inc., Fractal*, <http://en.wikipedia.org/wiki/Fractal>, 10 August 2005.
- [25] *Paul Bourke, Sierpinski Gasket*, <http://astronomy.swin.edu.au/~pbourke/fractals/gasket/>, 13 September 2005.
- [26] *Larry Riddle, Sierpinski Carpet*, <http://ecademy.agnesscott.edu/~lriddle/ifs/carpet/carpet.htm>, 14 September 2005.
- [27] *Larry Riddle, Koch Curve*, <http://ecademy.agnesscott.edu/~lriddle/ifs/kcurve/kcurve.htm>,

14 September 2005.

- [28] *Fractal Geometry*, <http://www.crystalinks.com/fractal.html>, 21 September 2005.
- [29] *Peter Jonsson, Fractal Antennas for RFID Applications*. [http://www.ite.mh.se/~elektro/forskningsweb/research/groups/system/rfid\\_3.htm](http://www.ite.mh.se/~elektro/forskningsweb/research/groups/system/rfid_3.htm), 27 August 2005.
- [30] *Fractal Antenna – Mobile Devices*. <http://www.fractenna.com/commercial/mobile.htm>, 1 September 2005.
- [31] *Fractal Antenna – RFID*. <http://www.fractenna.com/commercial/rfid.html>, 1 September 2005.
- [32] *Wireless Networks*. <http://www.fractenna.com/commercial/wireless.html>, 1 September 2005.
- [33] *Fractal Antenna – Telematics*. <http://www.fractenna.com/commercial/telematics.html>, 1 September 2005.
- [34] *David J. Jefferies, The Smith Chart*, <http://www.antennex.com/preview/Folder03/Oct4/smith.htm>, 26 September 2005.
- [35] *Jashwant S.Dahele. (1987). “On the Resonant Frequencies of the Triangular Patch Antenna.” IEEE Transactions on Antennas and Propagation, AP-35(1); 100-101.*

# APPENDIX A

## Dimension and Cell Calculator

**DIMENSION & CELL CALCULATOR**

For calculating the length and height of triangle, box dimensions, i.e. the cells in the simulation box (x and y dimensions and divisions  $\sim \Delta y$ ).  
All units are in millimeters.

A. Triangular patch sizes

Length  $x := \bullet$

Height  $y := \frac{\sqrt{3}x}{2}$   $y = \bullet$

B. Box Dimensions

i. Cells in the simulation box (X Divisions  $\sim \Delta x$ , Y Divisions  $\sim \Delta y$ )  
 $\Delta x := 112$        $\Delta y := 111$

ii. Cells in the x and y axis to draw the length and height of the triangular patch

Let,

$X\_cells := 64$        $Y\_cells := 63$

C. The Calculations for Cell Dimension

$X\_dimension := \frac{x \cdot \Delta x}{X\_cells}$        $Y\_dimension := \frac{y \cdot \Delta y}{Y\_cells}$

**RESULTS**       $X\_dimension = \bullet$        $Y\_dimension = \bullet$

Press F1 for help.      AUTO      Page 1

# APPENDIX B

## Substrates for Microstrip Antenna

Table B1: Properties of RT/Duroid High Frequency Laminates

Property	Typical Value		
	RT/Duroid 5870	RT/Duroid 5880	RT/Duroid 6002
Dielectric constant, $\epsilon_r$	2.33 2.33 $\pm$ 0.02 spec.	2.20 2.20 $\pm$ 0.02 spec.	2.94 $\pm$ 0.04
Dissipation factor, $\tan \delta$	0.0005 0.0012	0.0004 0.0009	0.0012
Thermal coefficient of $\epsilon_r$	-115	-125	+12
Volume Resistivity	$2 \times 10^7$	$2 \times 10^7$	$10^6$
Surface Resistivity	$3 \times 10^8$	$3 \times 10^8$	$10^7$
Standard thickness	0.127 mm 0.254 mm 0.381 mm 0.508 mm 0.787 mm 1.575 mm 3.175 mm	0.127 mm 0.254 mm 0.381 mm 0.508 mm 0.787 mm 1.575 mm 3.175 mm	0.127 mm 0.254 mm 0.508 mm 0.762 mm 1.524 mm 3.048 mm
Standard copper cladding	$\frac{1}{4}$ oz. (8 $\mu$ m) electrodeposited copper foil. $\frac{1}{2}$ oz. (17 $\mu$ m), 1oz. (35 $\mu$ m), 2 oz. (70 $\mu$ m) electrodeposited and rolled copper foil.		

Table B2: Properties of RO3000 Series High Frequency Laminates

Property	Typical Value		
	RT/Duroid 5870	RT/Duroid 5880	RT/Duroid 6002
Dielectric constant, $\epsilon_r$	3.00 ± 0.04	6.15 ± 0.16	10.2 ± 0.30
Dissipation factor, $\tan \delta$	0.0013	0.0020	0.0023
Thermal coefficient of $\epsilon_r$	13	-160	-280
Dimensional Stability	0.5	0.5	0.5
Volume Resistivity	$10^7$	$10^3$	$10^3$
Surface Resistivity	$10^7$	$10^3$	$10^3$
Standard thickness	0.13 mm 0.25 mm 0.50 mm 0.75 mm 1.52 mm	0.13 mm 0.25 mm 0.64 mm 1.28 mm	0.13 mm 0.25 mm 0.64 mm 1.28 mm
Standard copper cladding	$\frac{1}{2}$ oz. (17 $\mu$ m), 1 oz. (35 $\mu$ m), 2 oz. (70 $\mu$ m) electrodeposited copper foil.		